THE IMPACT OF MATERIAL CHARACTERISTICS ON TIRE PAVEMENT INTERACTION NOISE FOR FLEXIBLE PAVEMENTS

By

Salih Kocak

A THESIS

Submitted to
Michigan State University
in partial fulfillment of the requirements
for the degree of

MASTER OF SCIENCE

Civil Engineering

2011

ABSTRACT

THE IMPACT OF MATERIAL CHARACTERISTICS ON TIRE PAVEMENT INTERACTION NOISE FOR FLEXIBLE PAVEMENTS

By

Salih Kocak

Noise pollution has recently been one of the growing problems all over the world. While there are many sources of the noise, traffic noise is the main contributor to the total environmental noise. Although there are different sources for traffic noise, the tire pavement interaction noise is the most dominant component within most city and highway limits. One of the ways to reduce the tire pavement noise is to improve the material characteristics of the pavements such that they produce less noise. In this study, the relationship between basic material characteristics (e.g., Hot Mix Asphalt (HMA) volumetrics) and sound generation and absorption characteristics of flexible pavements was investigated. In addition, the effect of linear visco-elastic properties (e.g., dynamic modulus ($|E^*|$) and phase angle (δ)) on sound absorption was studied. In order to focus only on impact of material characteristics and overshadow the effect of surface texture, a novel laboratory tire pavement noise measurement simulator (TIPANOS) was developed. The statistical analysis results showed that although the individual material characteristics do not have appreciable influence on sound absorption, there is a significant correlation between sound pressure levels (SPL) and combination of several material and linear visco-elastic parameters.

To My Family

ACKNOWLEDGEMENTS

I would like to thank my advisor, Dr. Muhammed Emin Kutay, for his endless support, guidance and friendship throughout my graduate career. He always encouraged and gave me back my confidence whenever I lost it. I also would like to thank to the Civil and Environmental Department at Michigan State University for providing me with the opportunity to pursue my graduate degree. The efforts and inputs of Dr. Syed Waqar Haider and members of the advisory committee, Dr. Karim Chatti, and Dr. Neeraj Buch, are highly appreciated.

I would like to extend my appreciations to my colleagues, Ashvini Kumar Thottempudi, Hande Isik Ozturk, and Abrar Siddiqui for their invaluable discussions and supports.

Thanks to my family and friends for their continuous emotional support and encouragement. The research presented in this thesis was supported by the MSU's Intramural Research Grants Program (IRGP).

TABLE OF CONTENTS

LIST OF TABLES

LIST OF FIGURES

CHAPTER 1

INTRODUCTION

1.1 BACKGROUND

The noise pollution has been one of the most obtrusive problems all over the world recently. Traffic noise is one of the major contributors to total environmental noise. People living at a closer proximity to the highways, who are constantly exposed to the traffic noise, complain about physical and psychological health related problems (Kropp et al. 2007). While there are different sources of traffic noise, noise due to the tire/pavement interaction is dominant at high speeds greater than 30 miles/hr (Sandberg 2001, Kutay et al. 2010). To minimize the impact of tire/pavement interaction noise, tire manufacturers have been working on producing tires that generate less noise. On the other hand, constructing sound walls, to absorb the traffic noise, was the most commonly used sound mitigating solution by State Departments of Transportation (DOTs). However, the noise walls absorb a small percent of the noise and reflect most of the sound waves. This leads to driver discomfort. Moreover, the noise walls are expensive to construct (~$2.1 million per mile) (Hanson et al. 2004). Therefore, to solve the problem at the source, DOTs have been spending great effort to produce pavements having good sound absorption capacity.

One of the major contributors to the tire/pavement noise generation is the surface texture. Recent studies have primarily focused on measurement of texture using both 2D and 3D laser-based techniques and developed correlations between tire/pavement noise and certain parameters representing texture such as the mean profile depth. However, it was observed that the correlation between the texture characteristics and pavement noise is not always consistent (Rasmussen et al. 2006). This is possibly due to the material characteristics of the pavements that cause damping or amplification of the sound. Depending on the design of the pavement material, these characteristics may overshadow the effects of texture. Certain pavements with surface textures designed for low levels of tire/pavement noise were reported in the literature to lose their characteristics quickly over the years. Moreover, both microtexture and macrotexture result in the deformations on the tread of the tire and escorting to the vibrations of tire and all suspension system (Wayson 1998).

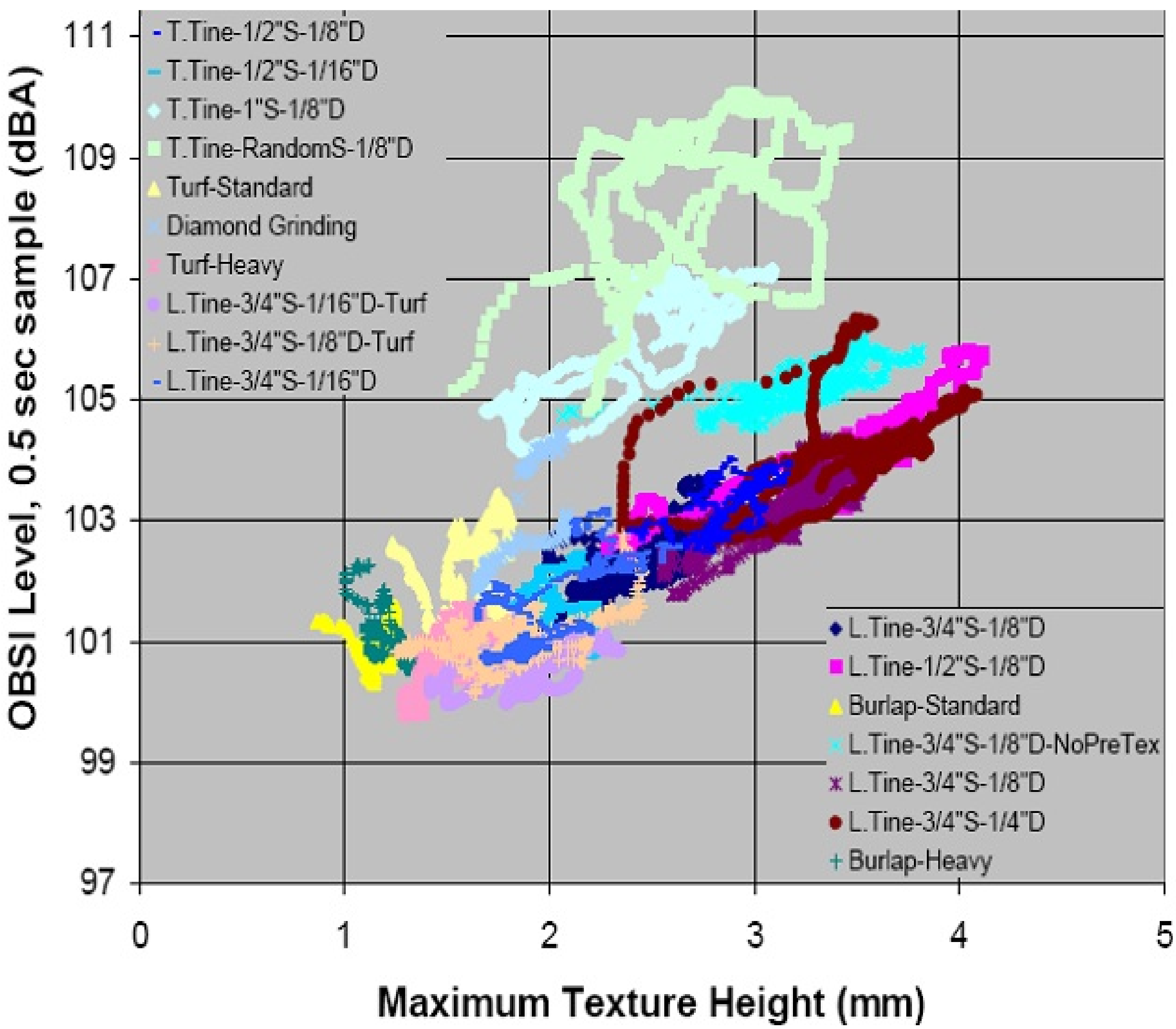

Figure 1.1 On-Board Sound Intensity (OBSI) levels versus the maximum texture height relationships for a variety of pavement surface (Rasmussen et al. 2006).
“For interpretation of the references to color in this and all other figures, the reader is referred to the electronic version of this thesis.”

Pavement surface can be textured to minimize tire/pavement noise. However, the degradation of the texture is dependent on the material properties such as the aggregate type and shape used in the mixture, asphalt binder characteristics...etc. Even though pavement material properties can have such a significant influence on the highway noise, there is a lack of literature on the relationship between the material properties and the generation of noise. Furthermore, the durability of surface texture calls for development of such relationships to better understand the tire/pavement noise generation and for a better design of long-lasting quiet pavements.

1.2 PROBLEM STATEMENT

As mentioned earlier, the noise generated by the pavement is dependent on the surface texture of the pavement, which is further dependent on the material properties such as aggregate type and shape, asphalt binder characteristics…etc. The primary aim of this research is to identify the fundamental material characteristics of asphalt pavements that affect the tire-pavement noise generation and propagation to lead to an improved pavement design for sustainable green highways in the future.

1.3 OBJECTIVES

The main objective of this research is to investigate relationship between tire/pavement noise generation/absorption and material characteristics of flexible pavements. It also presents the impact of material mix design characteristics as well as linear visco-elastic properties on sound absorption.

To accomplish the objective, a research plan consisting of three major tasks was developed and is presented in the next section.

1.4 RESEARCH PLAN

As stated above, the research plan for this study consists of the three tasks detailed below.

Task 1 – Information and Material Supply – In this task, mix design types, specifications and standards utilized by most of the state DOT’s were obtained and analyzed. The most suitable mix designs for the research were adopted. AASHTO standards were followed in both testing of the materials and constructing mix designs. The following steps can summarize the task 1,

- Getting familiar with the standards, specifications and DOT’s practices. All tests performed on aggregates, binders and HMAs follow AASHTO standards.
- Obtaining different mix designs typically used by DOTs and choosing the most suitable designs for the research.
- Acquiring ample aggregate and binder samples for preparation of HMAs.
- Gathering the information and ideas to construct a system capable of measuring the tire/pavement interaction noise in the laboratory environment without taking into account the effect of surface texture.
- Getting familiar with the laboratory equipment for tests and specimen preparation.

Task 2 — Evaluation of Materials and Preparation of Specimens- All material supplies used in the study were tested according to the corresponding AASHTO standards. Only those materials complying with the AASHTO standards are used in this research. The assessment and preparation of specimens include:

- Testing as-received supplies according to the AASHTO standards. These tests include all performance grading (PG) tests for binders and physical property tests of aggregates. The materials were assessed if they conformed to the specifications after testing part was performed.
- Performing mix designs. Superpave (SP) 9.5mm, SP 12.5 mm, SP 25 mm, open graded friction course (OGFC) and stone matrix asphalt (SMA) are the mix designs performed.

- Preparation of specimens. All specimens were prepared by using a laboratory slab compactor with shearing capabilities.

Task 3 – Laboratory Testing and Data Analysis – The cylindrical specimens prepared during the previous task were tested for dynamic modulus measurements and sound pressure levels. Since both the tests are non-destructive in nature, same specimens were used. Statistical analyses were performed on the measured dynamic modulus and sound pressure levels. This task includes:

- Dynamic modulus measurement by using Asphalt Mixture Performance Tester (AMPT).
- Tire/pavement interaction noise measurements via the laboratory device developed in this research (Tire-Pavement Noise Measurement Simulator (TIPANOS)).
- Statistical analysis of relationship between individual material characteristics and sound pressure levels.

CHAPTER 2

LITERATURE REVIEW

2.1 INTRODUCTION

Noise pollution has recently been one of the most important problems in the United States and other countries all over the world. Loss of hearing, anxiety, sleeplessness, aggression, speech interference, increase in heart rate and stress are just few common examples of physical and psychological health related problems caused by noise pollution (Shatanawi et al. 2008, SCDREA 1999). While there are many sources of the noise, traffic noise is a major contributor to the total environmental noise. Traffic noise mainly composed of three different sources, which can be classified as propulsion, tire-pavement interaction, and aerodynamic noises. Sounds generated from the engine, exhaust, intake and other power-train components constitute the propulsion noise type. This kind of noise governs the total noise at low speeds (Rasmussen et al. 2007). The sound generated by the interaction of tire and pavement surface is called tire-pavement noise, which becomes dominant when a crossover speed is reached. Crossover speed is between 10-25 mph for cars and 35-50 mph for trucks (Rasmussen et al. 2007). With today's technology in manufacturing quieter engines, crossover speed has been decreasing significantly. The third kind of noise is the aerodynamic noise and it is generated as a result of the air turbulence around a vehicle. This type of noise becomes dominant at very high speeds. In city and highway speed limits, tire pavement interaction noise controls the overall noise generated by moving vehicles. To reduce the noise generated by running traffic, both the vehicle and tire manufacturers have shown significant accomplishments in this multidisciplinary problem. As the third party in the solution of the traffic noise problem, the road owners also have been sharing the responsibility by conducting or supporting research on quite pavements. In order to meet the public demand, Federal Highway Administration (FHWA) recommends six traffic noise abatement methods (FHWA 1997). The most commonly used method is construction of noise barriers. Besides being costly (~$2.1 million per mile), the noise walls are not very effective and desirable because of the driveway access, height limitation and their aesthetical view. Typical concrete noise barriers have high acoustic reflectivity with 95% or above and very limited sound absorption (Campbell 2000, Zhu et al. 2008). Therefore, they can only alter the direction of propagation. Redirected noise from the barriers adversely affects the passengers and drivers using the roads. Moreover, Campbell (2000) showed the inefficiency of concrete noise barriers in controlling and reducing the impact of traffic noise by both field measurements and modeling studies. Constructing quieter pavements is anticipated to be a more economic and sustainable way in reducing the tire pavement interaction noise. The low noise road surface is defined as the "road surface which, when interacting with a rolling tire, influences the vehicle noise in such a way as to cause at least a 3 dB (A) lower vehicle noise than that obtained on conventional and most common road surfaces" (Sandberg et al. 2002). The definition of common road surface differs from country to country. In the ISO standards, it corresponds to the reference surface with dense, smooth- textured asphalt concrete surface with a maximum aggregate size between 11 mm. to 16 mm (ISO 1997).

2.2 TIRE-PAVEMENT NOISE MECHANISM

The interaction between tire and pavement results in generation of noise. Depending on the type of the tire and pavement surface, the noise level can vary greatly. There are several mechanisms that explain the generation of the sound at the interface between the tire and pavement. Moreover, there are some other factors that can contribute to the amplification of the mechanisms.

All mechanisms can be gathered under three categories. These are air resonant, radial vibration and adhesion mechanisms.

2.2.1 Air Resonant Mechanism

Air resonant mechanism includes three main components and becomes dominant after 1000 Hz frequency level. The first one is the pipe resonance which amplifies the sound generated in another place inside the grooves of the tire tread and on channels along the surface the tire (Sandberg 1992, Rasmussen 2007). Another component is the Helmholtz resonance that occurs when the air in the tire tread cavity behaves as a spring which resonates with the mass of air in between the cavity and the atmospheric air while the tire rotates. The last one is the air pumping. It forms in between the tire tread and pavement surface texture as the gaps in between filled with air. While the tire rolls over the pavement, either air is squeezed out or trapped and compressed. When tire loses the contact with pavement at a point, trapped air is forced to out. This process is repeated hundreds of times in a second and results in a large amount of air turbulence and as a result noise (Leasure et al. 1975, Rasmussen 2007).

2.2.2 Radial Vibration Mechanism

The radial vibration mechanism occurs as the tire rolls over the pavement. It is more pronounced at frequencies below 1000 Hz. In this mechanism, the vibrations (noise) are induced by small deflections due to the interactions between pavement texture and the tread of the tire and propagate to the air. It can be described by a hammer physical analogy. It can be visualized by assuming each tread as a hammer stroking to the pavement thousands of times a second.

2.2.3 Adhesion Mechanism

The adhesion mechanism includes two components. As in the case of air resonant mechanism, adhesion mechanism is more pronounced at 1000 Hz and higher frequencies. Stick-slip is the first component and it occurs as a result of the vibrations due to tangential slippage of the tire tread between tire and the road surface. The second constituent is stick-snap. It happens when the rubber adheres and is released vertically from the road surface as the tire rotates. The physical analogy for stick-snap can be seen as suction cup. There are some other components of the tire pavement interaction noise that amplify the mechanisms explained as well.

2.3 QUITE PAVEMENTS

The research on quite pavements first started in Europe in 1970's, and one-decade later, Japan researchers began to implement low noise pavements. A few decades ago, the importance of the quite pavements was realized by FHWA and research projects were initiated in this field in United States (Meiarashi 1999, Rasmussen et al. 2007).

There are three typical types of hot mix asphalt (HMA) designs used in the high volume highways: Open Graded Friction Course (OGFC), Dense Graded HMA Mix (DGA), and Stone Matrix Asphalt (SMA) mix (Hanson et al. 2004). In literature, porous pavements also known as OGFC, gap graded asphalt or drainage asphalt, are reported to be one of the quietest pavement types. Studies have shown that an OGFC can reduce the noise level 3 to 5 dB (A), when compared to a dense HMA pavement. This is because the air voids in the pavement provide a means for air trapped between the tire and the pavement surface to escape, and lead to increased sound absorption. To be able to damp the noise successfully, the pores need to be interconnected (Sandberg et al. 2002). Furthermore, porous surfaces have an advantage of efficient drainage of water and reduce the splash and spray behind vehicles during rainfalls (Malcom et al. 2003). However, one of the important challenges associated with the porous pavements is their durability and effectiveness over years. Fine particulate on the roadways can quickly clog the voids reducing pavement's capability to absorb noise. The recent researches to solve the clogging of surface with dirt and dust from environment and snow removal operations and durability issues related with OGFC wearing surfaces have suggested the use of two layer system (Hanson et al. 2004). Otherwise, clogging can become a serious problem especially in urban areas and periodic cleaning operations are needed, which creates additional costs. A surface named as Twinlay has been optimized to have a long acoustical lifetime for urban applications at speeds around 50 kilometer per hour (km/h). In the applications of porous pavements where the traffic speed is 90-130 km/h, there is a self-cleaning of the pavement surface and the acoustic lifetime can be acceptable even without cleaning (Sandberg 1999).

2.4 PARAMETERS AFFECTING NOISE

There are several geometrical and road pavement parameters affecting the sound absorption of porous pavement surfaces. Porosity, pore size distribution, air void, tortuosity, coarseness of the aggregate mix, thickness of the porous layer and the airflow resistance per unit length are parameters typically related to noise (Malcolm et al. 2003, Nelson et al. 2008).

Typical in-place air voids in dense HMA is 5-7%, whereas, the percent air void in porous mixes ranges from 15% to 30%. While the tortuosity or shape factor is a measure of the shape of air voids passages, the airflow resistance is the resistance experienced by air when it passes through open pores in the pavement (Malcolm et al. 2003). It has been shown that airflow resistance and air void content play an important role on peak sound absorption coefficient of porous surfaces with 40 mm thick and tortuosity value of 5 (Von Meier 1998, Von Meier et al. 1990).

The frequency range of the traffic noise, which is undesirable for the public, lies between 250 Hz. and 4000 Hz (Lapcik 1998). The thickness of the porous mixes changes both the value and the shape of the absorption peak. Hamet et al. (1990) performed the measurement of sound absorption of various surfaces ranging from 50 mm to 400 mm thick. While 50 mm thick porous surface had a sharp peak with almost unity at about 900 Hz, 100 mm surface had first peak in 450 Hz with a smooth peak and second sharp peak at 1,350 Hz. Moreover, the 150 mm thick pavement had three different peak values at 300, 900 and 1,500 Hz (Hamet et al. 1990). The thickness of the porous surface has a significant effect on both sharpness and peak frequency. In general, as the thickness of the surface layer increases, peak frequency decreases. It is worth to note that the most objectionable noise to human ear occurs between frequencies of 800 and 1200 Hz. Hence, the frequency at which the maximum acoustic absorption occurs could be manipulated by changing the thickness of the surfaces (Narayanan et al. 2004). When the peak absorption is desired at a frequency approximately 1000 Hz, which is the interstate highway noise frequency for vehicles with most of the tire and road combinations, a porous surface between 1.5 and 2.0 inch thick can be used effectively (Malcolm et al. 2003, Sandberg 2003). To shift the absorption maxima to low frequency region when the traffic speed is low as in the case of in city conditions and/or the percentage of heavy vehicles of the traffic volume is high, the use of thicker asphalt pavement layer is suggested (Kropp et al. 2007). In particular, for the frequency ranges below 1000 Hz sound waves show less attenuation inside the material, the sound absorption coefficient peaks at a frequency at which the anti phase condition is satisfied between the multi reflective waves in the material and the sound wave reflected from the front surface of the material. Moreover, for the frequencies above 1000 Hz, attenuation gradually increases while the interference decreases (Yamaguchi et al. 1999). Since the thickness, air void and the interconnectivity of the air voids play an important role in sound absorption, most of the researchers have been working on these characteristics to increase the efficiency. While dense asphalt mixes' air voids vary between 4% and 8%, with absorption coefficients ranging from 0.1 to 0.2, open graded mixes with air void content 15% absorption coefficients of 0.4 to 0.7 are easily achieved (Hanson et al. 2004). In order to obtain reasonable noise reduction, which is around 8 dB(A), it is advised to construct a pavement with an air void content 20% and minimum thickness of 40-50 mm by using small chippings in the top layer. However, the pavements thicker than 100 mm do not show significant sound absorption (Sandberg 1999).

2.5 IMPROVING MATERIAL CHARACTERISTICS TO REDUCE NOISE

Besides trying to increase the efficiency and durability of porous surfaces, some other researchers have been working on different ways of reducing the tire pavement interaction noise. One of the study areas is to use different kinds of bitumen and mixes. Use of crumb rubber or polymer-modified binder in asphalt to increase the sound absorption has been one of the mostly funded areas in this field recently. Especially the use of crumb rubber modified binder has more than one advantage. While resulting in a decrease in noise level generated by tire pavement interaction, it also helps environment by recycling the old tires inside asphalt. Crumb rubber is obtained by re-processing (shredding) the disposed automobile tires into small pieces after removing the fiber and the metal present inside (Zhu et al. 1999). Even though the idea of using old tires to make asphalt was started in United States in 1940's, the idea has not gained much momentum. However, nowadays it has been gaining more popularity both in the States and all over the world and it is used with confidence (SCDERA 1999). Using crumb rubber inside the asphalt pavement also helps solving environmental problems caused by disposal of automobile tires (Zhu et al. 1999). Furthermore, the presence of crumb rubber particles inside the binder affected the volumetric properties of the mixtures such as permeability and the binder content that in return have effect on the sound absorption (Shatanawi et al. 2008). A study in University of Waterloo, Ontario revealed that crumb rubber modified open friction course absorbed 9% of the sound generated (Ahammed et al. 2010). In another research performed, the surface of the aged and cracked Portland Cement Concrete Pavement was overlaid by crumb rubber modified asphalt (CRM). The noise measurements just before and after placement of the CRM asphalt layer showed a decrease of 6.1 dB (A) in residential areas which are almost 40 ft away from the roadway. Also, the noise level inside the car was measured and in average the noise reduction was 5.2 dB (A) compared to the previously existing pavement surface. Upon the extremely positive public opinion in the area, the City of Phoenix allocated new funds for rehabilitation of roads with CRM asphalt (Carlson et al. 2005). The similar analysis was performed in the eight streets in the City of Thousand Oaks, Sacramento. Before and after laying the asphalt rubber overlay, the noise measurements were taken from 50 ft or more from the roadway centerlines. The results indicated that traffic noise level reductions were between 3 and 7 dB (A) on freshly resurfaced roadways compared to old one and 2 to 5 dB (A) of total noise reduction was attributed by asphalt rubber overlay. Noise reduction was even more on the sites where traffic speed is higher (Bucka 2002). As the time passed and pavements aged under temperature and pressure applied by vehicles, the reduction in noise level decreased; however, it still stayed noticeable around 1 to 3 dB (A). In his research, Meiarashi (1999) measured the annual noise absorption degradation in drainage asphalt is about 1 dB (A)/year. From the literature review on acoustic properties of pavements, using drainage surface with two layer system and crumb rubber modified binder with anticipated thickness by considering the frequency of traffic according to the flow speed will yield the maximum reduction in traffic noise. The reduction in noise level degrades as the time passes but above-mentioned pavement surface never loses all its ability to absorb noise compared to dense graded asphalt mixes (Meiarashi 1999).

2.6 SENTHESIS OF THE PREVIOUS WORK AND MOTIVATION FOR THE CURRENT STUDY

Since one of the major contributors to the tire/pavement noise generation is the surface texture, most of the recent studies focused on measurement of surface texture by using newly developed techniques. The researchers worked on developing correlations between tire/pavement noise and certain parameters representing texture such as the mean profile depth. However, it was observed that the correlation between the texture characteristics and pavement noise is not always consistent (Rasmussen et al. 2006). This might be because of the effect of pavements' material characteristics (causing damping or amplification) overshadowing the effects of surface texture on the tire/pavement noise. Some other researchers studied the relation between individual material parameters and tire pavement interaction noise. In their research, Kaloush et al. (2006) analyzed the relation between the dynamic modulus (|E*|) test parameters for conventional and asphalt rubber mixtures and tire/road noise characteristics. However, they focused only on the individual correlations between the |E*| and noise levels and did not investigate combined effect of other materials characteristics such as HMA volumetrics and aggregate properties. The primary motivation for this research was that there was very limited or no information on the relation between the material characteristics of HMA pavements and their ability to absorb tire/pavement noise. These characteristics include (i) HMA mix design parameters (e.g., binder and air void content, voids in mineral aggregate (VMA), voids filled with asphalt (VFA)…etc.), (ii) aggregate properties (e.g., nominal maximum aggregate size (NMAS), coefficient of uniformity (Cu) …etc.) and (iii) linear viscoelastic properties (e.g., |E*|, phase angle, storage modulus (E'), loss modulus(E") …etc.). Also, there was no realistic and practical sound absorption measurement system that can be used on the laboratory-size asphalt samples. Such system is important for evaluating different HMA types at the mix design stage so that the future pavements can be designed by taking into account the HMA's ability to absorb noise.

CHAPTER 3

MATERIAL AND MIXTURE PROPERTIES

This chapter covers the physical properties of aggregates, binders and mixtures along with their sources. The aggregates were obtained from different locations in the State of Michigan (MI). Michigan Paving and Materials Company (a.k.a. Spartan Asphalt) and Rieth-Riley Construction Co., Inc. were the two companies providing the aggregates in Lansing, MI for the research. Light weight aggregates used to investigate the effect of aggregates in a wider range were supplied by Buildex Incorporated in Ottawa, Kansas.

The main supplier of the asphalt binder was Mathy Technology and Engineering (MTE) Services in Onalaska, Wisconsin. MTE provided original and polymer modified binders used during the research. Crumb rubber modified binders were supplied by Seneca Petroleum Co. Inc located at Crestwood, Illinois.

All material tests were performed according to the corresponding AASHTO and ASTM standards at Michigan State University (MSU) Advanced Asphalt Characterization Laboratory (AACL).

3.1 PHYSICAL PROPERTIES OF AGGREGATES

The aggregates used during the research were mainly river gravels with at least one crush face. Limestone was another mostly used aggregate type to produce specimens. Besides the regular aggregates, some of the specimens were prepared by using commercially available light weight aggregates which is also known as hydite. The more detailed information about the physical properties of the aggregates is presented in job mix formula (JMF) tables in Appendix A. Table 3.1 shows the basic properties of the coarse, fine and light weight aggregates used throughout the research.

Table 3.1Particle size and physical properties of aggregates

Sieve Opening		River Gravel Specific Gravity	River Gravel Absorption	Light Weight Agg. Specific Gravity
	in mm			
3/4	19.5	2.706	1.66%	NA
1/2	12.5	2.702		1.202
3/8	9.5	2.684		1.208
#4	4.75	2.633		1.212
#8	2.36	2.814	0.73%	1.351
#16	1.18	2.821		1.501
#30	0.6	2.802		1.711
#50	0.3	2.632		1.902
#100	0.15	2.695		2.101
#200	0.075	2.695		2.303
Dust	<0.075	2.604		NA

As it can be seen from the table above, the specific gravities of the coarser light weight aggregates are less than half of the specific gravities of river gravels. However, as the particle size gets smaller, the difference between the specific gravities reduces. Since researchers and manufactures of the light weight aggregates have been conducting tests for potential use in asphalt and concrete mixtures, this research also aimed to study the effect of light weight aggregates on tire pavement interaction noise.

3.2 PHYSICAL PROPERTIES AND ENGINEERING CHARACTERISTICS OF ASPHALT BINDERS

Binders used throughout the research were evaluated according to AASHTO performance grade standards. Since the binder determines the visco-elastic properties and climatic condition that asphalt pavements can resist, it needs to be investigated deeply. In this research, other than original binder, polymer and crumb rubber modified binders were used to analyze the effect of modified binders on sound absorption capacity of the asphalts as well. Performance grade (PG) of the binders is performed according to AASHTO R-29 and M-320 protocols. PG tests include;

- Flash Point by Cleveland Open Cup, AASHTO-48
- Viscosity Determination of Asphalt Binder by Using Rotational Viscometer (RV), AASHTO T-316
- Determining the Rheological Properties of Asphalt Binder Using a Dynamic Shear Rheometer (DSR), AASHTO T-315
- Effect of Heat and Air on a Moving Film of Asphalt, Rolling Thin Film Oven (RTFO), AASHTO T-240
- Accelerated Aging of Asphalt Binder Using a Pressurized Aging Vessel (PAV), AASHTO R-28
- Determining the Flexural Creep Stiffness of Asphalt Binder Using the Bending Beam Rheometer (BBR), AASHTO T-313

The Table 3.2 summarizes the performance grade (PG), flash point, viscosity and specific gravity of asphalt binders used in the research.

Table 3.2 Properties of binders used during the research

Binder Type	**PG**	**Flash Point**	**Viscosity (at 135 ^{o}C)**	**Specific Gravity**
		^{o}C	**Pa.s**	
Original Binder	58-28	272	0.34	1.023
Polymer Modified (PM)	70-28	314	1.26	1.029
5% Crumb Rubber Modified (CRM)	70-28	298	1.29	1.031
10% Crumb Rubber Modified (CRM)	76-28	335	2.20	1.033

Moreover, the mixing temperature (MT) and compaction temperature (CT) of the hot mix asphalts can be obtained by using RV. According to AASHTO T312- Preparing and Determining the Density of Hot Mix Asphalt Specimens by Means of the Superpave Gyratory Compactor, MT and CT can be obtained by running the RV more than one temperature level and demonstrating them on semi-log paper. Temperatures corresponding to 170 ± 20 milipascals-seconds (mPa.s) and 280 ± 30 mPa.s kinematic viscosities will give MT and CT of HMA prepared by that asphalt binder (AASHTO T-312). Table 3.3 summarizes mixing and compaction temperatures of the HMAs prepared by using each binder type. It is noted that the mixing and compaction temperatures of CRM binders were recommended by the manufacturer.

Table 3.3 Mixing and compaction temperatures for the binders used in the research

Binder Type	**Mixing Temp.**	**Compaction Temp.**
	^{o}C	**^{o}C**
Original	149	138
Polymer Modified	175	165
5% CRM	180	170
10% CRM	180	170

Since HMA containing modified binders follows manufacturer's recommendations, Figure 3.1 shows how to obtain MT and CT of the original binder used in the research.

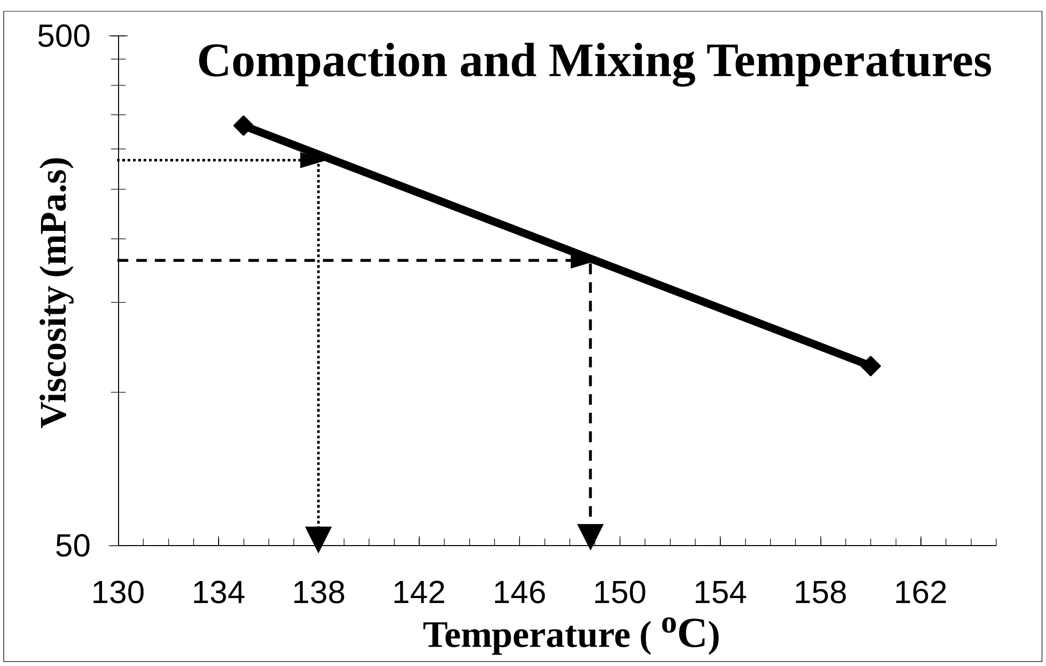

Figure 3.1 Compaction and mixing temperature determination for original binder

3.3 Physical Properties of HMA

After the physical properties of the aggregates and binders used in HMA preparation are explored, the next step is to prepare asphalt specimens and check their properties whether they conform to standards. The most important criteria to be checked is the air void content.

This section covers the aggregate gradations, control mix design parameters and process and preparation of the specimens.

3.3.1 Gradation of Aggregates and Sieve Analysis

The effect of mix design parameters on sound absorption characteristics of pavements has been investigated by performing five different mix designs: (i) Superpave (SP) 12.5 mm, (ii) SP 9.5 mm, (iii) SP 25.0mm, (iv) stone matrix asphalt (SMA) and (v) open graded friction course (OGFC). Table 3.4 and Figure 3.2 provide the aggregate gradations for each type of the mix designs.

Table 3.4 Aggregate gradations used in the research mix designs

Sieve Size	**Percent Retained in Each Sieve**				
mm	**SP-9.5 mm**	**SP-12.5 mm**	**SP-25 mm**	**SMA**	**OGFC**
25.000	0.0%	0.0%	3.0%	0.0%	0.0%
19.000	0.0%	0.0%	8.0%	0.0%	0.0%
12.500	0.0%	3.1%	14.0%	6.0%	0.0%
9.500	9.0%	7.0%	8.0%	29.0%	0.0%
4.750	35.0%	18.0%	13.0%	35.0%	62.0%
2.360	18.0%	19.0%	13.0%	10.0%	28.0%
1.180	12.0%	18.0%	11.0%	5.0%	4.0%
0.600	10.0%	15.4%	8.0%	3.0%	2.0%
0.300	6.0%	7.3%	7.0%	2.0%	1.0%
0.150	3.0%	4.7%	5.0%	4.0%	0.0%
0.075	2.0%	3.6%	7.0%	2.0%	0.4%
(dust)	5.0%	4.0%	3.0%	4.0%	2.6%
TOTAL	100.00%	100.00%	100.00%	100.00%	100.00%

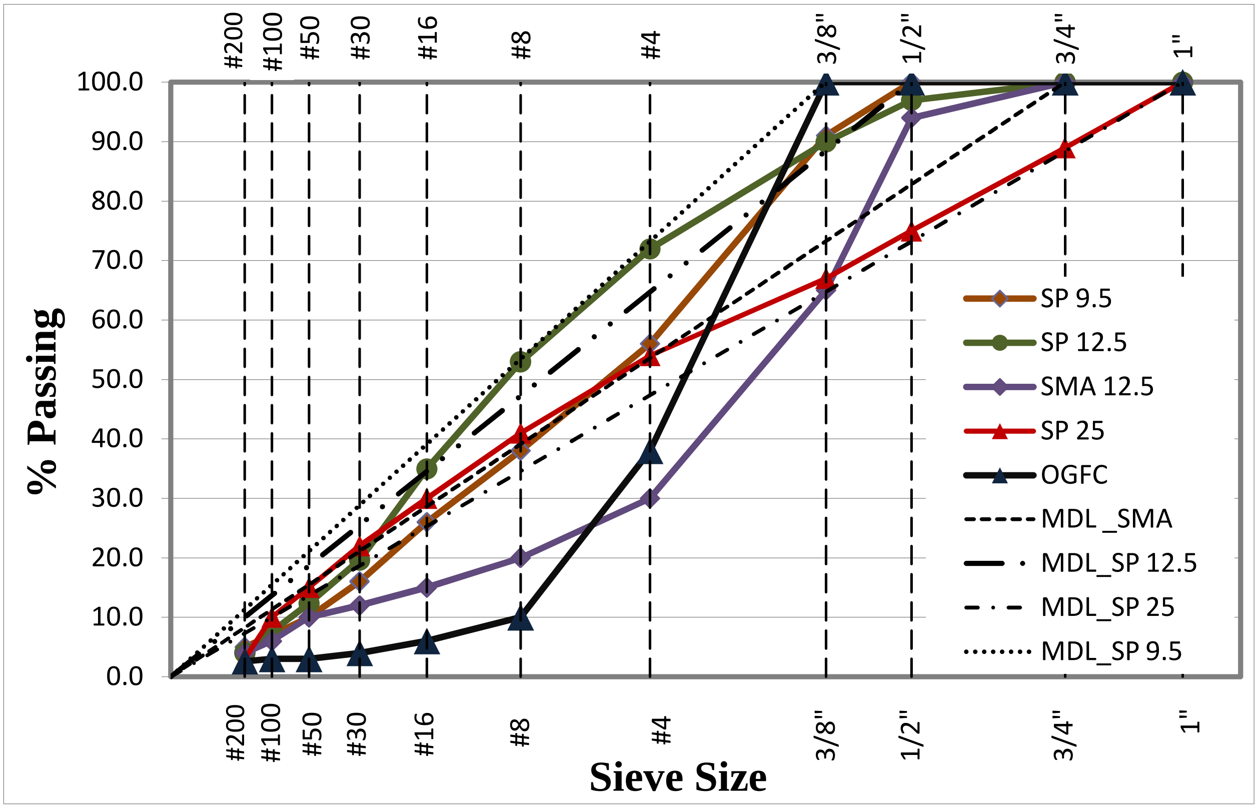

Figure 3.2 Aggregate gradation curves and maximum density lines (MDL)

Superpave mix design with maximum aggregate size 12.5 mm was chosen as the control mix design since it has been very commonly used in asphalt pavement projects in Michigan. SMA mixture design uses superpave mix design with some modifications (AASHTO M-325 & R-46, 2009). National Pavement Asphalt Association's (NAPA 1999) designing and constructing SMA mixtures and NCHRP report 425 (Brown et al. 1999) were two other sources studied for SMA mixture design. Since the amount of binder was considerably high in SMA and OGFC mix designs, cellulose fibers were introduced to the mixtures to prevent the draindown. The amount of fiber added was 0.2% and 0.3% by weight of the mixture, in SMA and OGFC, respectively (Kumar et al. 2005). Fibers were not kept in the oven with aggregates since they might catch fire easily. They were introduced mixture during mixing period. Furthermore, 1% hydrated lime was added to the OGFC mix design as an antistripping agent. Since OGFC mixtures have high air void content compared to other mix designs, water can freely infiltrate to entire depth of the pavement. To prevent the moisture damage to the asphalt, using hydrated lime as an antistripping agent on OGFC mixtures is the most commonly used technique (Cooley et al. 2004).

3.3.2 Control Mix Design Parameters

The aggregate gradation for the control mix design can be seen in Table 3.4 as SP -12.5. Furthermore, in this section detailed information about the findings of control mix design is presented. AASHTO M323- Superpave Volumetric Mix Design and R35- Superpave Volumetric Design for Hot Mix Asphalt were two main sources used for mix designs. Table 3.5 shows the standard sieve sizes, maximum and minimum control points specified in standards and three different gradations chosen to conduct the test. Figure 3.3 demonstrates the three trial gradations on 0.45 power curve.

Table 3.5 Initial gradations and control points for control mix design

Sieve Size (SS)	$SS^{0.45}$	Gradation 1 % retained	Gradation 2 % retained	Gradation 3 % retained	12.5mm Superpave mixture gradation limits	
mm					Min. (%)	Max. (%)
19.5	3.81	0.0	0.0	0.0	100	
12.5	3.12	10.0	5.5	3.4	90	100
9.5	2.75	8.5	8.1	7.0		90
4.75	2.02	22.0	19.0	18.0		
2.36	1.47	21.0	21.0	19.0	28	58
1.18	1.08	20.0	19.0	18.0		
0.6	0.79	8.0	11.0	15.3		
0.3	0.58	4.0	6.0	7.3		
0.15	0.43	2.0	3.4	4.7		
0.075	0.31	1.3	3.0	3.6	2	10
0	0.00	3.2	4.0	4.0		

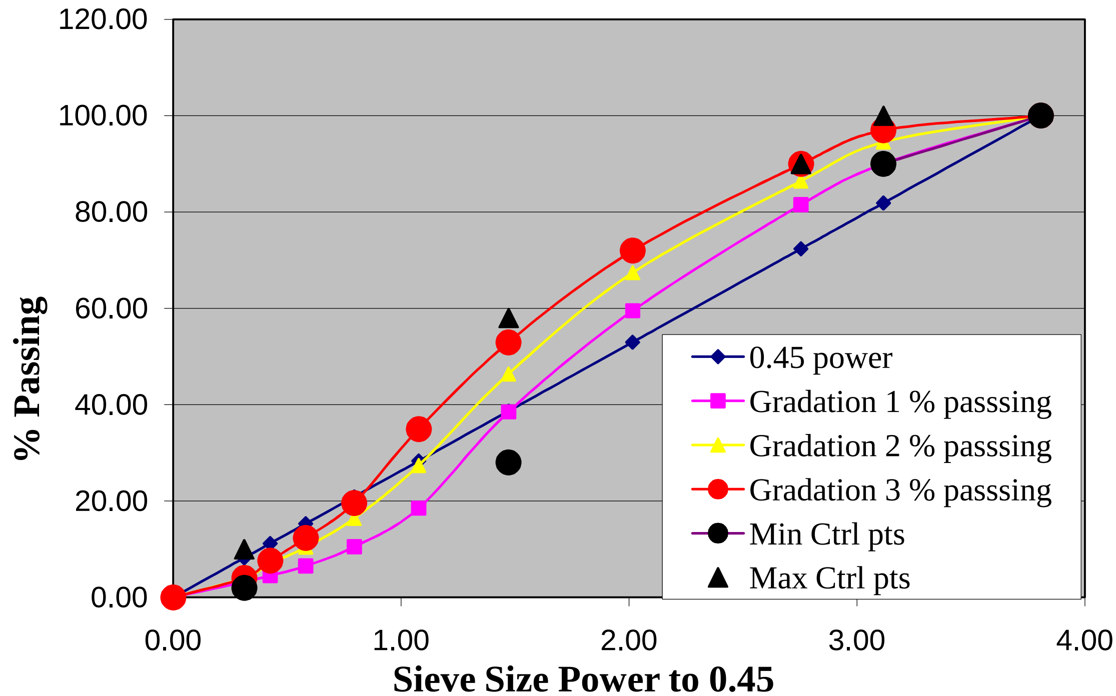

Figure 3.3 Superpave control mix design gradations on 0.45 power graph

After determining three aggregate gradations, the next step was to choose one binder content and it was taken as 5% by using the previous experience with aggregates. At the end of the first step of Superpave mix design, third gradation with 5.1 % estimated optimum binder content was the closest one to the Superpave mix design requirements. During the second step of the design process, specimens with third gradation and having optimum, optimum +/-0.5% and optimum +1.0% binder contents were prepared and analyzed. The results of the analysis include the change in theoretical maximum specific gravity (G_{mm}), bulk specific gravity (G_{mb}) and air void content (V_a). Figures 3.4 through 3.7 show the results of values obtained during the first step of control mix design.

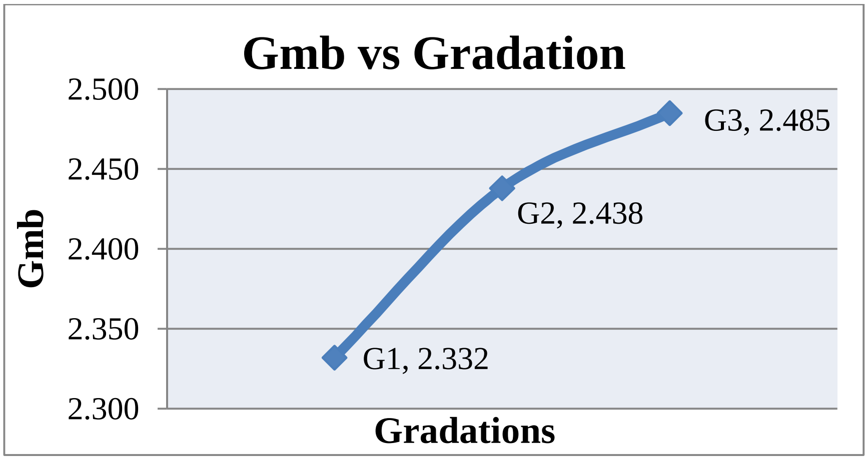

Figure 3.4 G_{mb} values for 3 gradations and 1 binder content

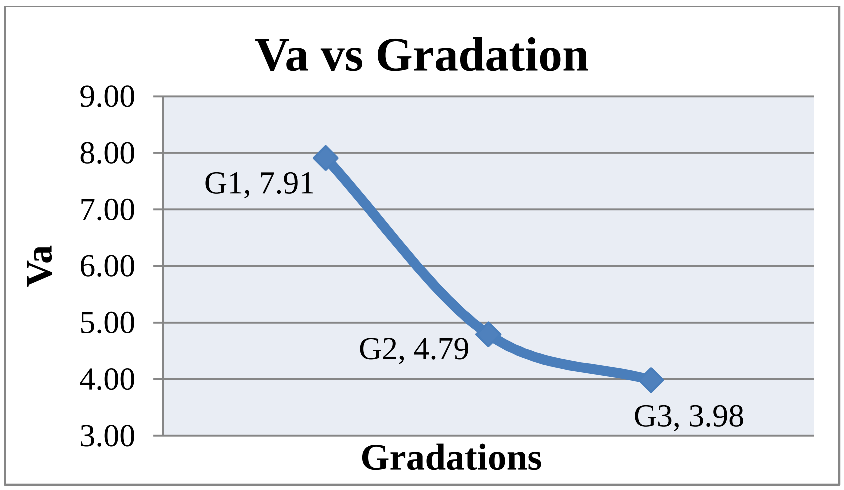

Figure 3.5 V_a values for 3 gradations and 1 binder content

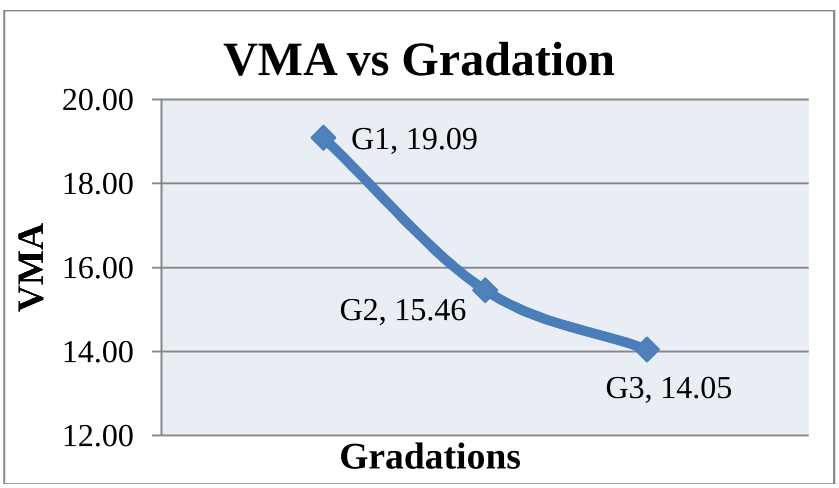

Figure 3.6 VMA values for 3 gradations and 1 binder content

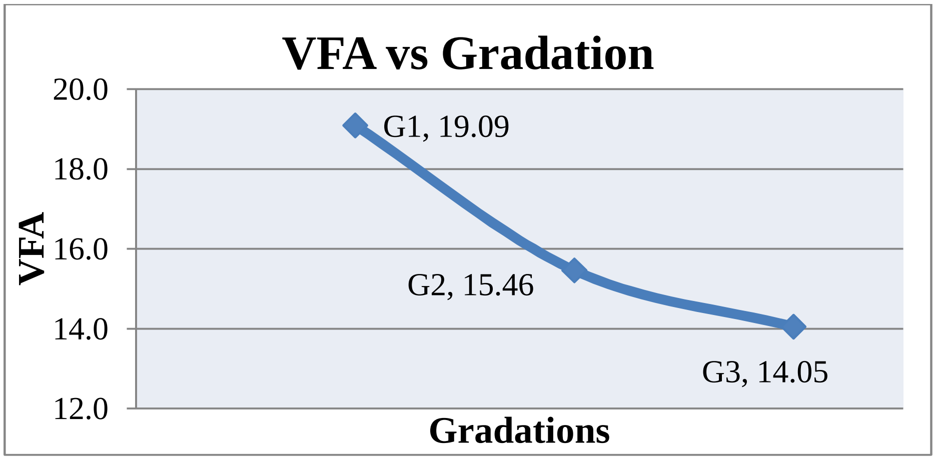

Figure 3.7 VFA values for 3 gradations and 1 binder content

Equivalent single axle load (ESAL) for the design life was assumed a value in between $3x10^6$ to $30x10^6$. According to this value, minimum voids in mineral aggregate (VMA), target voids filled with asphalt binder (VFA) and number of gyrations to be applied to compact the specimens to target air content (V_a) were obtained from AASHTO design tables. The design criteria and results obtained for the Superpave mix design NMAS 12.5 mm are given in the Table 3.6.

Table 3.6 Superpave design criteria for control mix and obtained results

	Design Criteria	Results
V_a target	4.00%	4.00%
VMA (min)	14.00%	14.41%
VFA target	65-75	72.28
ESAL (20 years)	$>3x10^6$ and $<30x10^6$	$>3x10^6$ and $<30x10^6$
N_{des} (gyration)	100	100

Superpave mix design criteria for other NMAS values are important to mention. It is important to note how the volumetric values change with NMAS although all other design requirements are kept the same for the research purposes. SP mix design criteria for NMAS 9.5 mm and 25 mm are also provided in the Table 3.7.

Table 3.7 Superpave mix design criteria for NMAS 9.5 and 25 mm (AASHTO R-35)

Requirements	Superpave Mix Design Criteria	
	NMAS 9.5 mm	**NMAS 25 mm**
V_a target	4.00%	4.00%
VMA (min)	15.00%	12.00%
VFA target	65-75	65-75
ESAL (20 years)	$>3x10^6$ and $<30x10^6$	$>3x10^6$ and $<30x10^6$
N_{des} (gyration)	100	100

The common point for all SP mix designs is the anticipated traffic loading. Both the aggregate and mixture volumetric properties change with amount of ESALs. It is also important to understand that the numbers of ESALs are based upon the expected traffic on the design lane over 20 - year period. The actual roadway design life is most probably different than the design lane assumptions. Table 3.8 shows the mix design calculations for all the mixes performed during the tire/pavement interaction noise study.

Table 3.8 Mix designs and basic mixture-volumetric values

	Mix Design Type				
	Superpave			**SMA**	**OGFC**
NMAS	**9.5 mm**	**12.5 mm**	**25 mm**	**12.5 mm**	**4.75 mm**
$\mathbf{G_{mm}}$	2.648	2.583	2.624	2.587	2.497
$\mathbf{G_{mb}}$	2.542	2.480	2.519	2.484	2.122
$\mathbf{G_b}$	1.023	1.023	1.023	1.023	1.023
$\mathbf{G_{se}}$	2.876	2.819	2.840	2.867	2.912
$\mathbf{G_{sb}}$	2.849	2.747	2.802	2.819	2.664
$\mathbf{P_s}$	95.24	94.80	95.37	94.00	91.00
$\mathbf{P_b}$	4.76	5.20	4.63	6.00	9.00
$\mathbf{P_{ba}}$	0.34	0.95	0.49	0.61	3.27
$\mathbf{P_{be}}$	4.44	4.30	4.16	5.43	6.02
$\mathbf{P_{200}}$	0.05	0.04	0.03	0.04	0.03
$\mathbf{P_{200}/P_{be}}$	1.13	0.93	0.72	0.74	NA
VMA	15.02	14.41	14.26	17.19	NA
VFA	73.35	72.28	71.94	76.72	NA
$\mathbf{V_a}$ **(%)**	4.00	4.00	4.00	4.00	15.02

It is important to note the parameters provided in Tables 3.6 and 3.7 are only for Superpave mix designs. AASHTO specifies the dust to binder ratio (P_{200}/P_{be}) for mix designs as 0.6-1.2 (AASHTO M-323). Moreover, VMA for SMA mix design should not be less than 17 and voids in coarse aggregate of the compacted mix (VCA_{MIX}) should be less than dry-rodded voids in coarse aggregates (VCA_{DRC}) of the coarse fraction (AASHTO R-46 and AASHTO M-325). These conditions are satisfied for SMA mix design.

Figure 3.8 demonstrates the job mix formula (JMF) for control mix design. The JMFs for other type of mix designs are provided in the Appendix A. Since all the aggregate sources were graded to each sieve size, pit number and percent values on the right hand side of the JMF are either blank or assigned as not available (NA). Furthermore, JMF were prepared according to the original virgin binder with PG 58-28. Although the specific gravities (G_b) of the binders used were so close to each other, volumetric parameters were checked by using new binder G_b. All of the values conformed to the standards.

All specimens, while applying the mix design procedures, were prepared by using gyratory compactor which was capable of recording the properties at initial, design and maximum gyrations. The volumetric properties measured on prepared specimens. The same process was performed for each mix design. Once the gradation and optimum binder content was obtained for each mix design type, the specimens were produced by using presbox shear compactor (a.k.a slab compactor). The preparation of the specimens by using slab compactor is explained under section 3.3.3.

<table>
<tr><th colspan="12">JOB MIX FORMULA</th></tr>
<tr><th colspan="12">HMA FIELD COMMUNICATION</th></tr>
<tr><td colspan="3">CONTROL SECTION
CONTROL MIX DESIGN</td><td colspan="2">JOB NO.
0.01</td><td colspan="4">PROJECT ENGINEER
Salih KOCAK</td><td colspan="3">DATE EFFECTIVE
07/21/2009</td></tr>
<tr><td colspan="3">MIXTURE TYPE
SUPERPAVE</td><td colspan="4">MIX DESIGN NO.
NMAS 12.5</td><td colspan="5">PLANT LOCATION
EAST LANSING</td></tr>
<tr><td colspan="2">ANGULARITY
47.0</td><td colspan="2">% AIR VOIDS
4.00</td><td colspan="2">VMA
14.41</td><td>VFA
72.28</td><td colspan="3">COMP.TEMP
138 C</td><td colspan="2">MIX. TEMP
149 C</td></tr>
<tr><td>Gmm
2.583</td><td colspan="2">Gmb
2.480</td><td>Gb
1.023</td><td>Gse
2.819</td><td colspan="2">Gsb
2.747</td><td colspan="2">P200/Pbe
0.93</td><td colspan="3">% AIR VOIDS
4.00</td></tr>
<tr><th colspan="4">MIX/AGG. GRADATION, %</th><th colspan="8">MIX/AGG. PROPORTION, %</th></tr>
<tr><th colspan="3">ITEM</th><th>PERCENT</th><th colspan="6">MATERIAL/PRODUCER</th><th colspan="2">PIT NO.</th></tr>
<tr><td colspan="3">ASPHALT,%</td><td>5.20%</td><td colspan="6">SPARTAN & RIETH-RILEY</td><td colspan="2">N/A</td></tr>
<tr><td colspan="3">P 1-1/2" (37.5 mm)</td><td>100.00%</td><td colspan="6">SPARTAN & RIETH-RILEY</td><td colspan="2">N/A</td></tr>
<tr><td colspan="3">P 1" (25.0 mm)</td><td>100.00%</td><td colspan="6">SPARTAN & RIETH-RILEY</td><td colspan="2">N/A</td></tr>
<tr><td colspan="3">P 3/4" (19.0 mm)</td><td>100.00%</td><td colspan="6">SPARTAN & RIETH-RILEY</td><td colspan="2">N/A</td></tr>
<tr><td colspan="3">P 1/2" (12.5 mm)</td><td>96.95%</td><td colspan="6">SPARTAN & RIETH-RILEY</td><td colspan="2">N/A</td></tr>
<tr><td colspan="3">P 3/8" (9.5 mm)</td><td>89.95%</td><td colspan="6">SPARTAN & RIETH-RILEY</td><td colspan="2">N/A</td></tr>
<tr><td colspan="3">P No. 4 (4.75 mm)</td><td>71.95%</td><td colspan="6">SPARTAN & RIETH-RILEY</td><td colspan="2">N/A</td></tr>
<tr><td colspan="3">P No. 8 (2.36 mm)</td><td>52.95%</td><td colspan="6">SPARTAN & RIETH-RILEY</td><td colspan="2">N/A</td></tr>
<tr><td colspan="3">P No. 16 (1.18 mm)</td><td>34.95%</td><td colspan="6">SPARTAN & RIETH-RILEY</td><td colspan="2">N/A</td></tr>
<tr><td colspan="3">P No. 30 (600 µm)</td><td>16.90%</td><td colspan="6">SPARTAN & RIETH-RILEY</td><td colspan="2">N/A</td></tr>
<tr><td colspan="3">P No. 50 (300 µm)</td><td>12.30%</td><td colspan="3">RECLAIMED</td><td colspan="5">NO RAP</td></tr>
<tr><td colspan="3">P No. 100 (150 µm)</td><td>7.60%</td><td colspan="3" rowspan="2">ASPHALT
BINDER</td><td colspan="5">Supplier: MTE</td></tr>
<tr><td colspan="3">P No. 200 (75 µm)</td><td>4.00%</td><td colspan="5">GRADE: PG 58-28</td></tr>
<tr><td colspan="3">CRUSHED 1 FACE</td><td>100%</td><td colspan="8">PRODUCER LOCATION: MSU-CEE-AACL</td></tr>
<tr><td colspan="3">CRUSHED 2 FACES</td><td>100%</td><td colspan="8">REGULAR TESTING</td></tr>
</table>

Figure 3.8 Job mix formula for Superpave mix design NMAS 12.5 mm (control mix)

3.3.3 Preparation of Specimens for |E*| and Laboratory Noise Testing Using TIPANOS

Specimens for both |E*| and TIPANOS testing were compacted by using slab compactor. The advantage of using slab compactor is to be able to obtain three (3) 100 mm diameter 150 mm tall cylindrical HMA replicates from a single slab. This reduced the preparation time, labor and the amount of the material wasted. Table 3.9 shows the material test matrix with corresponding air voids, aging condition and control parameter for each slab.

Table 3.9 Material notation and parameters controlled

Slab No	**Sample Code**	**Gradation (NMAS)**	**Aging Condition**	**Air Voids ***	**Control Parameter**
#1	125SA4	12.5 mm	4 hours	7.35%	Control Mixture
#2	125SA48	12.5 mm	48 hours	6.98%	Aging Performed
#3	125SA4PM	12.5 mm	4 hours	7.38%	PM** Binder
#4	125SA4CR5	12.5 mm	4 hours	7.20%	5% CRM*** Binder.
#5	125SA4CR10	12.5 mm	4 hours	6.92%	10% CRM Binder
#6	125SA4LW	12.5 mm	4 hours	7.05%	Lightweight Aggregate
#7	095SA4F	9.5 mm	4 hours	6.94%	Fine Gradation
#8	25SA4C	25.0 mm	4 hours	6.74%	Coarse Gradation
#9	0475OA4	4.75 mm	4 hours	15.87%	OGFC Mix Design
#10	0475OA4CR10	4.75 mm	4 hours	13.20%	OGFC-10%CRM Binder
#11	125SMAA4	12.5 mm	4 hours	4.90%	SMA Mix Design
#12	125SMAA4CR10	12.5 mm	4 hours	4.32%	SMA-10% CRM Binder

*Air void content is the average of three replicates for each slab, **PM- Polymer modified, ***CRM- Crumb rubber modified.

Total twelve slabs were prepared for this research. Each slab yielded three (3) 100 mm diameter, 150 mm tall replicates, which resulted in total 36 specimens. First slab is the control mixture with NMAS of 12.5 mm (125SA4 in Table 3.9). Second slab is prepared by using the same Superpave mix design however the binder was aged for 48 more hours (125SA48 in Table 3.9). Similar to the second one, the other consecutive three slabs were prepared by just altering the binder types. They include polymer modified (125SA4PM in Table 3.9), 5% and 10% crumb rubber modified binders (125SA4CR5, 125SA4CR10 in Table 3.9), respectively. The last SP-12.5 mm slab is prepared by changing the aggregate type. Instead of gravel, it includes light weight aggregates (125SA4LW in Table 3.9). Slab #7 is prepared by SP mix design with NMAS of 9.5 mm (095SA4F in Table 3.9) and slab#8 with NMAS of 25 mm (25SA4C in Table 3.9). The following two slabs are constructed according to OGFC mix design procedure with original and 10% CRM binders (0475OA4, 0475OA4CR10), respectively. The last two slabs follow the SMA mix design procedure. Slab#11 includes original binder (125SMAA4) whereas slab#12 has 10% CRM binder (125SMAA4CR10).

Figure 3.9 illustrates the schematic representation of the material matrix tested during the research.

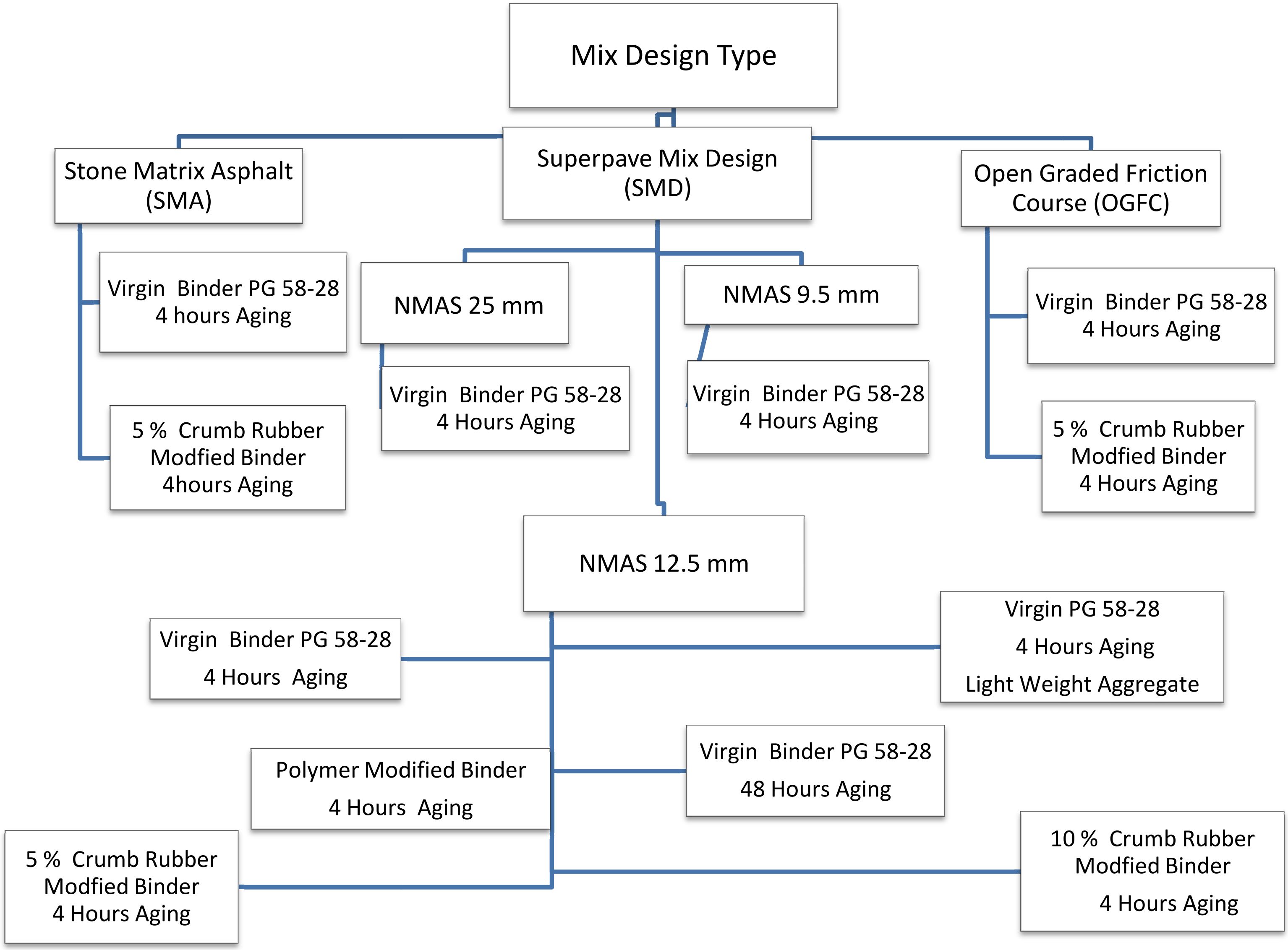

Figure 3.9 Flow chart showing the material matrix

CHAPTER 4

LABORATORY INVESTIGATIONS AND INSTRUMENTATION

Laboratory investigations included three different measurements on the specimens during and after the specimen preparation periods. They were aggregate consensus properties and HMA volumetric measurements/calculations, tire pavement interaction noise measurement using TIPANOS and dynamic modulus (|E*|) measurement by means of asphalt mixture performance tester (AMPT). Aggregate properties can be found in chapter 3 and on the JMF tables provided in the Appendix A. Table 4.1 provides the gradation and volumetric properties for the laboratory prepared specimens.

Table 4.1 Properties of the laboratory prepared specimens

Design Type	Sample Code	V_a	VMA	VFA	C_u	C_c	P_b
SP- Control	125SA4	7.35%	17.08	57.0%	14.27	1.35	5.20%
SP- Aged	125SA48	6.98%	16.75	58.3%	14.27	1.35	5.20%
SP- PM Binder	125SA4PM	7.38%	17.11	56.9%	14.27	1.35	5.20%
SP- CRM 5%	125SA4CR5	7.20%	16.95	57.5%	14.27	1.35	5.20%
SP- CRM 10%	125SA4CR10	6.92%	16.68	58.6%	14.27	1.35	5.20%
SP- 9.5 mm	095SA4F	6.94%	14.63	52.5%	17.64	1.54	4.76%
SP- 25 mm	25SA4C	6.74%	14.88	54.8%	46.28	1.38	4.63%
OGFC-Virgin Bin.	0475OA4	15.87%	27.08	42.0%	2.73	1.09	9.00%
OGFC-CRM 10%	0475OA4CR10	13.19%	24.88	47.1%	2.73	1.09	9.00%
SMA-Virgin Bind.	125SMAA4	4.90%	14.77	66.8%	29.40	8.53	6.00%
SMA-CRM 10%	125SMAA4CR10	4.32%	14.25	69.6%	29.40	8.53	6.00%

4.1 TIRE PAVEMENT INTERACTION NOISE MEASUREMENTS

To simulate the tire/pavement interaction noise generation and the measurement on laboratory size specimens, tire/pavement noise simulator (TIPANOS) was developed (Figure 4.2). The simulator is explained in detail in the subsequent parts of the chapter.Tire pavement interaction noise measurement was the first test performed by using non destructive laboratory measurement device TIPANOS. Tests were performed at room temperature. Each design type had three replicates and the resulting sound pressure was recorded as the average of all three measurements. Each specimen was tested three times for repeatability concerns and satisfactory results were obtained. Coefficient of variation (COV) of repeatability test was around 4.2% overall. The results given in linear SPL scale were then converted into A-weighted scale. Table 4.2 demonstrates the averaged and A-scale converted SPL.

Table 4.2 SPL at 250 Hz and 23^{O}C

Sample Code		125SA4	125SA48	125SA4PM	125SA4CR5
SPL	**dB(A)**	91.4	91.8	89.8	90.7
Sample Code		125SA4CR10	095SA4F	125SA4LW	25SA4C
SPL	**dB(A)**	89.1	89.8	92.0	94.0
Sample Code		0475OA4	0475OA4CR10	125SMAA4	125SMAA4CR10
SPL	**dB(A)**	86.7	85.2	92.9	90.0

The peak SPL at interstate roads is experienced at around 1000 Hz. (Sandberg 2003). However, since TIPANOS tire and specimen's sizes are smaller, the peak SPL in laboratory conditions was acquired at 250 Hz. Figure 4.1 shows the SPL at 1/3 octave frequency band.

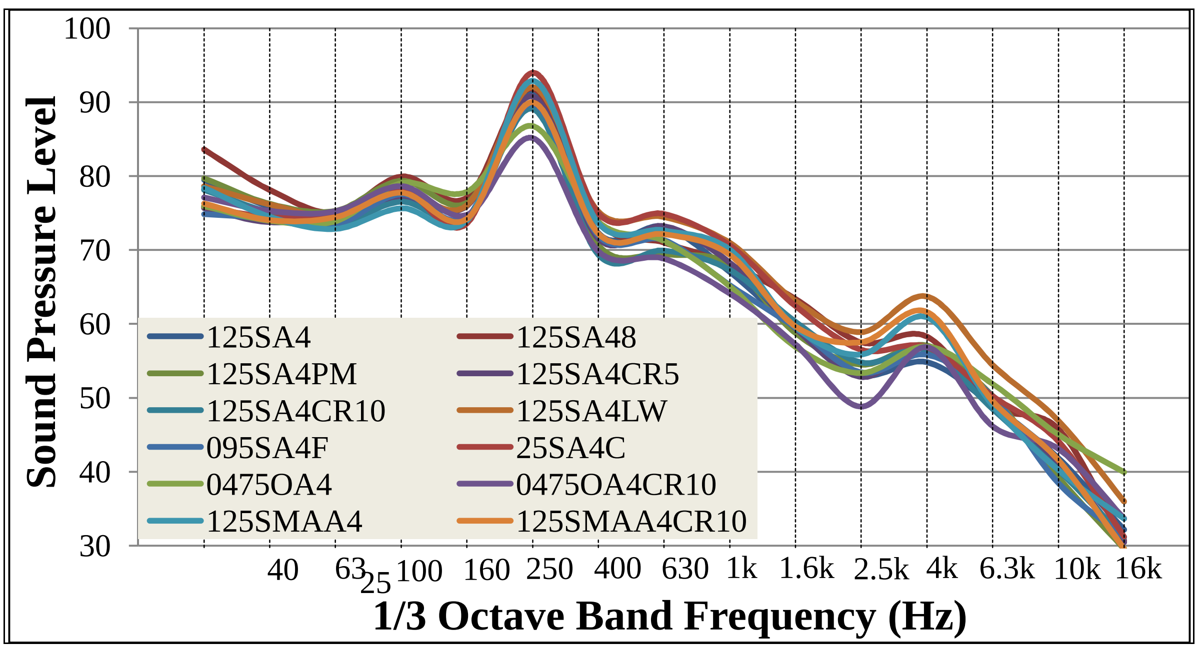

Figure 4.1 SPL versus 1/3 octave frequency of the specimens.

Moreover, the speed of the TIPANOS can be calculated at its highest rotation. For this calculation, a tachometer was used to record the rotational speed of the tire. It was measured as 810 revolutions per minute (rpm). Equations 4.1 through 4.5 show the computation steps for the speed of TIPANOS.

$$w = 810\, rpm \qquad 4.1$$

$$c = 2 \times \pi \times r = 2 \times \pi \times 2 = 4\,\pi \qquad 4.2$$

$$x = 810 \times 4\,\pi \approx 10179\, \frac{inch}{minute} \qquad 4.3$$

$$X = 60\, min. \times 10179 = 610740\, \frac{inch}{hour} \qquad 4.4$$

$$X = 610740 \times \frac{1}{63360} \approx 9.64\, \frac{mile}{hour} \qquad 4.5$$

4.1.1 Tire Pavement Noise Measurement Simulator (TIPANOS)

The set-up consists of a treaded tire rotating over the cored specimens. Dimensions of the specimens (100 mm diameter and 150 mm tall) used in TIPANOS have been chosen intentionally so that they can be used in dynamic modulus (|E*|) tests as well. Since the sound measurement test performed by TIPANOS is non-destructive, the same samples can be used in dynamic modulus tests conveniently by eliminating the cost, time and effort necessary for preparation of extra samples. As shown in the Figure 4.2, TIPANOS has two specimen holders to maintain the cored and sawed cylindrical specimens in place. They have 101 mm interior diameter and 15 mm lip thickness. To be able to simulate the sound generated on the roadways as closely as possible, a small scale threaded tire was used. The other two unthreaded tires support the specimen from bending at the bottom. The diameter of the tires is 100 mm and the width is 50 mm. Treaded tire has 2.5 mm width and 2.5 mm depth grooves on the surface and they are spaced at 6 mm. Both specimen holders and tires are kept in place by means of metal rods and these rods are supported by other metal arms attached to the main frame. Rotation is provided by an electric motor connected to the main frame via belt. Distance between motor and the pulley is 250 mm. The speed of the rotation can be easily adjusted to any level by using the tunable switch available on the motor. All system sits on a metal block having dimensions 50 cm length, 50 cm width and 5 cm thickness. To record the real time sound generated between tire and the specimen, an intensity microphone, dynamic signal analyzer and a computer are utilized. Microphone is pointed to the interface between threaded tire and the specimen from 250 mm distance and hold in place with a metal bar. Dynamic signal analyzer, which is connected to the microphone in one end and to the computational station on the other end, is capable of measuring, analyzing and recording the sound pressure level (SPL) values to the computer between 0 and 20000 Hz.

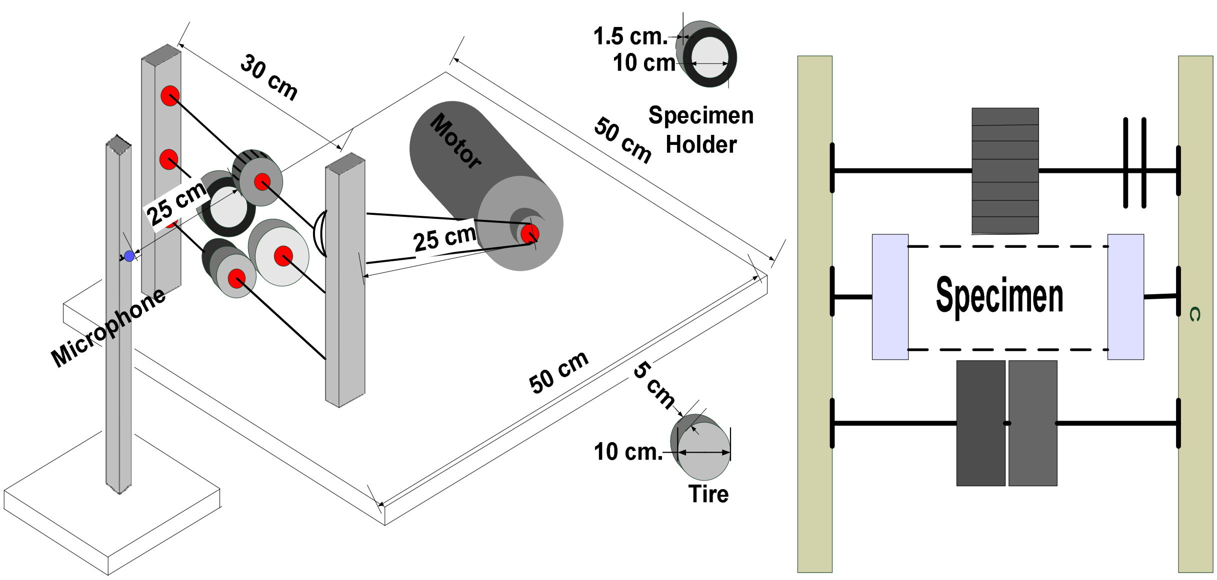

(a) (b)

Figure 4.2 (a) TIPANOS set-up, (b) TIPANOS plan view

4.1.2 Dynamic Signal Analyzer (DP-QUATTRO)

Data physics Quattro Dynamic Signal Analyzer (simply QUATTRO) hardware and SignalCalc Ace 240 software were used for recording and analyzing the real time sound data. Both the analyzer and the software are commercially available. Data acquisition system saves the data to a computer via USB connection. The capability of the software to record sound pressure level data is determined by the capability of microphone. After recording is performed, the data can be manipulated by converting other weighting scales. Traffic noise is generally analyzed and published according to A-weighing scheme. The A-scale converted data for all recorded frequencies can be reached in the Appendix B. Figure 4.3 illustrates the QUAATRO data acquisition system.

Figure 4.3 QUATTRO data acquisition hardware (www.dataphysics.com)

4.1.3 Free Field Microphone (G.R.A.S- Type 46AE)

GRAS Type 46 AE is the combination of ½-inch pre-polarized free field microphone 40 AE and the same size constant current power type 26CA. It is highly sensitive to sound pressure and can cover a frequency range of 3.15 Hz to 20000 Hz with its large dynamic range. As a free field microphone system, it can measure sound pressure and compensate for the influence of its presence in the sound field. One of the most important properties of the free field microphones is the need to point them towards the sound source. The incidence to the source other than 0 degree angle can affect the results, the effect is drastic at higher frequencies. Moreover, the presence of the microphone in the sound field has a small impact at low frequencies, however the effects of reflections and diffractions at higher frequencies can cause and increase in sound pressure level measurements. The connection between QUATTRO and amplifier is provided by using BNC co-axial connector. Figure 4.4 shows GRAS type 46 AE free field microphone unit.

Figure 4.4 GRAS type 40 AE free field microphone and CCP 26 CA preamplifier combination (http://www.gras.dk/)

4.1.4 Sound Calibrator (LD-CAL200)

Larson Davis CAL 200 (Figure 4.5) is used as a sound calibrator for ½-inch free field microphone. It has a calibration frequency of 1000 Hz and it provides an output level of 94 and 114 dB with National Institute of Standards and Technology (NIST). Figure 4.5 demonstrates the sound calibrator.

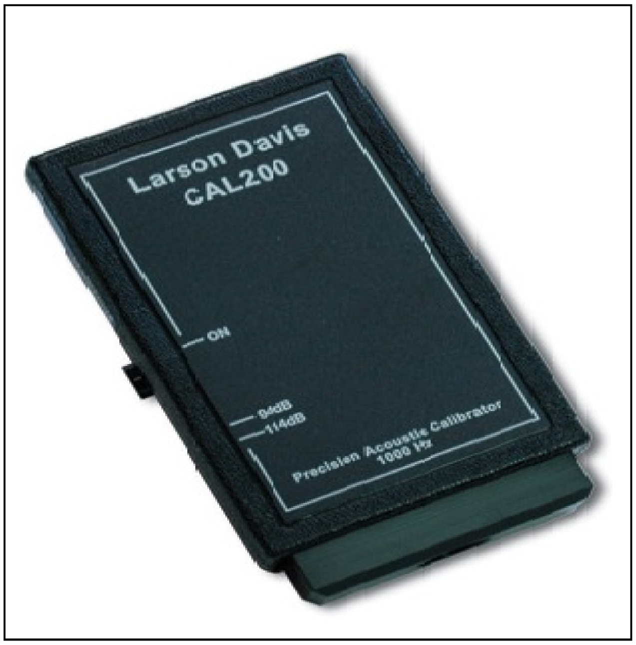

Figure 4.5 Larson Davis L 200 portable sound calibrator (www.larsondavis.com)

4.2 DYNAMIC MODULUS MEASUREMENTS

Dynamic modulus measurement was one of the most important parts of this study. Since the noise measurements are time consuming and expensive compared to dynamic modulus (|E*|) measurements, any relation between |E*| and the SPL could help the researchers and the asphalt producers understand the noise level that specific pavement causes.

Since noise measurement by using TIPANOS was non-destructive, the same specimens were tested in AMPT to obtain the |E*| master curve. The specimens were tested at 4, 21, 37 and 54 ^{o}C temperatures and 0.1, 0.5, 1, 5, 10 and 25 Hz frequencies. After the |E*| and phase angle (δ) values were averaged for all three replicates, |E*| master curves were constructed. Sigmoidal and Gaussian curves were fitted for |E*| and phase angle, respectively. Phase angle fit was performed by using commercially available curve fitting software “Curve Expert”. AASHTO TP 62 – Determining Dynamic Modulus of Hot Mix Asphalt (HMA) was the applied standard for |E*| measurements. It should be recalled that complex modulus (*E**) is actually a complex number with real and imaginary parts (i.e., $E^*=E'+E''i$). Real part ($E'=|E^*|cos\delta$) is known as storage or elastic modulus, whereas the imaginary part ($E'' =|E^*|sin\delta$) is called as loss or viscous modulus. The magnitude of complex modulus is defined as dynamic modulus and denoted by |E*|. The phase angle "δ" in degrees is also measured for each and every frequency and temperature levels. Since the asphalt mixtures exhibit linear visco-elastic behavior (at small deformations), when the stress is applied to the specimen, strain will be obtained after some time lag. This lag between applied stress and resultant strain is the phase angle and it ranges from 0 to 90 degrees. When phase angle is 0°, the material shows only elastic behavior. As δ increases, the viscous behavior of the material increases as well and when δ = 90°, the material behaves purely viscous. Table 4.3 shows the averaging process for sample 125SA4CR5 replicates.

Table 4.3 Averaging dynamic modulus and phase angles for sample 125SA4CR5

			Measured E* (MPa)							
			Replicate #1		*Replicate #2*		*Replicate #3*			
Specimen Code	**Temp (°C)**	**f (Hz)**	**|E*| (MPa)**	**δ**	**|E*| (MPa)**	**δ**	**|E*| (MPa)**	**δ**	**Avg. |E*|**	**Avg. δ**
125SA4CR5	4.0	25	11614	10.89	12486	11.09	13010	9.83	12370	10.6
125SA4CR5	4.0	10	10481	12.01	11137	12.12	11684	11.22	11101	11.8
125SA4CR5	4.0	5	9593	13.02	10083	13.04	10635	12.18	10104	12.7
125SA4CR5	4.0	1	7488	15.68	7831	15.74	8300	14.83	7873	15.4
125SA4CR5	4.0	0.5	6546	17.13	6876	17.12	7304	16.33	6909	16.9
125SA4CR5	4.0	0.1	4451	21.68	4837	21.49	5023	20.58	4770	21.3
125SA4CR5	21.0	25	4965	22.89	5286	23.67	5496	22.62	5249	23.1
125SA4CR5	21.0	10	3919	25.37	4162	26.15	4364	25.1	4148	25.5
125SA4CR5	21.0	5	3243	27.24	3413	27.97	3625	26.88	3427	27.4
125SA4CR5	21.0	1	1975	31.81	2036	32.44	2214	31.3	2075	31.9
125SA4CR5	21.0	0.5	1572	33.26	1601	33.59	1775	32.53	1649	33.1
125SA4CR5	21.0	0.1	863.3	36.68	863.7	36.47	983.5	35.81	904	36.3
125SA4CR5	37.0	25	1560	37.13	1555	36.68	1713	36.37	1609	36.7
125SA4CR5	37.0	10	1087	38.6	1087	37.91	1215	37.53	1130	38.0
125SA4CR5	37.0	5	819.8	39.04	817.6	38.34	920.4	37.92	853	38.4
125SA4CR5	37.0	1	402.5	39.65	402.5	39.03	464.5	38.41	423	39.0
125SA4CR5	37.0	0.5	301.4	38.7	299.5	38.12	347.7	37.41	316	38.1
125SA4CR5	37.0	0.1	151.9	36.54	150.3	36.28	175.2	35.51	159	36.1
125SA4CR5	54.0	25	442.2	38.82	412.7	39.16	409.7	38.24	422	38.7
125SA4CR5	54.0	10	288.9	37.47	271.6	37.77	267.9	37.03	276	37.4
125SA4CR5	54.0	5	211.1	35.85	196.1	36.35	196.9	35.53	201	35.9
125SA4CR5	54.0	1	106	32.5	97.9	32.97	98.2	32.1	101	32.5
125SA4CR5	54.0	0.5	83.7	30.44	77.9	30.85	80.3	30.08	81	30.5
125SA4CR5	54.0	0.1	51.9	26.71	38.6	25.29	51.1	26.65	47	26.2

In order to obtain quality data, data quality indicators (DQI) were maintained in the limits (AASHTO PP-62). Only high quality data is used in the calculations. Load standard error, deformation standard error, deformation uniformity and phase uniformity were the parameters checked each and every temperature-frequency combinations. Table 4.4 shows the basic calculations to obtain the master curve for sample 125SA4CR5.

Table 4.4 Master curve construction for sample 125SA4CR5

T (C)	f (Hz)	Avg. |E*| (MPa)	Avg. δ	log(aT)	f_R (Hz)	Log f_R (Hz)	Phase Angle Fit	Sigmoid Fit, |E*| MPa	$Error^2$
4.0	25	12370	10.6	2.10	3.2E+03	3.5E+00	1.1E+01	12187	4.1903E-05
4.0	10	11101	11.8	2.10	1.3E+03	3.1E+00	1.1E+01	11022	9.497E-06
4.0	5	10104	12.7	2.10	6.3E+02	2.8E+00	1.2E+01	10096	1.1641E-07
4.0	1	7873	15.4	2.10	1.3E+02	2.1E+00	1.6E+01	7868	8.1833E-08
4.0	0.5	6909	16.9	2.10	6.3E+01	1.8E+00	1.8E+01	6912	5.2095E-08
4.0	0.1	4770	21.3	2.10	1.3E+01	1.1E+00	2.3E+01	4828	2.7369E-05
21.0	25	5249	23.1	-0.12	1.9E+01	1.3E+00	2.2E+01	5333	4.7154E-05
21.0	10	4148	25.5	-0.12	7.6E+00	8.8E-01	2.5E+01	4236	8.1581E-05
21.0	5	3427	27.4	-0.12	3.8E+00	5.8E-01	2.7E+01	3490	6.2791E-05
21.0	1	2075	31.9	-0.12	7.6E-01	-1.2E-01	3.3E+01	2088	7.355E-06
21.0	0.5	1649	33.1	-0.12	3.8E-01	-4.2E-01	3.5E+01	1630	2.6236E-05
21.0	0.1	904	36.3	-0.12	7.6E-02	-1.1E+00	3.7E+01	871	0.00025502
37.0	25	1609	36.7	-1.85	3.6E-01	-4.5E-01	3.5E+01	1591	2.565E-05
37.0	10	1130	38.0	-1.85	1.4E-01	-8.5E-01	3.7E+01	1120	1.3096E-05
37.0	5	853	38.4	-1.85	7.1E-02	-1.1E+00	3.8E+01	848	6.4792E-06
37.0	1	423	39.0	-1.85	1.4E-02	-1.8E+00	3.8E+01	430	4.9656E-05
37.0	0.5	316	38.1	-1.85	7.1E-03	-2.1E+00	3.6E+01	319	1.5752E-05
37.0	0.1	159	36.1	-1.85	1.4E-03	-2.8E+00	3.1E+01	161	2.2402E-05
54.0	25	422	38.7	-3.30	1.3E-02	-1.9E+00	3.7E+01	408	0.00020199
54.0	10	276	37.4	-3.30	5.0E-03	-2.3E+00	3.6E+01	275	3.466E-06
54.0	5	201	35.9	-3.30	2.5E-03	-2.6E+00	3.3E+01	204	4.4047E-05
54.0	1	101	32.5	-3.30	5.0E-04	-3.3E+00	2.4E+01	105	0.00040226
54.0	0.5	81	30.5	-3.30	2.5E-04	-3.6E+00	1.9E+01	81	7.2687E-08
54.0	0.1	47	26.2	-3.30	5.0E-05	-4.3E+00	1.5E+00	46	0.0001827
								Error sum	**0.00152672**

Figure 4. 6 and Figure 4.7 show the master curve for dynamic modulus and Gaussian fitting for phase angle after the data in Table 4.4 is analyzed and studied.

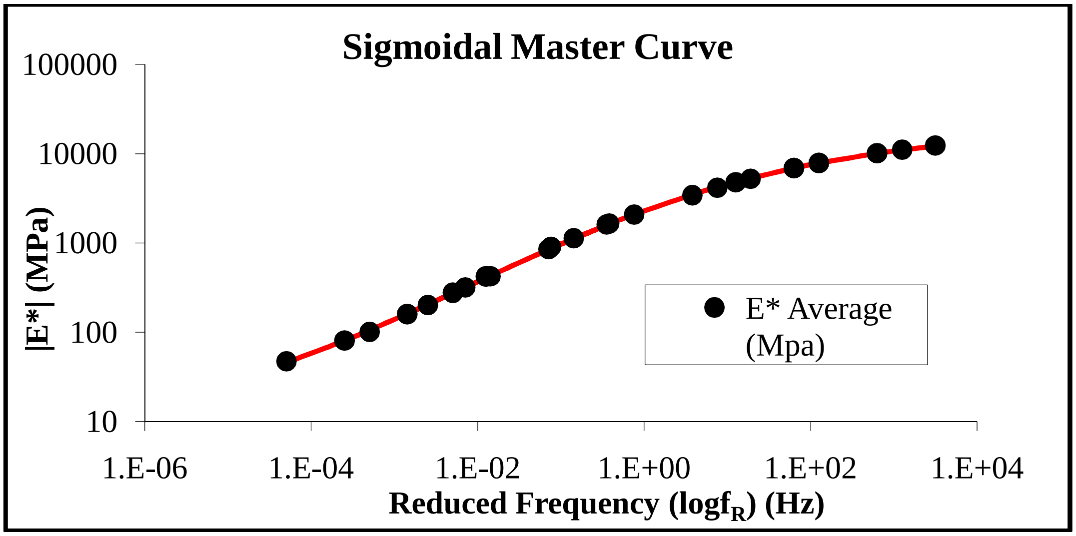

Figure 4.6 Sigmoidal master curve for sample 125SA4CR5

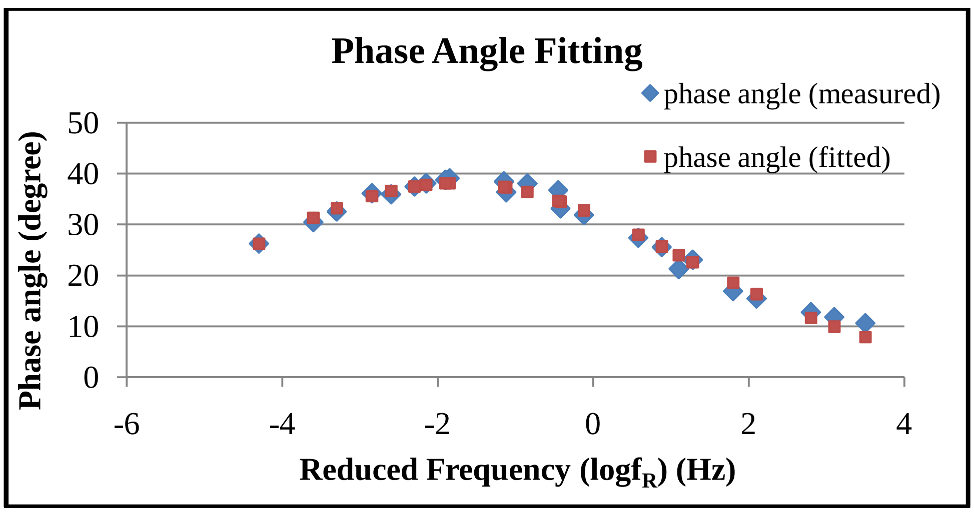

Figure 4.7 Phase angle fitting for sample 125SA4CR5

Master curve for |E*| is constructed by using the data provided in Table 4.4. AASHTO PP 61 - Developing Dynamic Modulus master curves for Hot Mix Asphalt (HMA) Using the Asphalt Mixture Performance Tester (AMPT) and AASHTO PP 62- Developing Dynamic Modulus master curves for Hot Mix Asphalt (HMA) were the two standards used to construct the master curves for all samples. Equations 4.6 and 4.7 demonstrate the formulations for calculations used during construction of master curves.

$$\log\left(a(T)\right) = a_1 T^2 + a_2 T + a_3 \qquad 4.6$$

$$\log(|E^*|) = \delta + \frac{\alpha}{1+e^{\beta+\gamma\left(\log f_R\right)}} \qquad 4.7$$

where;

a_1, a_2, a_3 are the shift coefficient factors,

α,β, γ, δ are sigmoid coefficients,

f_R is reduced frequency given in Table 4.3

The values of the shift and sigmoid coefficients are provided in Table 4.5. These coefficients were obtained by using the solver option available in excel spread sheets.

Table 4.5 Shift and sigmoid coefficients for sample 125SA4CR5

Shift Factor Coefficients	a_1	a_2	a_3	T_{ref} (C)	a_T at T_{ref}
	6.85E-04	-1.48E-01	2.68E+00	20.0	2.35E-06
Sigmoid Coefficients	α	β	γ	δ	
	3.55	1.01	0.49	0.76	

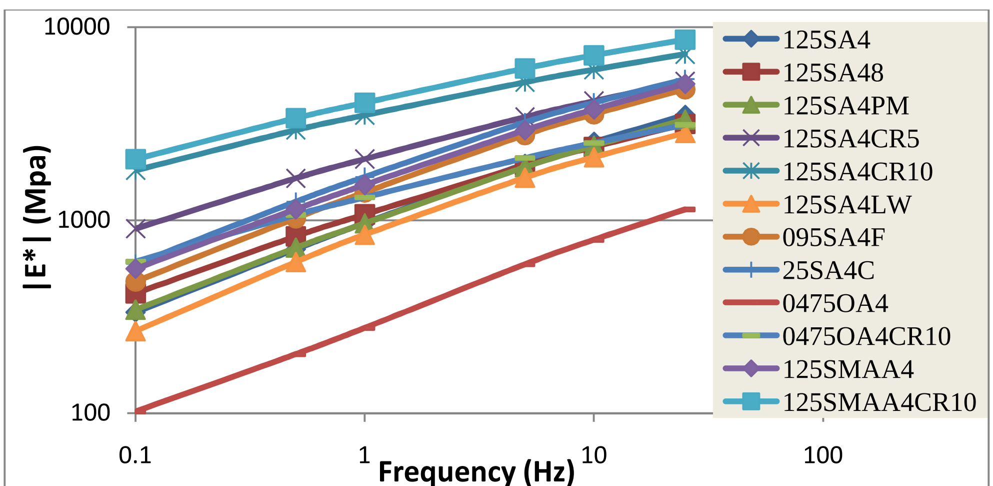

Figure 4.8 |E*| versus frequency for all samples at 21 ^{O}C

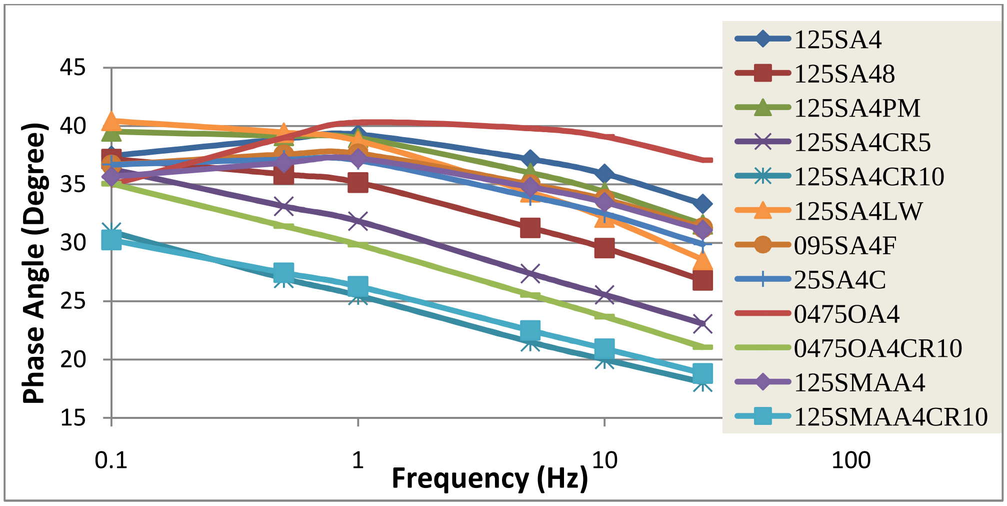

Figure 4.9 Phase angle versus frequency for all samples at 21^{O}C

Figure 4.8 and 4.9 illustrate |E*| and δ versus frequency change for all the samples at 21^{O}C, respectively.

4.2.1 Asphalt Mixture Performance Tester (IPC-AMPT)

Dynamic modulus tests were performed by using asphalt mixture performance tester (AMPT) (previously known as Simple Performance Tester (SPT)). AMPT was developed after the adaptation of Superpave mix design process almost two decades ago. First studies started in 1996 in University of Maryland at College Park (UMCP). Three years later National Cooperative Highway Research Program (NCHRP) task C took the effort under project 9-19 “Superpave Support and Performance Models Management” (NCHRP 2002). The definition of the simple performance test is described in NCHRP (2002) report as follows:

“A test method(s) that accurately and reliable measures a mixture response characteristics or parameter that is highly correlated to the occurrence of pavement distress (e.g., cracking and rutting) over a diverse range of traffic and climatic condition.”

Being one of the oldest triaxial compression tests, dynamic modulus test includes the application of haversine compressive stress to cylindrical test specimens in confined or unconfined condition. The relationship between stress and strain of a linear viscoelastic material under continuously applied sinusoidal loading is defined by a complex number which is called as complex modulus and denote as E*.

In the NCHRP project 9-29 phase 2, the SPT was constructed having the properties investigated and published in project 9-19. At the end of the research, small bottom loading, servo-hydraulic equipment with testing chamber serving both as an environmental chamber and confining pressure cell was constructed. Today's IPC AMPT uses circulating conditioned air through the test chamber to maintain the desired temperature. Figure 4.10 demonstrates the IPC's AMPT.

Figure 4.10 IPC Global AMPT

4.2.2 Environmental Chamber

Since the dynamic modulus measurements were performed at 4 different temperatures, Russell environmental chamber was used to control the temperature of the samples. Specimens were conditioned in the environmental chamber according to AASHTO specifications.

CHAPTER 5

DATA ANALYSIS

5.1 CORRELATION OF INDIVIDUAL MATERIAL CHARACTERISTICS AND SOUND PRESSURE LEVEL (SPL)

Aggregates and binder are the two main ingredients in asphalt pavements. Although the behavior of aggregates is well established, the behavior of the binders is very complex and has not been completely discovered yet. The same complexity of asphalt pavements is valid for their sound absorption capacities as well. The investigation of the contribution of each component to the noise level is crucial to understand and manipulate the sound absorption of pavements. The effect of individual material characteristics on sound pressure level was studied throughout the chapter. The analyses include the mutual correlations between SPL and linear visco-elastic parameters, mixture volumetric properties and aggregate gradations of HMA specimens.

5.1.1 Relation between Linear Visco-Elastic Parameters of Asphalt and SPL

Asphalt mixtures have complex mechanical behavior which changes with temperature and rate of loading. This behavior can be characterized in the linear visco-elastic domain by different dynamic material functions such as dynamic (complex) modulus and phase angle. New mechanistic- empirical approach for asphalt pavement design and analysis makes the use of complex modulus test data essential. Any relation between linear visco-elastic parameters and SPL would simplify the noise studies by saving time, budget and effort since SPL measurements of the pavements are more complex and expensive and time consuming compared to dynamic modulus test.

In order to investigate the relation between linear visco-elastic parameters and SPL, novel laboratory tire pavement noise measurement system (TIPANOS) was constructed. TIPANOS focuses on the noise due to asphalt material characteristics by overshadowing the impact of surface texture.

Dynamic modulus test was run at 4, 21, 37 and 54^{o}C with 25, 10, 5, 1, 0.5and 0.1 hertz (Hz) frequencies at each temperature level. The correlations for each combination have been studied for a trend and they can be reached in the Appendix C. However, the relation between linear visco-elastic parameters and SPL is presented at 23^{0}C and 212 Hz which are the temperature and frequency of the TIPANOS measurements according to the load impulse approach. It is important to calculate the frequency of impact when a point on the tire makes the contact with the pavement surface. Since the frequency that pavement experience is important to compute the dynamic modulus and phase angle, the equation 5.6 shows the calculation of the impact frequency on pavement. The revolution of TIPANOS is obtained by using a digital hand tachometer. At the highest speed, the reading was 810 revolutions per meter (rpm). Moreover, the contact length between the tire and the asphalt specimen surface was measured around 10 mm. As explained in the chapter 4, the diameter of the tire is 100 mm (with r =0.05m.). The following computations show how to calculate the frequency at which TIPANOS runs at its maximum speed.

$$\Delta x = \Delta t \times v \tag{5.1}$$

$$v = w \times r \tag{5.2}$$

$$w = 810 \frac{revolutions}{minute} \times (2\pi \ / \ revolution)/(60 \ seconds) \tag{5.3}$$

$$w \approx 84.82 \ \ radians/seconds \tag{5.4}$$

$$\Delta t = \Delta x/(w \times r) = (10\ )/(84.82 \times 50) = \ 0.0023 \ seconds \ (sec) \tag{5.5}$$

$$f = 1/(2 \times \Delta t) = 1/(2 \times 0.0023) \approx 212\ Hz \qquad 5.6$$

where;

r = radius of the tire (mm)

w= angular velocity (rpm)

Δx= contact length of tire and HMA specimen (mm)

Δt= contact time (sec)

f= frequency (Hz), calculated by diving 2 Δt since it is impulse frequency.

Table 5.1 summarizes the fundamental linear visco-elastic properties of the each HMA specimen at 212 Hz frequency at 23^{O}C as well as the sound pressure level (SPL) at 250 Hz and at the same temperature.

Table 5.1 Specimens linear visco-elastic properties at 212 Hz and 23^{O}C

Sample Code	**|E*|**	**δ**	**sin δ**	**|E*| / sin δ**	**E'**	**E"**	**SPL**
	MPa	Degree		MPa	MPa	MPa	dB(A)
125SA4	5949.5	23.85	0.404	14715.1	5441.6	2405.5	91.4
125SA48	6096.5	21.68	0.369	16501.4	5665.2	2252.4	91.8
125SA4PM	5466.2	25.32	0.428	12779.3	4940.9	2338.1	89.8
125SA4CR5	7456.4	17.27	0.297	25113.8	7120.2	2213.8	90.7
125SA4CR10	9523.3	13.92	0.241	39581.4	9243.6	2291.3	89.1
095SA4F	7816.2	23.95	0.406	19253.3	7143.2	3173.1	89.8
25SA4C	8012.7	23.78	0.403	19869.4	7332.3	3231.3	94.0
0475OA4	2056.3	30.22	0.503	4085.0	1776.8	1035.1	86.7
0475OA4CR10	4306.2	17.03	0.293	14700.3	4117.3	1261.4	85.2
125SMAA4	8386.6	23.47	0.398	21054.2	7692.5	3340.6	92.9
125SMAA4CR10	11389.0	14.76	0.255	44693.0	11013.0	2902.3	90.0

In the Figure 5.1, resultant sigmoidal curves for frequency-temperature combinations are shown for all asphalt samples tested.

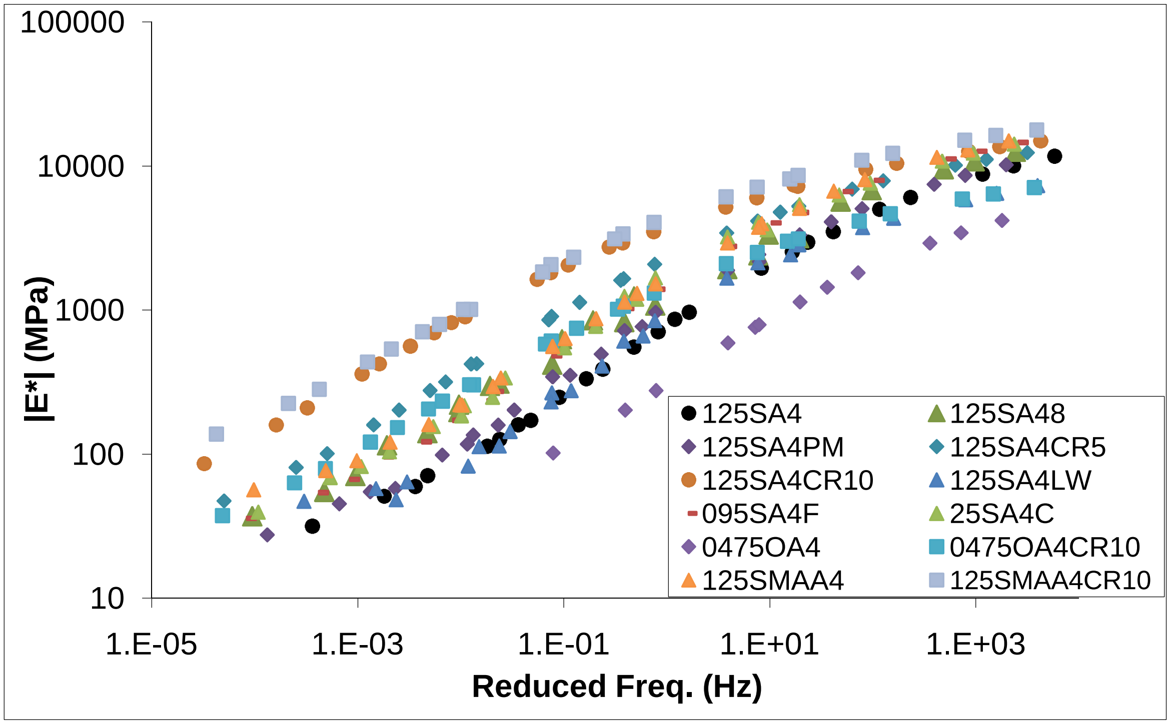

Figure 5.1 |E*| versus reduced frequency curves for specimens

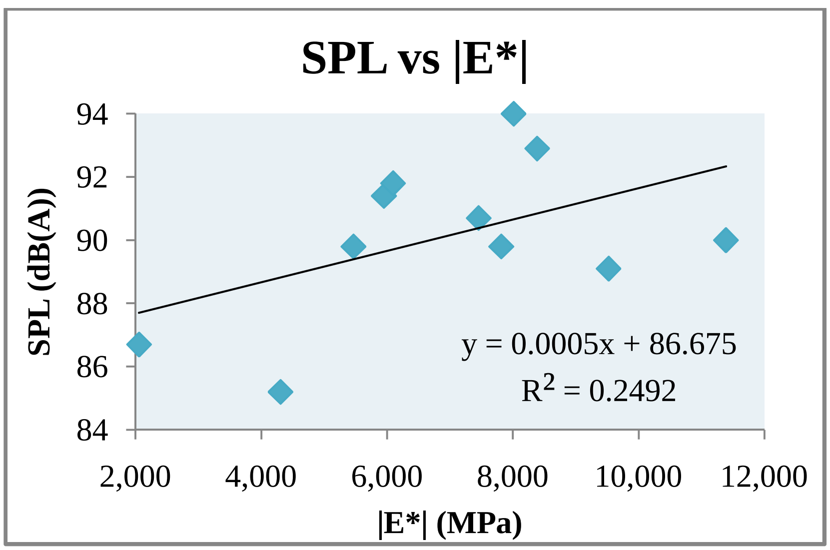

Figure 5.2 Change in SPL with change in |E*|

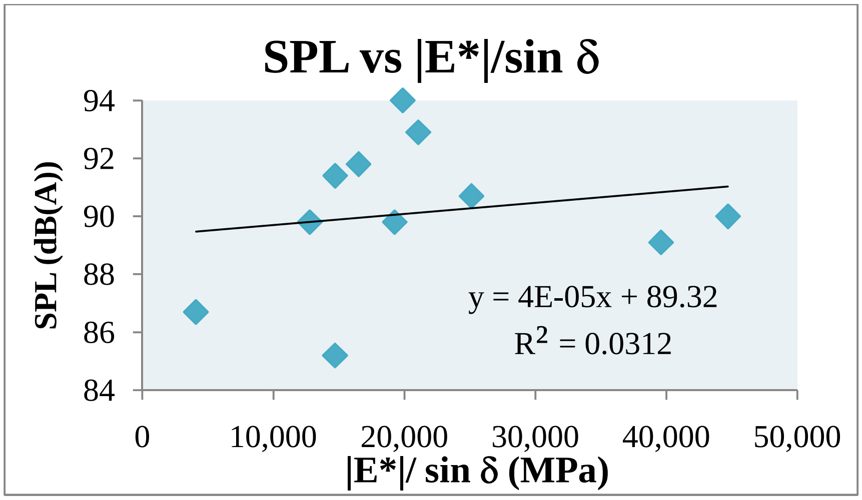

Figure 5.3 Change in SPL with change in |E*|/sin δ

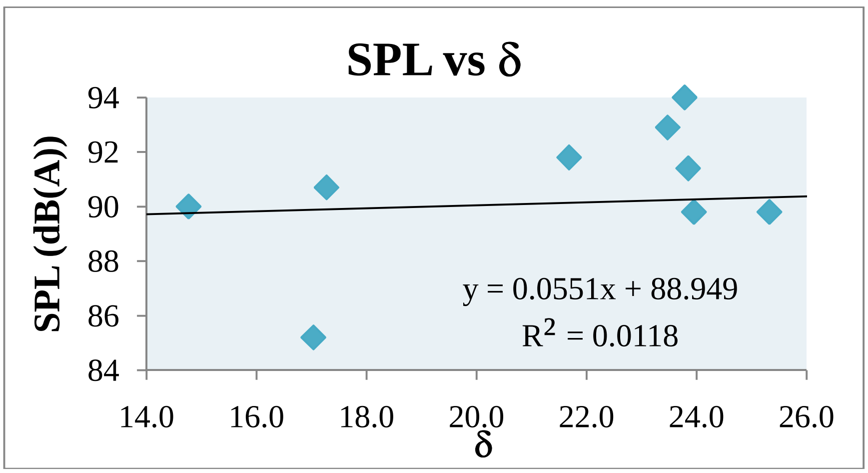

Figure 5.4 Change in SPL with change in δ

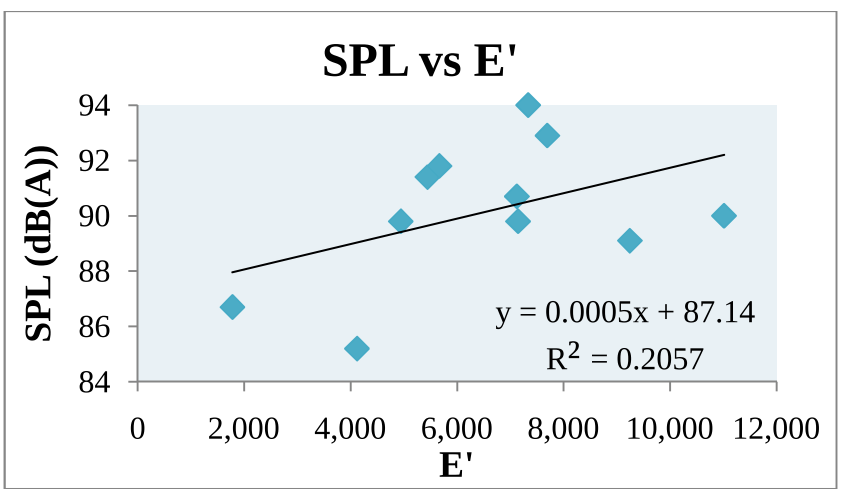

Figure 5.5 Change in SPL with change in E’

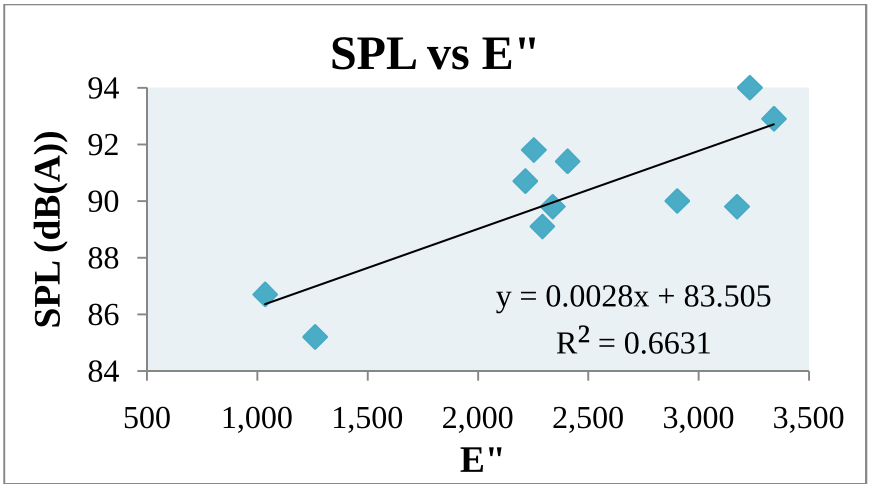

Figure 5.6 Change in SPL with change in E”

The correlations between SPL and linear visco-elastic parameters at 212 Hz and 23^{o}C are shown on the Figures 5.2 through 5.6. Figure 5.2 demonstrates the relation between SPL and dynamic modulus |E*|. Positive correlation between the variables with R^2=0.2492 is achieved. However, it should be observed that the relation becomes very weak if the lowest two values are ignored. Hence, it can be concluded that the correlation between |E*| and SPL is almost negligible. The same rationale applies for |E*|/sin δ, sin δ and E’ versus SPL relations where the relation is very weak. The last correlation for linear visco-elastic parameters is performed between SPL and E”. As explained and formulated in chapter 4, E” is the viscous, or loss, modulus. The relation between E” and SPL is positive with R^2=0.6631. With an increase in E”, SPL values increases as well. Another important finding is the sound absorption behavior of the asphalt mixture by changing time and frequency. Although all the volumetric parameters are somehow correlated positively with SPL at the mentioned temperature and frequency combination, the relation demonstrates negative correlation at some other combinations. Thus, it is not always proper to make generalization for the relation between the linear visco-elastic parameters and SPL. More analyses have been performed at different temperature – frequency combinations for each specimen to disclose the relationship and some of them are presented in the Appendix C.

It is important to declare that specimens prepared by using light weight aggregates become outliers for the data analysis. They absorbed unrealistic amount of asphalt binder. Since they yield the misinterpretation of the data when included, they are assigned as outliers for all data analysis part. However, the measurements performed on light weight aggregate specimens are presented in SPL measurements for comparison reasons.

5.1.2 Relation between Mixture Volumetric Parameters and SPL

Superpave is a volumetric mix design. There are certain values that need to be accomplished to perform the mix design according to the design criteria of AASHTO standards. Since SMA is a modified version of the Superpave, it also conforms to the volumetric mix design requirements. Mixture volumetric parameters studied in this research are air void content (V_a), voids filled with asphalt (VFA), voids in mineral aggregates (VMA), binder content (P_b) along with theoretical maximum specific gravity (G_{mm}) and compacted bulk specific gravity (G_{mb}) of a mixture. The equations from 5.7 to 5.12 show how to calculate the volumetric properties for a mix.

$$Gmm = \frac{Ws + Wac}{Vs + Vac} \tag{5.7}$$

$$Gmb = \frac{Ws + Wac}{Vs + Vac + Va} \tag{5.8}$$

$$Va = \left(1 - \frac{Gmb}{Gmm}\right) \times 100 \tag{5.9}$$

$$VMA = 100 - \frac{Gmb \times Ps}{Gsb} \tag{5.10}$$

$$VFA = 100 \times \frac{VMA - Va}{VMA} \qquad 5.11$$

$$Pb = \frac{Wac}{Wmix} \qquad 5.12$$

where;

Ws = Weight of aggregates

Wac = Weight of asphalt cement (binder)

$Wmix$ = Weight of the asphalt mixture

Vs = Volume of aggregates

Vac = Volume of asphalt cement

Va = Volume of air voids

Ps = Aggregate content $(1 - Pb)$

Gsb = Bulk specific gravity of aggregates

Table 5.2 gives the volumetric properties of the asphalt specimens prepared for the research. It illustrates the parameters for all Superpave, SMA and OGFC mix designs.

Table 5.2 Volumetric parameters of the specimens

Sample Code	**V_a**	**VMA**	**VFA**	**G_{mm}**	**G_{mb}**	**P_b**
125SA4	7.35	17.08	57.01	2.583	2.393	0.0520
125SA48	6.98	16.75	58.33	2.583	2.403	0.0520
125SA4PM	7.38	17.11	56.87	2.583	2.392	0.0520
125SA4CR5	7.20	16.95	57.52	2.583	2.397	0.0520
125SA4CR10	6.92	16.68	58.62	2.583	2.405	0.0520
095SA4F	6.94	14.63	52.50	2.648	2.464	0.0476
25SA4C	6.74	14.88	54.77	2.634	2.457	0.0463
0475OA4	15.87	27.08	41.98	2.497	2.105	0.0900
0475OA4CR10	13.19	24.88	47.05	2.497	2.168	0.0900
125SMAA4	4.90	14.77	66.76	2.587	2.460	0.0600
125SMAA4CR10	4.32	14.25	69.64	2.587	2.475	0.0600

Figures 5.7 to 5.11 illustrate the relation between individual volumetric properties of the asphalt mixtures with SPL. In figure 5.7, the correlation between air void content and sound pressure level is analyzed. There is an inverse; however, strong enough relation between the variables. It is the same for VMA versus SPL as well. This phenomenon can be explained with the travel of the sound waves. When there are more voids on the surface and internal structure of the asphalt, sound waves can freely move through them and be both absorbed and refracted. This results in less sound wave reflection and thus less SPL. The same logic applies for Figure 5.9. There is a mild relation between VFA and SPL. The more the voids are filled with asphalt, the more sound pressure level increases.

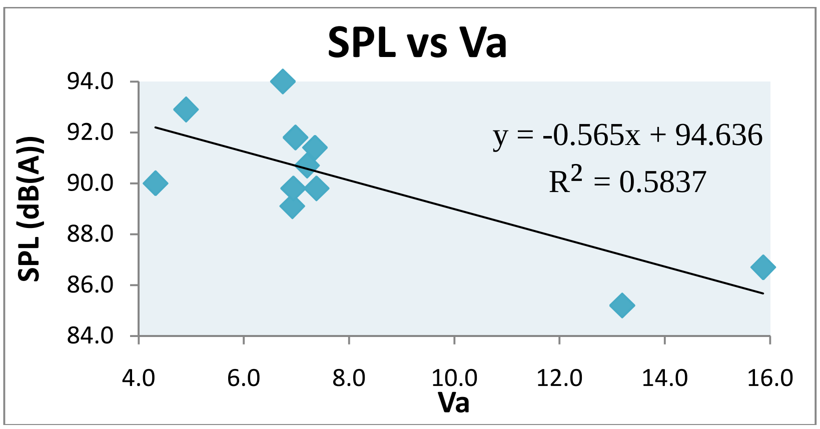

Figure 5.7 Change in SPL with change in air void content

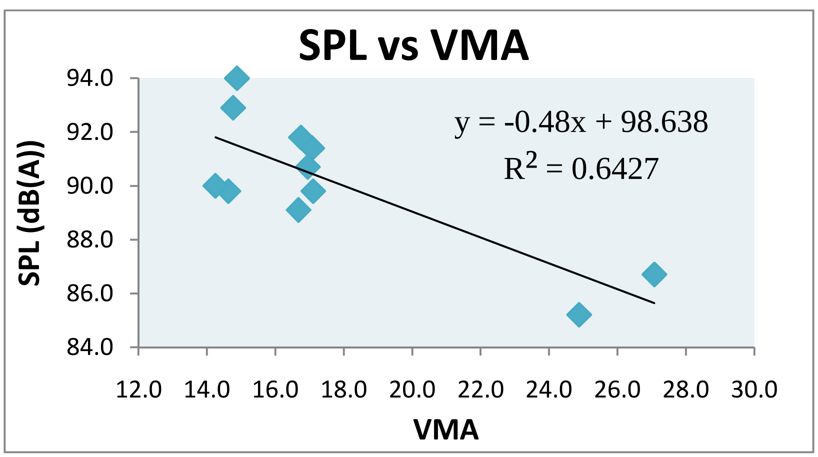

Figure 5.8 Change in SPL with change in voids in mineral aggregate

Figure 5.10 shows the relationship between P_b and SPL, where a negative correlation is visible.

Visco-elastic behavior of the binder and the mastic (binder + fine aggregate) may be the reason for such relationship. As the amount of binder is increased, the asphalt mixture becomes more in the viscous behavior side. Materials showing viscous behavior are quieter than the materials with elastic performance. However, it is noted that increase in asphalt content may yield the decrease in overall void content which is inversely correlated with SPL as well. There should be an optimum content for binder in which the highest sound reduction might be achieved. In order to discover this type of relation, there is a need for more tests covering a large enough range. Since the individual correlations with SPL do not contribute to the overall knowledge because of the material characteristics interactions, there is a need for multivariate data analysis and it will be presented in the section 5.2.

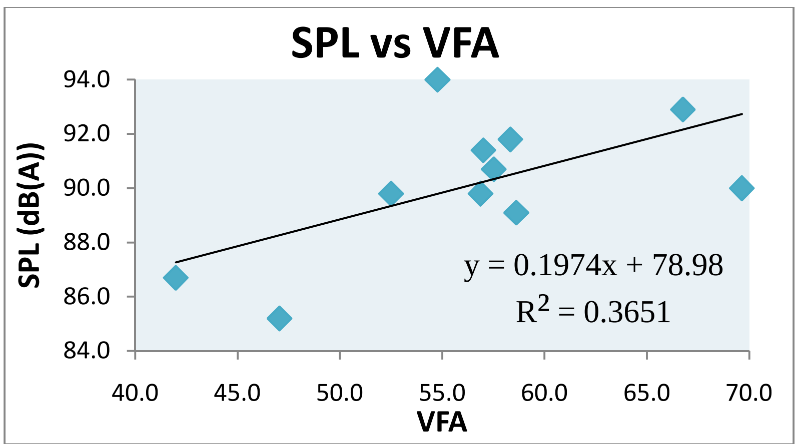

Figure 5.9 Change in SPL with change in voids filled with asphalt

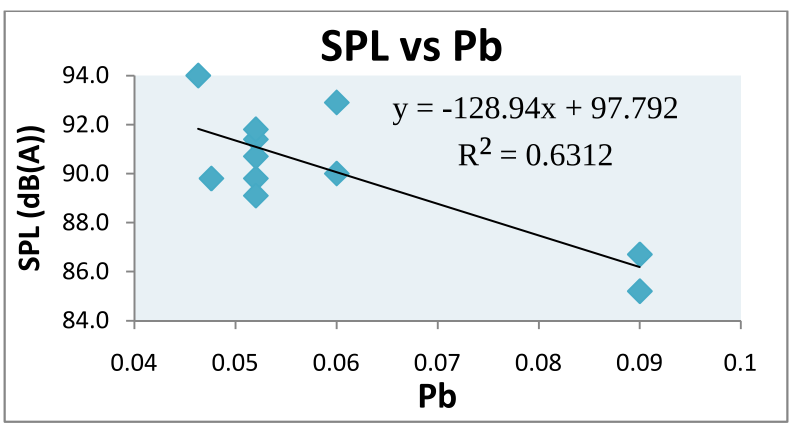

Figure 5.10 Change in SPL with change in binder content

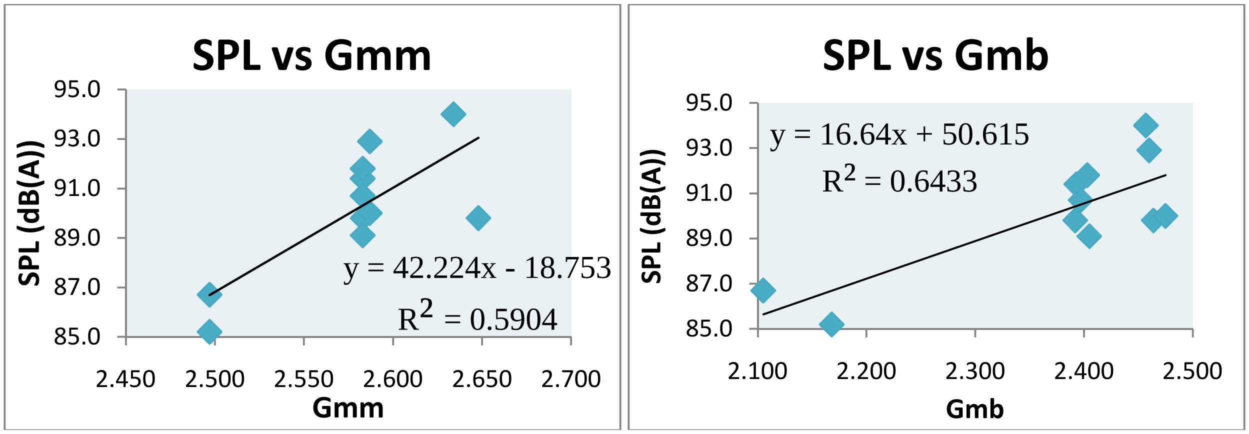

Figure 5.11 Change in SPL with change in G_{mm} and G_{mb}

For the figure 5.11, the relations are almost negligible if the lowest two values are ignored. Although the trend is positive for correlation between specific gravities and SPL, more data points are required to scrutinize and establish the relation acceptably.

5.1.3 Relation between Gradation Parameters, Material Types and SPL

Gradation of the aggregates is another important parameter analyzed for sound absorption\reflection capacities of the asphalt pavements. Gradation can be characterized according to the nominal maximum aggregate size (NMAS), coefficient of curvature (C_c) and coefficient of uniformity (C_u). The effect of NMAS, mix design type, binder aging, binder type, aggregate type on SPL can indirectly be seen in the figure 5.12. The decrease in NMAS for Superpave (SP) mix design results in the reduction on SPL as well. The drop in SPL between 25SA4C and 095SA4F specimens is approximately 4.2 dB (A). By choosing NMAS 12.5 mm instead of 25 mm for SP mix design yields around 3dB (A) more noise damping.

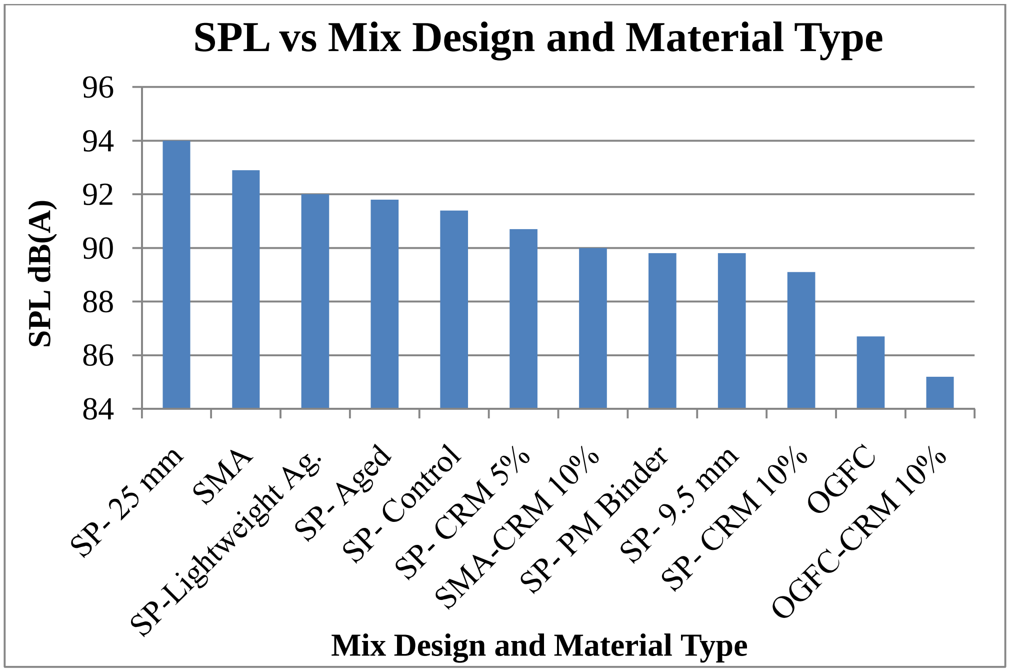

Figure 5.12 Peak SPL values at 250 Hz and 23^{o}C

Hence, as the HMA aggregate gradation gets finer, the sound pressure level decreases. The other obvious information that can be obtained from the figure is the impact of binder type on SPL. Modified binders work better for sound reduction on pavements. As the amount of crumb rubber increases in the binder, the SPL level decreases. Another deduction that can be seen is the effect of binder aging on SPL. The only difference between specimens 125SA4 and 125SA48 is the aging of the binder used. The variation is 0.4 dB (A) higher on aged specimen side. This can be explained by the visco-elastic behavior. Since the aged binder gets stiffer, it tends to become closer on elastic behavior side. It is known that elastic materials are not as good as viscous material on sound damping. The last conclusion is drawn from the figure is the type of material mix design. OGFC mix design has the best sound absorption capacity compared to SP and SMA. This can be attributed to the high air void content and connected void structure of the OGFC mixes.

Table 5.3 Gradation parameters and control parameters of the asphalt mixtures

Sample Code	**Gradation (NMAS)**	**Aging Condition**	**Air Voids ***	C_u	C_c	**Control Parameter**
125SA4	12.5 mm	4 hours	7.35%	14.27	1.35	Control Mixture
125SA48	12.5 mm	48 hours	6.98%	14.27	1.35	Aging Performed
125SA4PM	12.5 mm	4 hours	7.38%	14.27	1.35	PM*** Binder
125SA4CR5	12.5 mm	4 hours	7.20%	14.27	1.35	5% CRM** Binder.
125SA4CR10	12.5 mm	4 hours	6.92%	14.27	1.35	10% CRM Binder
125SA4LW	12.5 mm	4 hours	7.05%	14.27	1.35	Lightweight Aggregate
095SA4F	9.5 mm	4 hours	6.94%	17.64	1.54	Fine Gradation
25SA4C	25.0 mm	4 hours	6.74%	46.28	1.38	Coarse Gradation
0475OA4	4.75 mm	4 hours	15.87%	2.73	1.09	OGFC Mix Design
0475OA4CR10	4.75 mm	4 hours	13.20%	2.73	1.09	OGFC-10%CRM Binder
125SMAA4	12.5 mm	4 hours	4.90%	29.40	8.53	SMA Mix Design
125SMAA4CR10	12.5 mm	4 hours	4.32%	29.40	8.53	SMA-10% CRM Binder

*Air voids values are the average of three (3) replicates. CRM**-Crumb rubber modified. PM***-Polymer modified

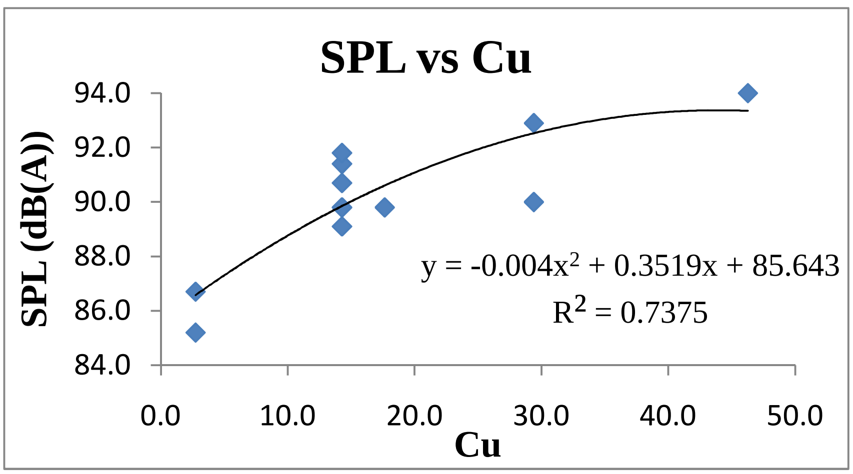

Figure 5.13 Change in SPL with change in C_u

The coefficient of uniformity is a measure of how well or poorly the aggregates are sorted. It can be calculated by using equation 5.13. Figure 5.13 shows the correlation between SPL and C_u.

$$Cu = D_{60}/D_{10} \qquad 5.13$$

$$Cc = (D_{30})\text{^}2/(D_{10} \times D_{60}) \qquad 5.14$$

where;

D_{60}= Grain diameter at 60% of the aggregates passing

D_{10} = Grain diameter at 10% of the aggregates passing

D_{30}= Grain diameter at 30% of the aggregates passing

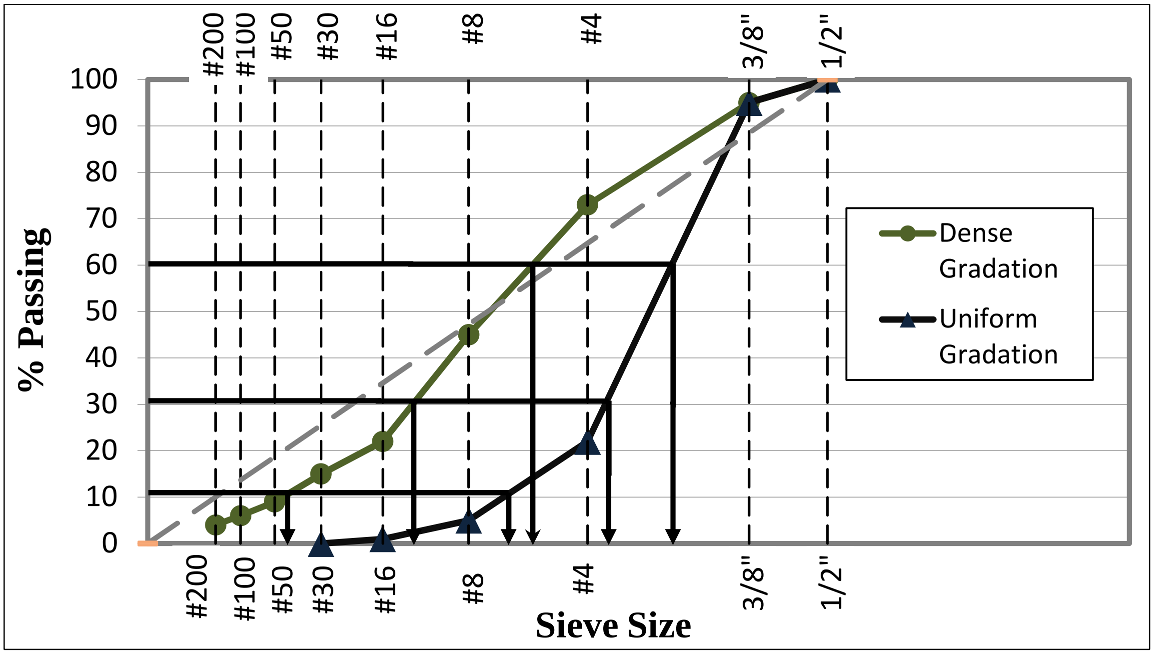

Figure 5.14 Dense and uniform gradation for maximum aggregate size 12.5 mm

According to Unified Soil Classification System (USCS), well graded (dense (non-uniformly) graded) aggregates are classified with $Cu > 4\ and\ 1 < Cc < 3$. If it does not satisfy the criteria, it is classified as poorly graded (uniform graded). Table 5.4 shows grain sizes and the gradation parameters C_u and C_c for the dense and uniform gradation examples demonstrated on figure 5.14.

Table 5.4 Gradation parameters for dense and uniform graded aggregates

	D_{10}	D_{30}	D_{60}	C_u	C_c
Uniform Gradation	3.06	5.27	7.23	2.36	1.25
Dense Gradation	0.35	1.59	3.64	10.40	1.99

It can be inferred from the USCS that increase in C_u results in well, i.e., non-uniform gradation. Hence, the uniformity coefficient is misnamed since as C_u gets smaller, the aggregate gradation becomes more uniform. It should actually be called the coefficient of non-uniformity. For instance, if C_u is equal to one (1), it means that there is only one grain size.

The relation between coefficient of uniformity and SPL is presented in figure 5.13, where a strong correlation between the variables (with R^2=0.74) was observed. This analysis can be further extended to discover the impact of C_u purely by overshadowing the interactions with other material characteristics. In order to better illustrate the effect of the Cu, only the specimens with unmodified binders were compared (i.e., mixtures with polymer modified and crumb rubber modified binders are not included). Also, the mixture with lightweight aggregates was not included in the analysis. Figure 5.15 illustrates the correlation between SPL and C_u. In this case, the relation becomes stronger with approximately R^2 = 0.96. This phenomenon can be explained with the compaction and void content. If C_u increases, the gradation becomes well graded having less air voids. When there are less air voids, more sound waves are reflected yielding higher SPL values. It still needs to be remembered that there are always other material interactions with SPL and multivariate analysis is required for better understanding.

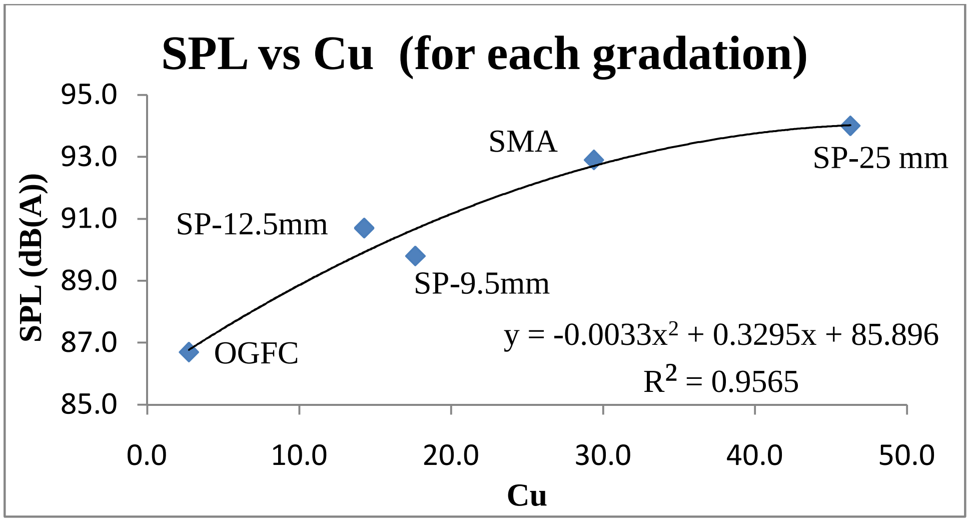

Figure 5.15 Change in SPL with change in Cu, only one for each gradation

The other gradation parameter is coefficient of curvature (C_c). The studies show that it almost has no impact on SPL. The correlation between C_c and SPL is given in the figure 5.16. R^2 = 0.0815 is also another indication very poor effect of C_c on SPL. Figure 5.16 demonstrates the correlations between SPL and C_c

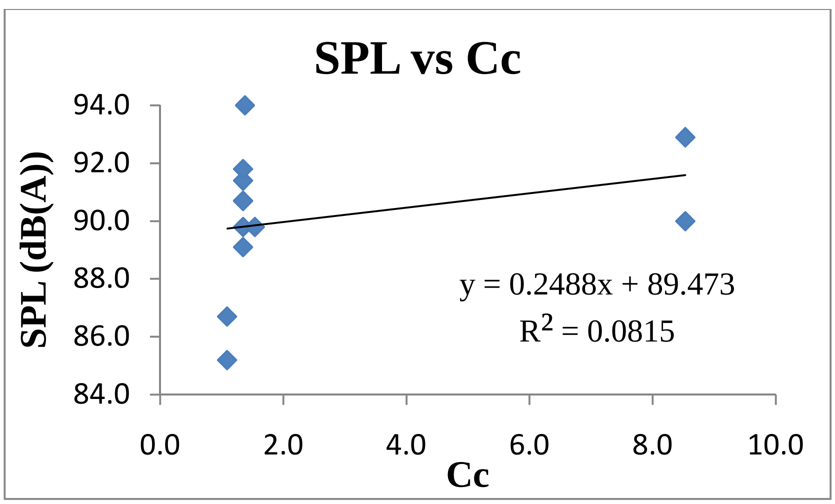

Figure 5.16 Change in SPL with change in C_c

In order to better understand the effect of gradation parameters on SPL, there is a need for an intensive study. Further research on this area is recommended.

5.2 MULTIVARIATE REGRESSION ANALYSIS

The individual relations between material characteristics of the asphalt pavements and the SPL reveal that there is a need for multivariate analyses for a better understanding about sound absorption behavior of asphalt. There are certain interactions between visco-elastic, volumetric and gradation parameters. As discussed in the previous sections, there is more than one parameter affecting the void content of the asphalt such as aggregate gradation, binder content and voids filled with asphalt. This occurrence can be elucidated by studying the interactions between parameters. Multivariate statistics by using commercially available software SPSS (statistical package for the social sciences) was performed to explore the relations. Multivariate regression analysis between linear visco-elastic, volumetric and gradation parameters of asphalt specimens and the SPL is studied to determine a formula which can be used to predict the SPL of the different asphalt mixtures by only using the data obtained at laboratory conditions. Such formulation might be helpful to fill the gap for future's quieter pavements by predicting the noise level of the asphalt pavements using basic mix design data.

The analyses performed show only the resultant significant parameters and results. SPSS were run on by using one of the backward, stepwise or enter methods on linear regression analyze mode. In any of the modes, the parameters were excluded from the model because of either collinearity between them or insignificancy according to setup criterion.

The first empirical prediction model included only linear visco-elastic parameters of the asphalt mixtures. The general denotation of the model utilized;

$$SPL = f\ (|E^*|, \sin\delta, |E^*|/\sin\delta, E', E'') \qquad 5.15$$

All the combinations between parameters were analyzed and the most suitable outcome was obtained as;

$$SPL = f(|E^*|, \sin\delta) \qquad 5.16$$

$$SPL = C_1 + (X_1 \sin\delta) + (X_2 |E^*|) \qquad 5.17$$

where C_1, X_1 and X_2 are the unstandardized coefficients obtained at the end of analysis and given in Table 5.5 which illustrates the results acquired from SPSS at the end of the run. The table consists only the basic values need to be reported.

Table 5.5 SPSS results for SPL and linear visco-elastic parameters

VARIABLES ENTERED/REMOVED					
Model	Var. Entered	Var. Removed	Method		
1	$\|E^*\|$, Sin δ	.	Enter		
MODEL SUMMARY					
Model	R	R Square	Adjusted R Square		
1	0.762	.581	.476		
ANOVA					
Model		Sum of Squares	df	F	Sig.
1	Regression	37.613	2	5.546	0.031
	Residual	27.128	8		
	Total	64.742	10		
COEFFICIENTS					
Model		Unstandardized Coefficients		t	Sig.
		B	Std. Error		
1	(Constant)	**C_1=74.742577**	5.029	14.862	**.000**
	Sin δ	**X_1=23.594655**	9.375	2.517	**.036**
	$\|E^*\|$	**X_2=.0009799**	.000	3.290	**.011**

The relation between SPL and $|E^*|$, $\sin\delta$ is not strong with $R^2 = 0.58$. The significance (sig) of the parameters to predict the model is good enough with sig value less than 0.05. However, the correlation between the independent variables is in an appreciable amount. This makes the model extremely weak to predict the SPL.

The second relation investigated was between SPL and gradation parameters. C_u and C_c were the two parameters studied for the effect of aggregate gradation on SPL. The prediction model was in the form of;

$$SPL = f\ (C_u, C_c) \tag{5.18}$$

Although Cu has a strong relation with SPL, it is weak for Cc. There is a need for a wider study to better understand the correlation between parameters studied. In the final prediction function, only Cu values are included since they seem to represent the impact of gradation on SPL better. Table 5.6 demonstrates the result obtained by SPSS. Backward criterion yielded for removal of C_c from the prediction since it does not make any contribution to predict the SPL in the model. The prediction model for gradation parameters is;

$$SPL = C_2+X_3.C_u \tag{5.19}$$

where X2 and A2 are the unstandardized coefficients. As in the individual correlations part, increase in C_u will result in an increase in SPL since the mixture becomes well graded.

Another prediction model was setup between mixture volumetric parameters and SPL.

$$SPL = f\ (V_a, VMA, VFA, G_{mm}, G_{mb}, P_b) \tag{5.20}$$

Since volumetric parameters were highly correlated, there was a problem of collinearity in the prediction model. SPSS excludes highly correlated variables by setting up the criteria and using the backward method. The strongest variable in the model above yielded to be P_b, V_a was the second significant parameter. They were used in the general prediction model along with other considerable gradation and visco-elastic parameters.

Table 5.6 SPSS results for SPL and gradation parameters

VARIABLES ENTERED/REMOVED			
Model	Var. Entered	Variables Removed	Method
1	C_c, C_u	.	Enter
2	.	C_c	Backward (criterion: Probability of F-to-remove >= .100)

MODEL SUMMARY				
Model	R	R Square	Adjusted R Square	Std. Error of the Est.
1	.813	.661	.576	1.657
2	.807	.651	.612	1.585

ANOVA						
Model		Sum of Squares	df	Mean Square	F	Sig.
1	Regression	42.768	2	21.384	7.785	0.01
	Residual	21.974	8	2.747		
	Total	64.742	10			
2	Regression	42.141	1	42.141	16.782	0
	Residual	22.601	9	2.511		
	Total	64.742	10			

COEFFICIENTS						
		Unstandardized Coefficients		Stand. Coef.		
Model		B	Std. Error	Beta	t	Sig.
1	(Constant)	87.2460188	.914		95.441	.000
	C_u	.1728447	.047	.858	3.694	.006
	C_c	-.0966415	.202	-.111	-.478	.646
2	(Constant)	**C_2=87.1793222**	.864		100.926	**.000**
	C_u	**X_3=.1625192**	.040	.807	4.097	**.003**

EXCLUDED VARIABLES			
Model		Partial Correlation	Collinearity Statistics (Tolerance)
2	C_c	-.167	.786

The general prediction model includes all the variables.

$$SPL = f\,(|E^*|, \sin\delta, |E^*|/\sin\delta, E', E'', C_u, C_c, V_a, VMA, VFA, G_{mm}, G_{mb}, P_b) \qquad 5.21$$

Although all the variables measured are shown in the model above, only the significant ones obtained in the previous analyses are included.

First considerable relation analyzed was

$$SPL = (|E^*|, C_u, P_b, VFA) \qquad 5.22$$

Runs were performed by using backward criterion of the SPSS so that the significant or highly collinear parameters were excluded from the model. Table 5.7 illustrates the results obtained by using important parameters at enter criterion of SPSS.

Table 5.7 SPSS results for SPL and significant parameters 1

VARIABLES ENTERED/REMOVED			
Model	Variables Entered	Variables Removed	Method
1	P_b, VFA, C_u, $\|E^*\|$	.	Enter

MODEL SUMMARY				
Model	R	R Square	Adjusted R Square	Std. Error of the Estimate
1	0.964	.930	.883	.869

ANOVA						
Model		Sum of Squares	df	Mean Square	F	Sig.
1	Regression	60.212	4	15.053	19.937	0.001
	Residual	4.530	6	.755		
	Total	64.742	10			

COEFFICIENTS						
Model		Unstandardized Coefficients		Std. Coef.	t	Sig.
		B	Std. Error	Beta		
1	(Constant)	**C_3=88.9664421**	3.458		25.730	**.000**
	$\|E^*\|$	**X_4=-.0006990**	.000	-.703	-3.172	**.019**
	VFA	**X_5=.1617178**	.065	.495	2.476	**.048**
	C_u	**X_6=.1319413**	.030	.655	4.367	**.005**
	P_b	**X_7=-92.5891333**	23.493	-.571	-3.941	**.008**

In the model all the parameters are significant with Sig. < 0.05 (very right column). The signs of the unstandardized parameter coefficients reveal the relation between parameter and SPL individually. VFA and Cu are positively correlated with SPL. It means that an increase in VFA or Cu or both will yield SPL to ascend as well. The reason for this kind of relation was explained under each individual parameter relation with SPL studies. On the other hand, rise in |E*| and/or P_b will cause decrease in SPL. The fact for P_b was clarified previously and the phenomenon for |E*| can be enlightened with following interpretations. This phenomenon can be enlightened with two interpretations. The first one is the range of |E*| data used. Since only one combination of temperature and frequency was utilized for visco-elastic parameter (212 Hz and 23^{o}C), the data used most probably does not cover the all range. The second reason might be the interaction between parameters in the model. The relations between independent parameters can cause inverse effect on certain parameters. In order to better understand the situation, more measurements of |E*| data and analysis need to be performed. The model has R^2 =0.930. This tells how close the predicted and measured SPL's are the ability of model to predict the SPL by using the engineering characteristics of the asphalt mixtures.

In this case the general prediction model yields the following SPL formula,

$$SPL = C_3 + (X_4.|E^*|) + (X_5.VFA) + (X_6.\ C_u) + (X_{7.}\ P_b) \qquad 5.23$$

where C_3, X_4, X_5, X_6 and X_7 are the coefficients given in Table 5.7.

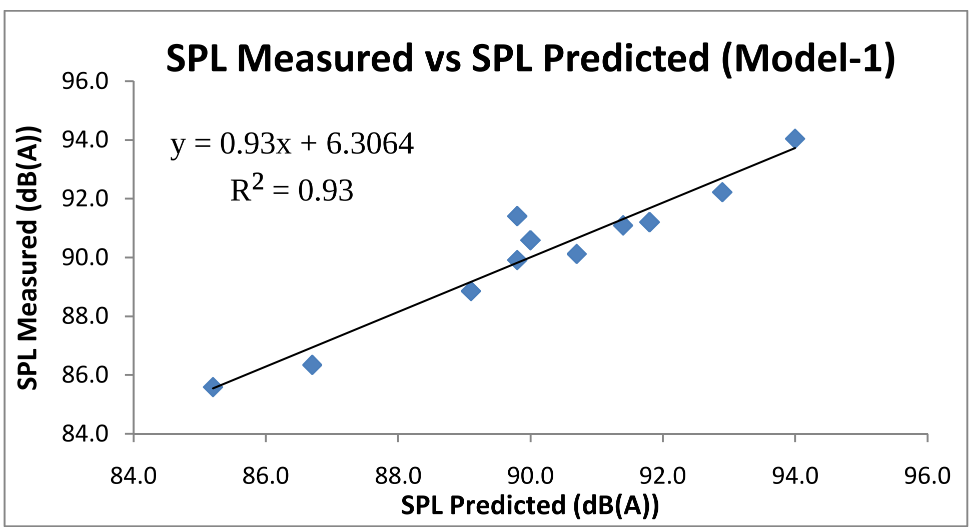

Figure 5.17 Measured and predicted SPL values for general prediction model 1

Figure 5.17 illustrated the relation between measured and predicted sound pressure levels which is obtained as a result of analysis of first general prediction model.

The second considerable relation performed was

$$SPL = (|E^*|, C_u, V_a) \qquad 5.24$$

Runs were performed by using backward criterion of the SPSS. All the parameters yielded to become significant according to the inherent removal criteria of SPSS. The aim of running a second general prediction model is to decrease the amount of variables to predict SPL. In this model, volumetric parameters VFA and P_b are replaced with another volumetric parameter V_a. Using only V_a as an independent variable in the model has some advantages. One of them is easier determination of V_a compared to VFA and P_b. The second advantage is to use less parameter to predict the model which in return results more efficient and time saving computations.

Table 5.8 demonstrates the SPSS results of general model 2. Although the relation is not as strong as in the model 1 (model1 R^2_1= 0.93 and model 2 R^2_2= 0.897), the significance of the parameters are better (Table 5.7 and Table 5.8).

Prediction formula in this model becomes,

$$SPL = C_4 + (X_8.|E^*|) + (X_9.C_u) + (X_{10}.V_a) \qquad 5.25$$

Figure 5.18 demonstrates the measured and predicted SPL values with trend line and equation of the line for general model 2.

Table 5.8 SPSS results for SPL and significant parameters 2

VARIABLES ENTERED/REMOVED						
Model	Variables Entered	Variables Removed	Method			
1	V_a, C_u, $\|E^*\|$	.	Enter			
MODEL SUMMARY						
Model	R	R Square	Adjusted R Square	Std. Error of the Estimate		
1	0.947	.897	.853	.9768393255844		
ANOVA						
Model		Sum of Squares	df	Mean Square	F	Sig.
1	Regression	58.062	3	19.354	20.283	0.001
	Residual	6.680	7	.954		
	Total	64.742	10			
COEFFICIENTS						
Model		Unstandardized Coefficients		Stand. Coef.	t	Sig.
		B	Std. Error	Beta		
1	(Constant)	**C_4=99.4611990**	3.089		32.194	**.000**
	|E*|	**X_8=-0.0008062**	.000	-.810	-3.300	**.013**
	Cu	**X_9=0.1288282**	.034	.640	3.784	**.007**
	Va	**X_{10}=-0.7601706**	.187	-1.028	-4.069	**.005**

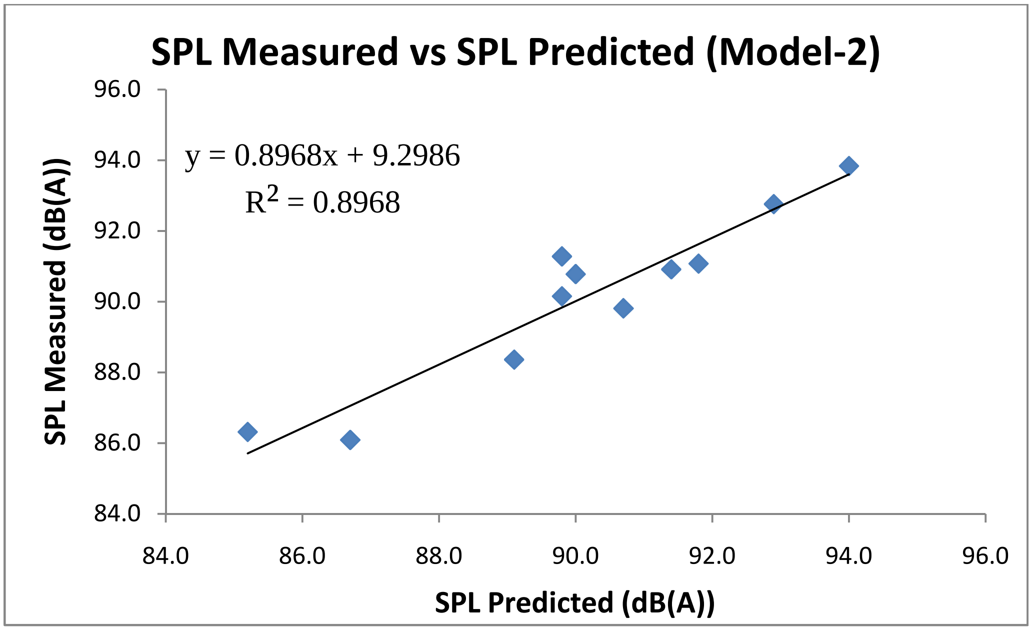

Figure 5.18 Measured and predicted SPL values for general prediction model 2

CHAPTER 6

SUMMARY AND CONCLUSIONS

6.1 SUMMARY

The impact of material properties on sound absorption of flexible pavements have been studied in this thesis. These material properties include asphalt linear visco-elastic properties, aggregate gradation parameters and mixture volumetrics. Analyses performed include both individual correlations and multivariate regressions between parameters and SPL. In order to focus on difference between sounds generated from the material properties, a novel laboratory tire pavement noise simulator (TIPANOS) was constructed. TIPANOS measurements were not influenced by the surface texture of pavement since tests were performed on laboratory AMPT specimens.

6.2 CONCLUSIONS

Based on the laboratory measurements of the samples and data analyses of the obtained results, the following conclusions were drawn:

- There is negative correlation between VMA and V_a, and SPL. As these parameters increase, there is possibility of more interconnected voids where sound waves can freely move and can be absorbed and refracted.
- A negative correlation between P_b and SPL was observed. This is logical because as the amount of binder increases, the asphalt mixture becomes more viscous (rather than elastic). Materials showing viscous behavior are typically quieter than the materials with elastic characteristics (because of damping). However, it should be noted that increase in asphalt content may yield to the decrease in void content, which may increase SPL.

Therefore, it can be suggested that, for sound absorption purposes, the binder content should be optimized such that the highest amount of binder is used, without excessively blocking the interconnected voids

- A very good correlation (with an R^2 of 0.89) between the C_u of aggregates used in the HMA and SPL was observed (SPL increased with increasing C_u). High C_u means well graded (more densely packed) aggregates, having less air void space between the aggregates. It is hypothesized that when there are less air voids, more sound waves are reflected yielding higher SPL values. However, there is a need for an intense study to discover the effect of C_c on SPL.
- Statistical analysis revealed that, among all the material parameters, the influence of |E*|, VFA, C_u and P_b on SPL is statistically significant. A predictive multivariate regression equation was developed. This regression equation revealed an R^2 of 0.93, which shows the significance of the combined effect of the parameters on the SPL.

APPENDICES

Appendix A

(Job Mix Formulas)

<table>
<tr><td colspan="12">JOB MIX FORMULA</td></tr>
<tr><td colspan="12">HMA FIELD COMMUNICATION</td></tr>
<tr><td colspan="3">CONTROL SECTION
CONTROL MIX DESIGN</td><td colspan="2">JOB NO.
0.02</td><td colspan="4">PROJECT ENGINEER
Salih KOCAK</td><td colspan="3">DATE EFFECTIVE
07/21/2009</td></tr>
<tr><td colspan="3">MIXTURE TYPE
SUPERPAVE</td><td colspan="5">MIX DESIGN NO.
NMAS 9.5</td><td colspan="4">PLANT LOCATION
EAST LANSING</td></tr>
<tr><td colspan="2">ANGULARITY
47.4</td><td colspan="2">% AIR VOIDS
4.00</td><td colspan="2">VMA
15.02</td><td colspan="2">VFA
73.35</td><td colspan="2">COMP.TEMP
138 C</td><td colspan="2">MIX. TEMP
149 C</td></tr>
<tr><td>Gmm
2.648</td><td colspan="2">Gmb
2.542</td><td>Gb
1.023</td><td colspan="2">Gse
2.876</td><td colspan="2">Gsb
2.849</td><td colspan="2">P200/Pbe
1.13</td><td colspan="2">% AIR VOIDS
4.00</td></tr>
<tr><td colspan="4">MIX/AGG. GRADATION, %</td><td colspan="8">MIX/AGG. PROPORTION, %</td></tr>
<tr><td colspan="2">ITEM</td><td colspan="2">PERCENT</td><td colspan="6">MATERIAL/PRODUCER</td><td colspan="2">PIT NO.</td></tr>
<tr><td colspan="2">ASPHALT,%</td><td colspan="2">4.76%</td><td colspan="6">SPARTAN & RIETH-RILEY</td><td colspan="2">N/A</td></tr>
<tr><td colspan="2">P 1-1/2" (37.5 mm)</td><td colspan="2">100.00%</td><td colspan="6">SPARTAN & RIETH-RILEY</td><td colspan="2">N/A</td></tr>
<tr><td colspan="2">P 1" (25.0 mm)</td><td colspan="2">100.00%</td><td colspan="6">SPARTAN & RIETH-RILEY</td><td colspan="2">N/A</td></tr>
<tr><td colspan="2">P 3/4" (19.0 mm)</td><td colspan="2">100.00%</td><td colspan="6">SPARTAN & RIETH-RILEY</td><td colspan="2">N/A</td></tr>
<tr><td colspan="2">P 1/2" (12.5 mm)</td><td colspan="2">100.00%</td><td colspan="6">SPARTAN & RIETH-RILEY</td><td colspan="2">N/A</td></tr>
<tr><td colspan="2">P 3/8" (9.5 mm)</td><td colspan="2">91.00%</td><td colspan="6">SPARTAN & RIETH-RILEY</td><td colspan="2">N/A</td></tr>
<tr><td colspan="2">P No. 4 (4.75 mm)</td><td colspan="2">56.00%</td><td colspan="6">SPARTAN & RIETH-RILEY</td><td colspan="2">N/A</td></tr>
<tr><td colspan="2">P No. 8 (2.36 mm)</td><td colspan="2">38.00%</td><td colspan="6">SPARTAN & RIETH-RILEY</td><td colspan="2">N/A</td></tr>
<tr><td colspan="2">P No. 16 (1.18 mm)</td><td colspan="2">26.00%</td><td colspan="6">SPARTAN & RIETH-RILEY</td><td colspan="2">N/A</td></tr>
<tr><td colspan="2">P No. 30 (600 µm)</td><td colspan="2">16.00%</td><td colspan="6">SPARTAN & RIETH-RILEY</td><td colspan="2">N/A</td></tr>
<tr><td colspan="2">P No. 50 (300 µm)</td><td colspan="2">10.00%</td><td colspan="3">RECLAIMED</td><td colspan="5">NO RAP</td></tr>
<tr><td colspan="2">P No. 100 (150 µm)</td><td colspan="2">7.00%</td><td colspan="3" rowspan="2">ASPHALT BINDER</td><td colspan="5">Supplier: MTE</td></tr>
<tr><td colspan="2">P No. 200 (75 µm)</td><td colspan="2">5.00%</td><td colspan="5">GRADE: PG 58-28</td></tr>
<tr><td colspan="2">CRUSHED 1 FACE</td><td colspan="2">100%</td><td colspan="8">PRODUCER LOCATION: MSU-CEE-AACL</td></tr>
<tr><td colspan="2">CRUSHED 2 FACES</td><td colspan="2">100%</td><td colspan="8">REGULAR TESTING</td></tr>
</table>

Figure A.1 Job Mix Formula for Superpave NMAS 9.5 mm

<table>
<tr><th colspan="4">JOB MIX FORMULA</th></tr>
<tr><th colspan="4">HMA FIELD COMMUNICATION</th></tr>
<tr><td>CONTROL SECTION
CONTROL MIX DESIGN</td><td>JOB NO.
0.03</td><td>PROJECT ENGINEER
Salih KOCAK</td><td>DATE EFFECTIVE
07/21/2009</td></tr>
</table>

<table>
<tr><td>MIXTURE TYPE
SUPERPAVE</td><td>MIX DESIGN NO.
NMAS 25.00</td><td>PLANT LOCATION
EAST LANSING</td></tr>
</table>

<table>
<tr><td>ANGULARITY
46.1</td><td>% AIR VOIDS
4.00</td><td>VMA
14.26</td><td>VFA
71.94</td><td>COMP.TEMP
138 C</td><td>MIX. TEMP
149 C</td></tr>
</table>

<table>
<tr><td>Gmm
2.624</td><td>Gmb
2.513</td><td>Gb
1.023</td><td>Gse
2.840</td><td>Gsb
2.802</td><td>P200/Pbe
0.72</td><td>% AIR VOIDS
4.00</td></tr>
</table>

<table>
<tr><th colspan="2">MIX/AGG. GRADATION, %</th><th colspan="3">MIX/AGG. PROPORTION, %</th></tr>
<tr><th>ITEM</th><th>PERCENT</th><th colspan="2">MATERIAL/PRODUCER</th><th>PIT NO.</th></tr>
<tr><td>ASPHALT,%</td><td>4.63%</td><td colspan="2">SPARTAN & RIETH-RILEY</td><td>N/A</td></tr>
<tr><td>P 1-1/2" (37.5 mm)</td><td>100.00%</td><td colspan="2">SPARTAN & RIETH-RILEY</td><td>N/A</td></tr>
<tr><td>P 1" (25.0 mm)</td><td>97.00%</td><td colspan="2">SPARTAN & RIETH-RILEY</td><td>N/A</td></tr>
<tr><td>P 3/4" (19.0 mm)</td><td>89.00%</td><td colspan="2">SPARTAN & RIETH-RILEY</td><td>N/A</td></tr>
<tr><td>P 1/2" (12.5 mm)</td><td>75.00%</td><td colspan="2">SPARTAN & RIETH-RILEY</td><td>N/A</td></tr>
<tr><td>P 3/8" (9.5 mm)</td><td>67.00%</td><td colspan="2">SPARTAN & RIETH-RILEY</td><td>N/A</td></tr>
<tr><td>P No. 4 (4.75 mm)</td><td>54.00%</td><td colspan="2">SPARTAN & RIETH-RILEY</td><td>N/A</td></tr>
<tr><td>P No. 8 (2.36 mm)</td><td>41.00%</td><td colspan="2">SPARTAN & RIETH-RILEY</td><td>N/A</td></tr>
<tr><td>P No. 16 (1.18 mm)</td><td>30.00%</td><td colspan="2">SPARTAN & RIETH-RILEY</td><td>N/A</td></tr>
<tr><td>P No. 30 (600 µm)</td><td>22.00%</td><td colspan="2">SPARTAN & RIETH-RILEY</td><td>N/A</td></tr>
<tr><td>P No. 50 (300 µm)</td><td>15.00%</td><td>RECLAIMED</td><td colspan="2">NO RAP</td></tr>
<tr><td>P No. 100 (150 µm)</td><td>10.00%</td><td rowspan="2">ASPHALT
BINDER</td><td colspan="2">Supplier: MTE</td></tr>
<tr><td>P No. 200 (75 µm)</td><td>3.00%</td><td colspan="2">GRADE: PG 58-28</td></tr>
<tr><td>CRUSHED 1 FACE</td><td>100%</td><td colspan="3">PRODUCER LOCATION: MSU-CEE-AACL</td></tr>
<tr><td>CRUSHED 2 FACES</td><td>100%</td><td colspan="3">REGULAR TESTING</td></tr>
</table>

Figure A.2 Job Mix Formula for Superpave NMAS 25 mm

JOB MIX FORMULA			
HMA FIELD COMMUNICATION			
CONTROL SECTION CONTROL MIX DESIGN	JOB NO. 0.04	PROJECT ENGINEER Salih KOCAK	DATE EFFECTIVE 07/21/2009

MIXTURE TYPE	MIX DESIGN NO.	PLANT LOCATION
SMA	12.5	EAST LANSING

ANGULARITY	% AIR VOIDS	VMA	VFA	COMP.TEMP	MIX. TEMP
45.0	4.00	17.19	76.72	138 C	149 C

Gmm	Gmb	Gb	Gse	Gsb	P200/Pbe	% AIR VOIDS
2.587	2.484	1.023	2.867	2.819	0.74	4.00

MIX/AGG. GRADATION, %		**MIX/AGG. PROPORTION, %**	
ITEM	**PERCENT**	**MATERIAL/PRODUCER**	**PIT NO.**
ASPHALT,%	6.00%	SPARTAN & RIETH-RILEY	N/A
P 1-1/2" (37.5 mm)	100.00%	SPARTAN & RIETH-RILEY	N/A
P 1" (25.0 mm)	100.00%	SPARTAN & RIETH-RILEY	N/A
P 3/4" (19.0 mm)	100.00%	SPARTAN & RIETH-RILEY	N/A
P 1/2" (12.5 mm)	94.00%	SPARTAN & RIETH-RILEY	N/A
P 3/8" (9.5 mm)	65.00%	SPARTAN & RIETH-RILEY	N/A
P No. 4 (4.75 mm)	30.00%	SPARTAN & RIETH-RILEY	N/A
P No. 8 (2.36 mm)	20.00%	SPARTAN & RIETH-RILEY	N/A
P No. 16 (1.18 mm)	15.00%	SPARTAN & RIETH-RILEY	N/A
P No. 30 (600 µm)	12.00%	SPARTAN & RIETH-RILEY	N/A
P No. 50 (300 µm)	10.00%	RECLAIMED	NO RAP
P No. 100 (150 µm)	6.00%	ASPHALT BINDER	Supplier: MTE
P No. 200 (75 µm)	4.00%		GRADE: PG 58-28
CRUSHED 1 FACE	100%	PRODUCER LOCATION: MSU-CEE-AACL	
CRUSHED 2 FACES	100%	REGULAR TESTING	

VCA (mix) & VCA (dry) conditions are satisfied, 0.2%fider was added.

Figure A.3 Job Mix Formula for Stone Matrix Asphalt

<table>
<tr><th colspan="4">JOB MIX FORMULA</th></tr>
<tr><th colspan="4">HMA FIELD COMMUNICATION</th></tr>
<tr><td>CONTROL SECTION
CONTROL MIX DESIGN</td><td>JOB NO.
0.05</td><td>PROJECT ENGINEER
Salih KOCAK</td><td>DATE EFFECTIVE
07/21/2009</td></tr>
</table>

<table>
<tr><td>MIXTURE TYPE
OGFC</td><td>MIX DESIGN NO.
4.75</td><td>PLANT LOCATION
EAST LANSING</td></tr>
</table>

<table>
<tr><td>ANGULARITY
47.0</td><td>% AIR VOIDS
4.00</td><td>VMA
NA</td><td>VFA
NA</td><td>COMP.TEMP
138 C</td><td>MIX. TEMP
149 C</td></tr>
</table>

<table>
<tr><td>Gmm
2.497</td><td>Gmb
2.122</td><td>Gb
1.023</td><td>Gse
2.912</td><td>Gsb
2.664</td><td>P200/Pbe
NA</td><td>% AIR VOIDS
15.00</td></tr>
</table>

<table>
<tr><th colspan="2">MIX/AGG. GRADATION, %</th><th colspan="2">MIX/AGG. PROPORTION, %</th></tr>
<tr><th>ITEM</th><th>PERCENT</th><th>MATERIAL/PRODUCER</th><th>PIT NO.</th></tr>
<tr><td>ASPHALT,%</td><td>9.00%</td><td>SPARTAN & RIETH-RILEY</td><td>N/A</td></tr>
<tr><td>P 1-1/2" (37.5 mm)</td><td>100.00%</td><td>SPARTAN & RIETH-RILEY</td><td>N/A</td></tr>
<tr><td>P 1" (25.0 mm)</td><td>100.00%</td><td>SPARTAN & RIETH-RILEY</td><td>N/A</td></tr>
<tr><td>P 3/4" (19.0 mm)</td><td>100.00%</td><td>SPARTAN & RIETH-RILEY</td><td>N/A</td></tr>
<tr><td>P 1/2" (12.5 mm)</td><td>100.00%</td><td>SPARTAN & RIETH-RILEY</td><td>N/A</td></tr>
<tr><td>P 3/8" (9.5 mm)</td><td>100.00%</td><td>SPARTAN & RIETH-RILEY</td><td>N/A</td></tr>
<tr><td>P No. 4 (4.75 mm)</td><td>38.00%</td><td>SPARTAN & RIETH-RILEY</td><td>N/A</td></tr>
<tr><td>P No. 8 (2.36 mm)</td><td>10.00%</td><td>SPARTAN & RIETH-RILEY</td><td>N/A</td></tr>
<tr><td>P No. 16 (1.18 mm)</td><td>6.00%</td><td>SPARTAN & RIETH-RILEY</td><td>N/A</td></tr>
<tr><td>P No. 30 (600 µm)</td><td>4.00%</td><td>SPARTAN & RIETH-RILEY</td><td>N/A</td></tr>
<tr><td>P No. 50 (300 µm)</td><td>3.00%</td><td>RECLAIMED</td><td>NO RAP</td></tr>
<tr><td>P No. 100 (150 µm)</td><td>3.00%</td><td rowspan="2">ASPHALT BINDER</td><td>Supplier: MTE</td></tr>
<tr><td>P No. 200 (75 µm)</td><td>2.60%</td><td>GRADE: PG 58-28</td></tr>
<tr><td>CRUSHED 1 FACE</td><td>100%</td><td colspan="2">PRODUCER LOCATION: MSU-CEE-AACL</td></tr>
<tr><td>CRUSHED 2 FACES</td><td>100%</td><td colspan="2">REGULAR TESTING</td></tr>
</table>

1% hydrated lime & 0.3% fiber by weight were added

Figure A.4 Job Mix Formula for Open Graded Friction Course

Appendix B

(TIPANOS SPL Measurement Results)

Table B.1 Sound pressure level at 1/3 octave band frequencies

Frequency	Sound Pressure Level of Samples dB(A)											
Hz	Sample Code 125SA4				Sample Code 125SA48				Sample Code 125SA4PM			
	1-1	**1-2**	**1-3**	**Average**	**2-1**	**2-2**	**2-3**	**Average**	**3-1**	**3-2**	**3-3**	**Average**
25.0	76.9	81.5	80.0	79.5	91.9	78.4	80.5	83.6	79.3	81.4	78.4	79.7
40.0	74.0	75.7	77.9	75.9	80.2	75.4	78.8	78.1	76.3	75.8	76.6	76.2
63.0	73.3	72.7	76.7	74.3	72.2	75.9	77.1	75.1	76.1	72.5	77.3	75.3
100.0	78.5	74.0	79.8	77.4	76.4	82.1	81.3	79.9	80.4	78.8	79.0	79.4
160.0	75.1	72.1	76.0	74.4	76.8	76.7	77.8	77.1	77.3	77.6	74.4	76.4
250.0	90.6	92.0	91.8	91.4	92.5	91.4	91.6	91.8	90.8	88.5	90.0	89.8
400.0	67.0	75.7	74.2	72.3	75.2	72.3	74.1	73.9	71.1	69.4	71.4	70.6
630.0	67.6	75.3	76.9	73.3	73.7	70.1	70.1	71.3	67.6	68.3	72.7	69.5
1000.0	66.6	66.7	67.7	67.0	67.9	67.7	68.5	68.0	66.7	66.3	71.3	68.1
1600.0	55.0	58.8	63.9	59.2	62.4	64.5	63.2	63.4	57.1	59.4	59.7	58.7
2500.0	53.5	51.9	54.0	53.1	52.2	61.2	59.1	57.5	54.1	52.6	56.8	54.5
4000.0	58.3	51.4	54.7	54.8	55.2	59.4	60.3	58.3	56.4	55.6	59.2	57.1
6300.0	47.7	49.2	50.1	49.0	49.4	47.2	50.2	48.9	51.9	49.5	49.2	50.2
10000.0	41.7	41.6	42.3	41.9	44.9	47.2	45.2	45.8	36.8	39.9	41.0	39.2
16000.0	32.2	32.1	32.2	32.2	29.3	30.0	32.7	30.7	28.7	30.3	29.7	29.6

Table B.2 Sound pressure level at 1/3 octave band frequencies (continued)

Frequency	Sound Pressure Level of Samples dB(A)											
Hz	Sample Code 125SA4CR5				Sample Code 125SA4CR10				Sample Code 125SA4LW			
	4-1	**4-2**	**4-3**	**Average**	**5-1**	**5-2**	**5-3**	**Average**	**6-1**	**6-2**	**6-3**	**Average**
25.0	76.7	76.7	73.7	75.7	81.8	75.5	77.1	78.1	79.0	78.8	78.1	78.6
40.0	74.6	75.1	71.6	73.8	77.2	72.7	75.4	75.1	76.3	75.7	76.5	76.1
63.0	75.4	76.6	72.4	74.8	75.2	71.2	74.0	73.5	75.3	73.6	74.9	74.6
100.0	77.6	77.8	76.0	77.1	77.7	74.2	77.7	76.5	77.7	79.0	76.7	77.8
160.0	74.5	77.9	75.5	76.0	77.7	72.5	72.7	74.3	75.2	76.3	76.6	76.0
250.0	91.8	90.9	89.6	90.7	88.7	89.4	89.0	89.1	92.2	92.6	91.2	92.0
400.0	70.9	73.3	70.3	71.5	71.3	68.6	68.2	69.4	73.9	75.4	76.2	75.2
625.0	75.5	72.3	73.5	73.8	70.1	71.3	69.1	70.2	73.7	74.4	76.2	74.7
1000.0	71.3	66.8	66.8	68.3	68.0	68.0	65.9	67.3	69.5	71.9	71.5	71.0
1600.0	59.1	58.5	60.6	59.4	64.6	58.5	57.7	60.3	59.6	64.1	65.6	63.1
2500.0	52.4	52.8	53.3	52.8	54.8	57.3	52.2	54.8	57.7	56.2	62.8	58.9
4000.0	57.0	56.5	57.2	56.9	53.8	58.1	57.5	56.5	64.0	64.2	62.9	63.7
6300.0	47.7	48.5	50.0	48.8	48.4	49.8	47.2	48.5	52.6	54.5	56.1	54.4
10000.0	40.5	40.3	42.8	41.2	38.5	42.4	39.8	40.2	45.4	48.8	46.5	46.9
16000.0	30.1	31.5	29.8	30.5	29.7	29.5	34.1	31.1	36.1	36.6	35.2	36.0

Table B.3 Sound pressure level at 1/3 octave band frequencies (continued)

Frequency	Sound Pressure Level of Samples dB(A)											
Hz	Sample Code 095SA4F				Sample Code 255SA4C				Sample Code 0475OA4			
	7-1	**7-2**	**7-3**	**Average**	**8-1**	**8-2**	**8-3**	**Average**	**9-1**	**9-2**	**9-3**	**Average**
25.0	72.6	74.3	77.7	74.9	77.4	73.7	76.5	75.9	76.6	78.3	72.9	75.9
40.0	72.4	73.6	76.8	74.3	75.6	72.9	74.8	74.4	75.4	75.7	70.6	73.9
63.0	73.1	72.4	74.9	73.5	75.4	74.8	74.3	74.8	74.7	75.3	71.6	73.9
100.0	77.6	75.6	79.5	77.6	77.4	81.1	75.9	78.1	77.9	80.5	78.7	79.0
160.0	75.5	72.8	74.9	74.4	73.2	72.5	75.0	73.6	76.9	77.4	79.3	77.9
250.0	89.3	90.0	90.0	89.8	93.9	93.8	94.2	94.0	85.1	87.2	87.9	86.7
400.0	72.5	72.2	71.3	72.0	76.2	73.8	74.8	74.9	76.0	72.9	72.5	73.8
625.0	72.0	69.3	74.4	71.9	72.4	76.7	75.9	75.0	72.3	72.4	69.5	71.4
1000.0	66.3	63.5	66.0	65.2	68.4	70.0	73.5	70.6	64.7	65.4	65.2	65.1
1600.0	62.8	56.7	59.1	59.5	60.0	63.0	64.2	62.4	57.7	58.4	54.6	56.9
2500.0	52.8	51.1	56.4	53.4	53.3	55.1	61.1	56.5	52.2	54.1	53.7	53.3
4000.0	56.3	54.1	57.1	55.8	57.3	54.9	58.3	56.9	57.9	54.7	58.2	56.9
6300.0	52.2	46.9	51.4	50.2	48.6	51.4	50.6	50.2	52.3	50.9	52.5	51.9
10000.0	37.3	41.3	36.8	38.5	42.0	45.8	44.6	44.1	45.2	46.2	43.7	45.0
16000.0	31.3	30.4	31.9	31.2	31.6	29.7	32.3	31.2	39.3	38.6	41.9	39.9

Table B.4 Sound pressure level at 1/3 octave band frequencies (continued)

Frequency	Sound Pressure Level of Samples dB(A)											
Hz	Sample Code 0475OA4CR10				Sample Code 125SMAA4				Sample Code 125SMAA4CR10			
	10-1	**10-2**	**10-3**	**Average**	**11-1**	**11-2**	**11-3**	**Average**	**12-1**	**12-2**	**12-3**	**Average**
25.0	76.0	75.0	77.1	77.1	76.3	79.7	79.2	78.4	74.7	76.6	77.5	76.3
40.0	75.1	75.2	75.3	75.3	73.1	76.1	74.3	74.5	73.5	73.9	74.8	74.0
63.0	74.3	75.0	75.2	75.2	72.9	73.5	72.2	72.9	73.7	74.3	75.3	74.4
100.0	82.4	76.5	78.6	78.6	76.9	74.3	75.8	75.6	76.4	79.6	77.3	77.8
160.0	77.5	74.0	74.8	74.8	74.3	73.0	74.6	74.0	73.9	74.8	74.0	74.2
250.0	88.5	86.7	85.2	85.2	92.8	92.4	93.5	92.9	90.8	89.6	89.4	90.0
400.0	74.2	67.3	69.8	69.8	75.1	73.6	72.2	73.6	70.3	72.0	74.4	72.2
625.0	68.9	69.5	69.2	69.2	74.1	72.8	72.2	73.0	71.6	74.7	71.2	72.5
1000.0	64.8	68.4	64.1	64.1	69.9	68.9	71.4	70.0	70.1	68.2	69.8	69.4
1600.0	56.7	55.9	57.2	57.2	59.4	61.2	57.9	59.5	57.7	60.7	60.6	59.7
2500.0	49.0	48.1	48.8	48.8	56.2	56.2	55.2	55.9	59.9	53.9	58.8	57.5
4000.0	53.1	58.1	56.9	56.9	62.6	59.6	60.5	60.9	60.3	61.7	62.8	61.6
6300.0	49.8	49.8	46.2	46.2	49.0	47.9	50.0	49.0	50.1	48.5	50.1	49.6
10000.0	40.8	43.2	43.1	43.1	40.4	38.8	41.5	40.2	43.9	40.6	40.2	41.6
16000.0	34.6	38.9	33.7	33.7	36.1	30.5	34.3	33.6	31.9	28.2	28.6	29.6

Appendix C

(Correlations between Linear Visco-Elastic Parameters and SPL at Different Frequency and Temperature Combinations)

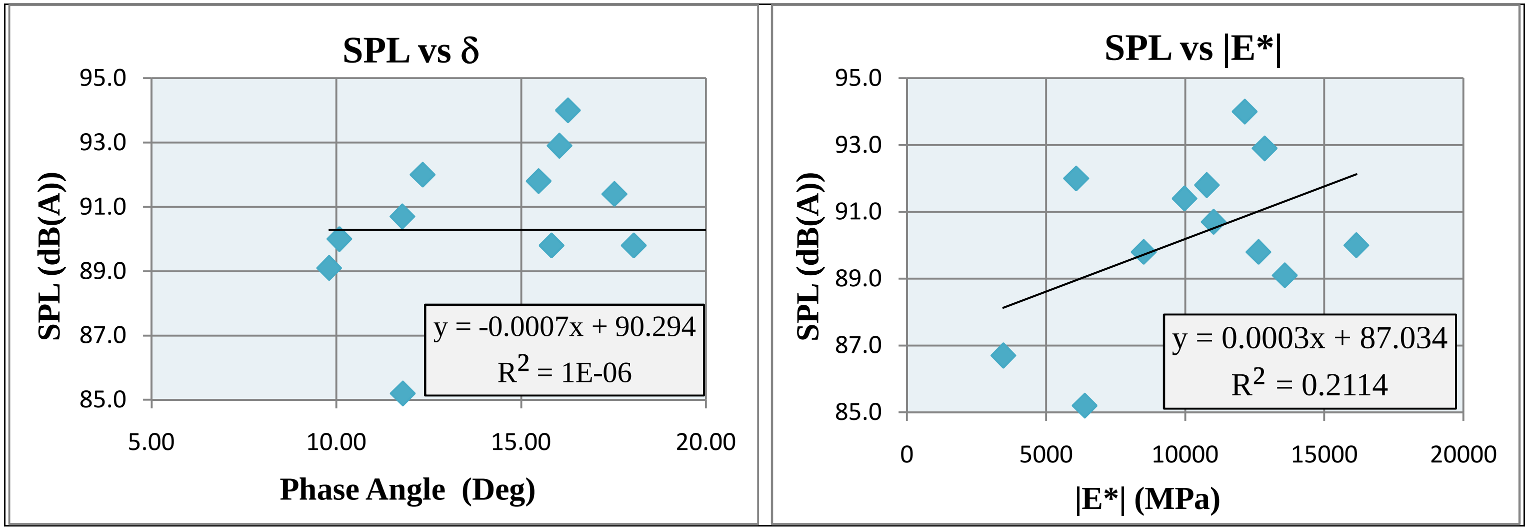

(a) (b)

Figure C.1 SPL versus (a) Phase angle (b) Dynamic modulus at 4^oC and 10 Hz

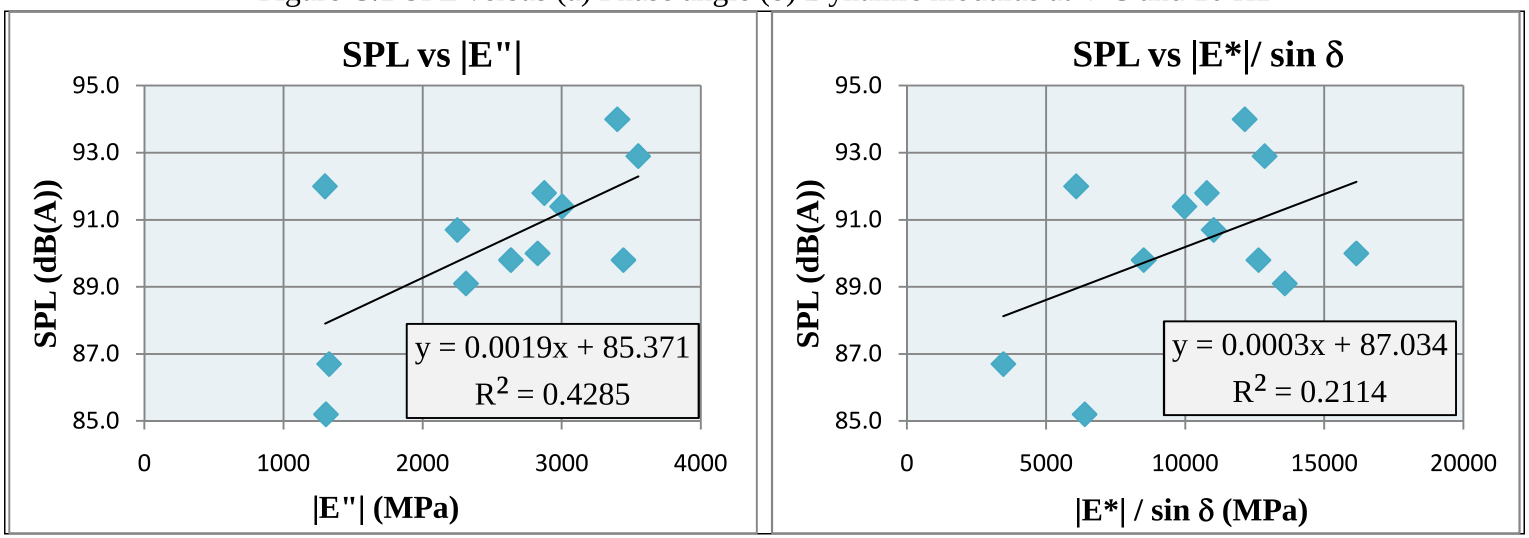

(a) (b)

Figure C.2 SPL versus (a) |E”| (b) |E*|/sin δ at 4^oC and 10 Hz

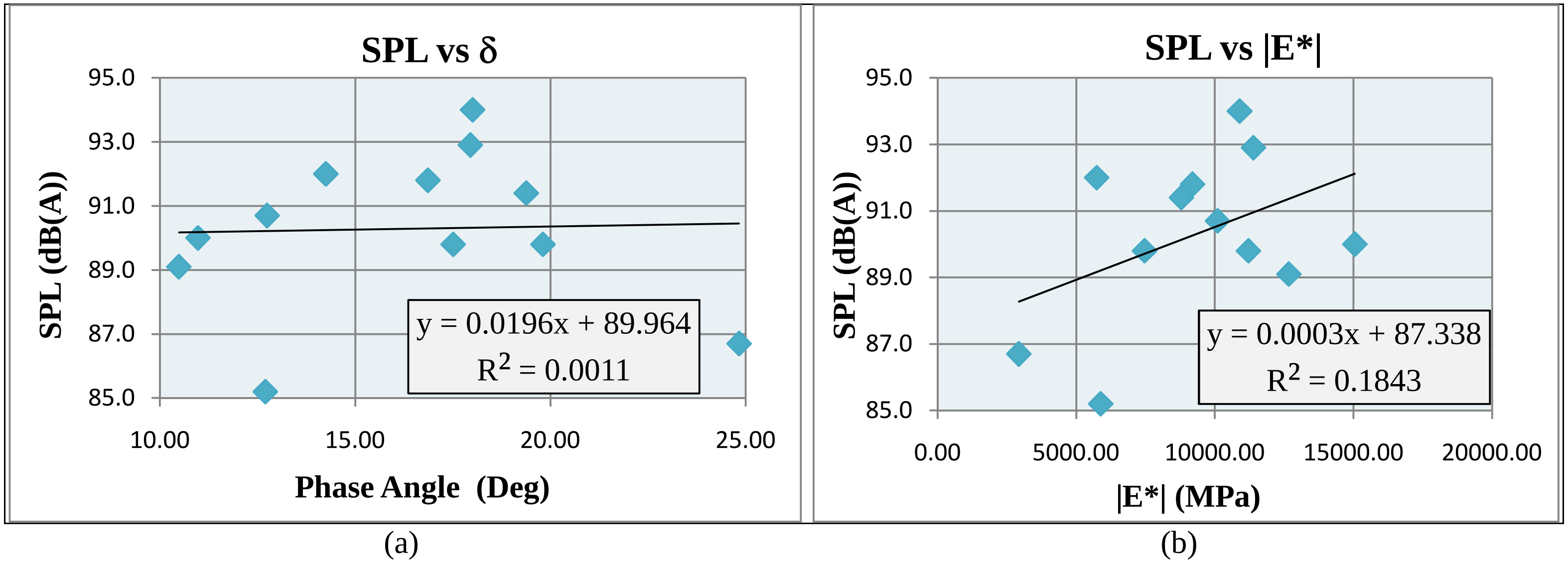

Figure C.3 SPL versus (a) Phase angle (b) Dynamic modulus at 4^{o}C and 5 Hz

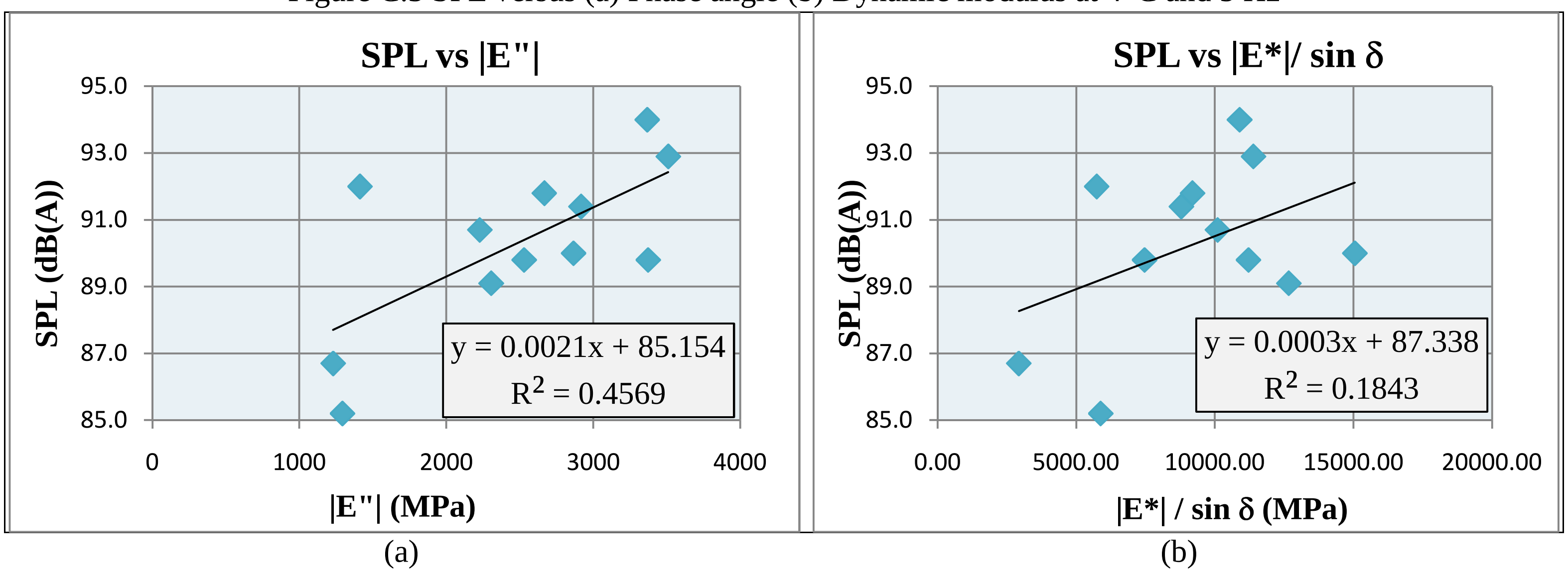

Figure C.4 SPL versus (a) |E"| (b) |E*|/sin δ at 4^{o}C and 5 Hz

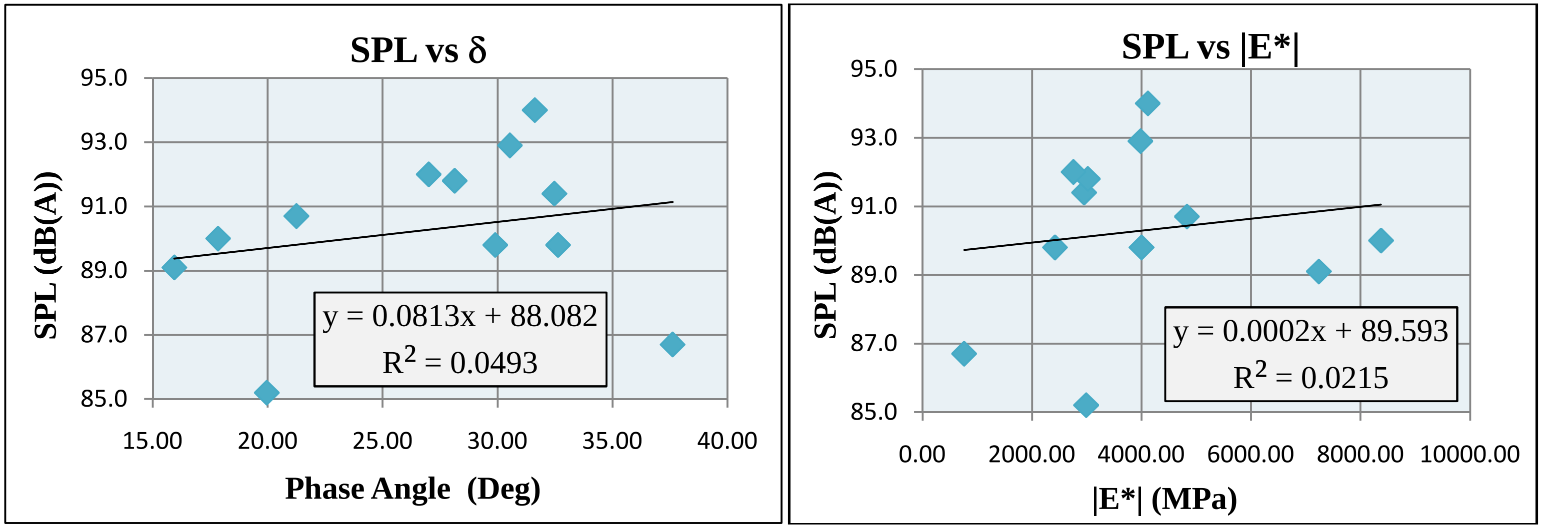

(a) (b)

Figure C.5 SPL versus (a) Phase angle (b) Dynamic modulus at 4^{o}C and 0.1 Hz

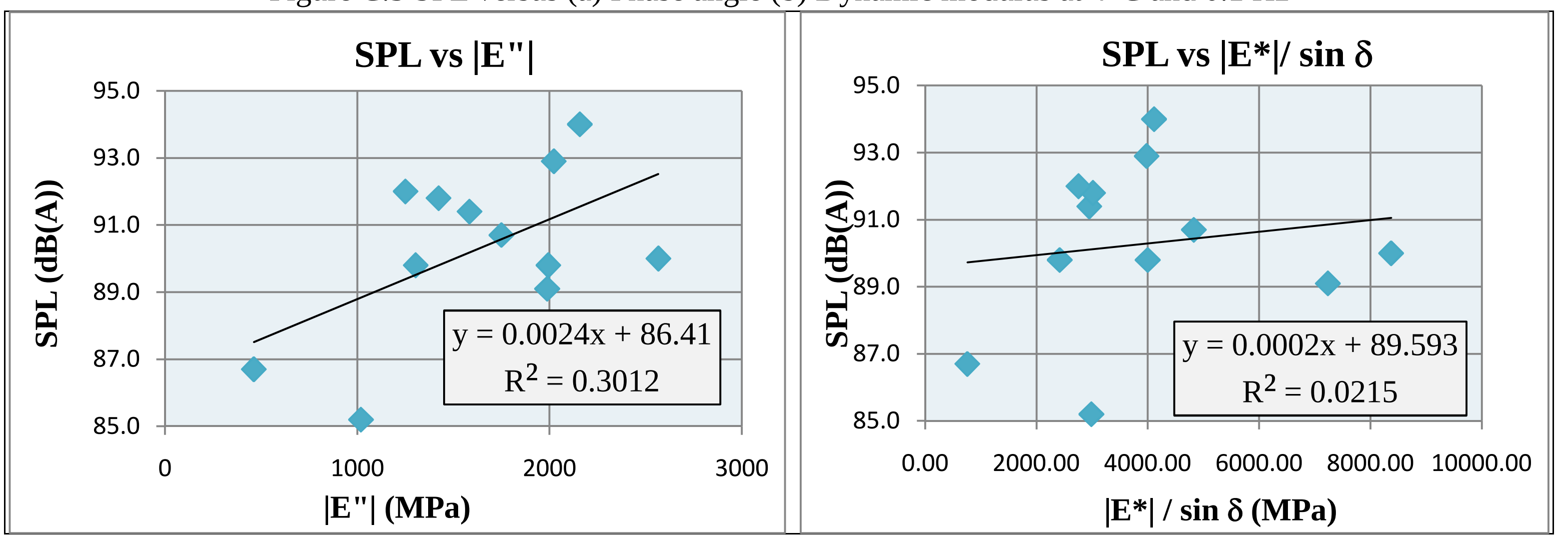

(a) (b)

Figure C.6 SPL versus (a) |E”| (b) |E*|/sin δ at 4^{o}C and 0.1 Hz

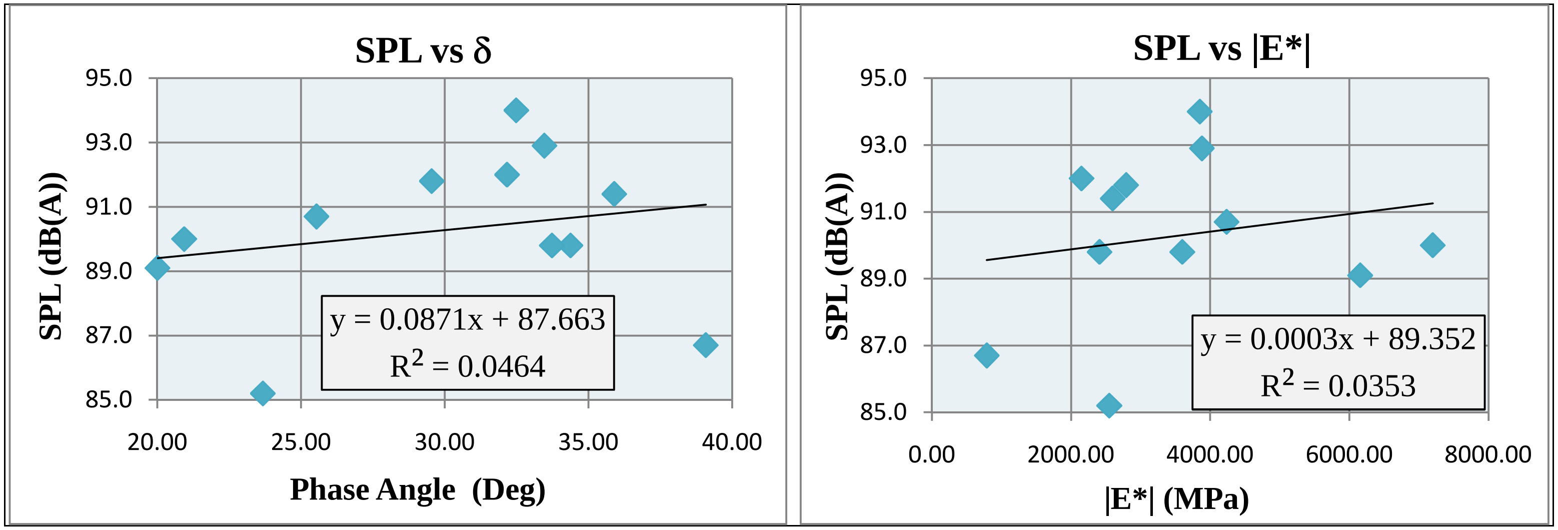

(a) (b)

Figure C.7 SPL versus (a) Phase angle (b) Dynamic modulus at 21^{o}C and 10 Hz

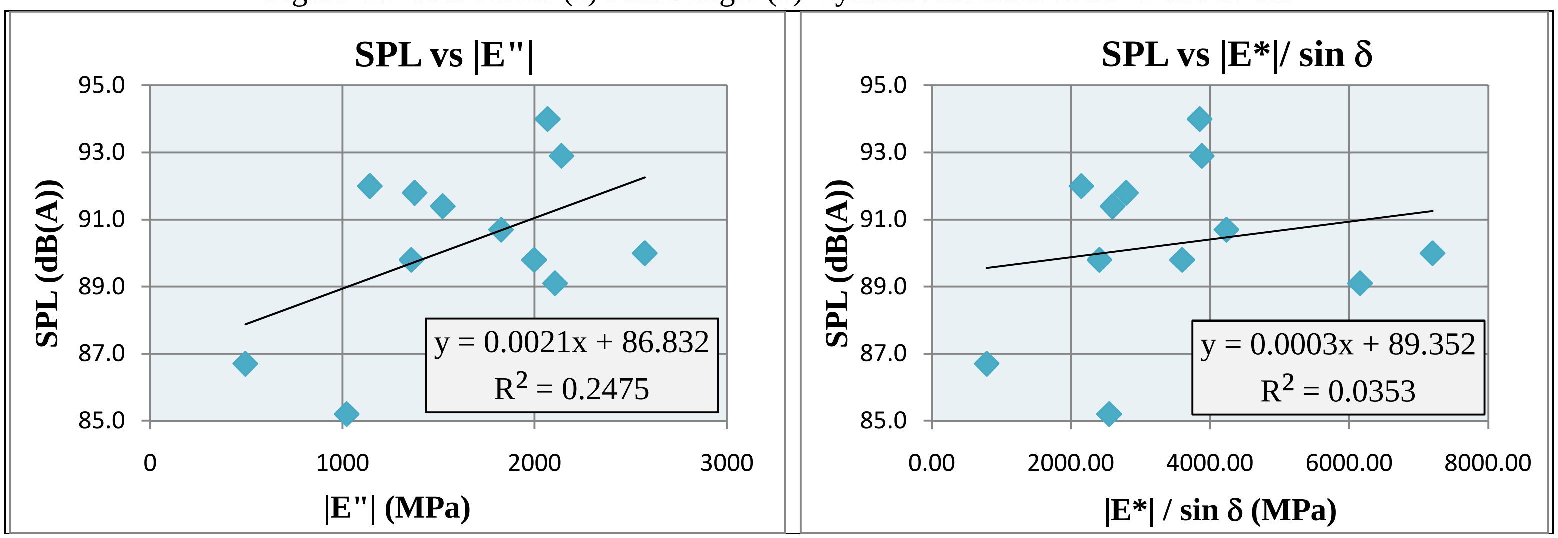

(a) (b)

Figure C.8 SPL versus (a) |E”| (b) |E*|/sin δ at 21^{o}C and 10 Hz

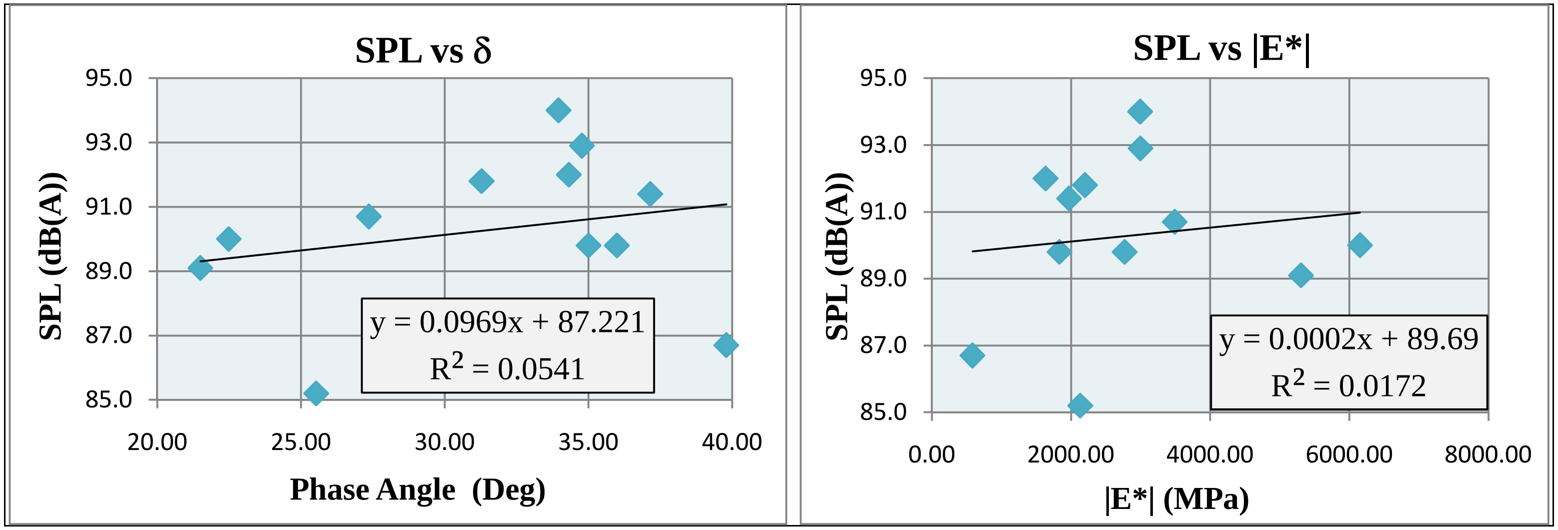

(a) (b)

Figure C.9 SPL versus (a) Phase angle (b) Dynamic modulus at 21^{o}C and 5 Hz

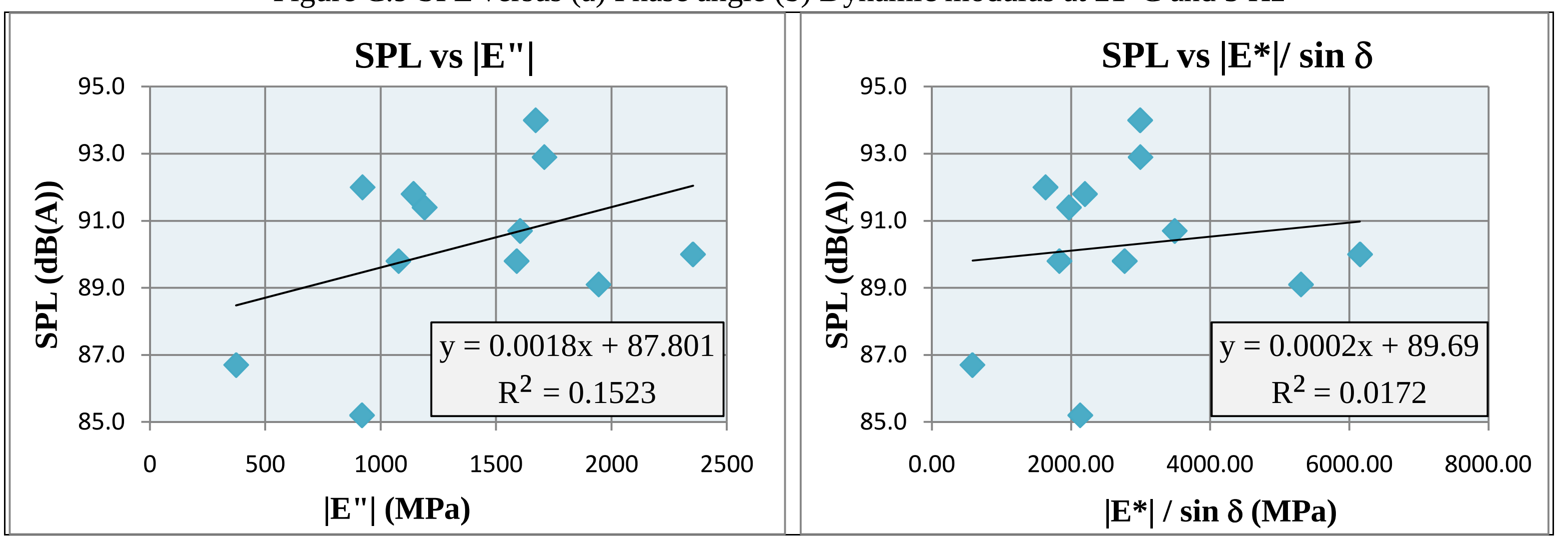

(a) (b)

Figure C.10 SPL versus (a) |E”| (b) |E*|/sin δ at 21^{o}C and 5 Hz

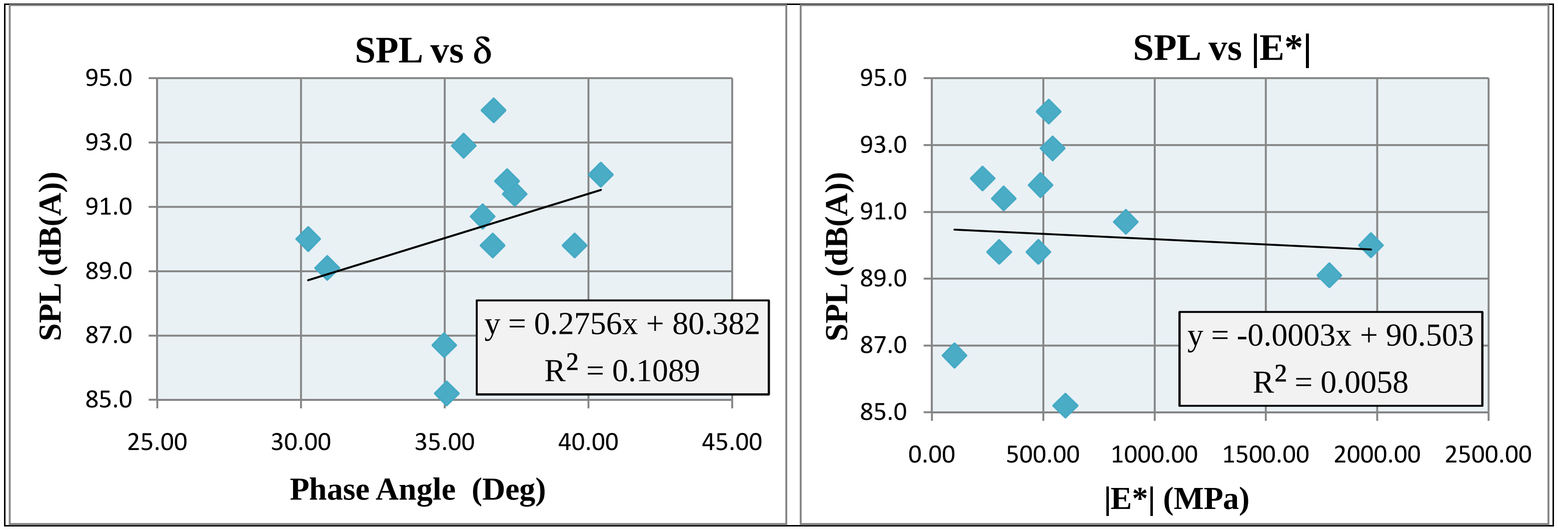

(a) (b)

Figure C.11 SPL versus (a) Phase angle (b) Dynamic modulus at 21^{o}C and 0.1 Hz

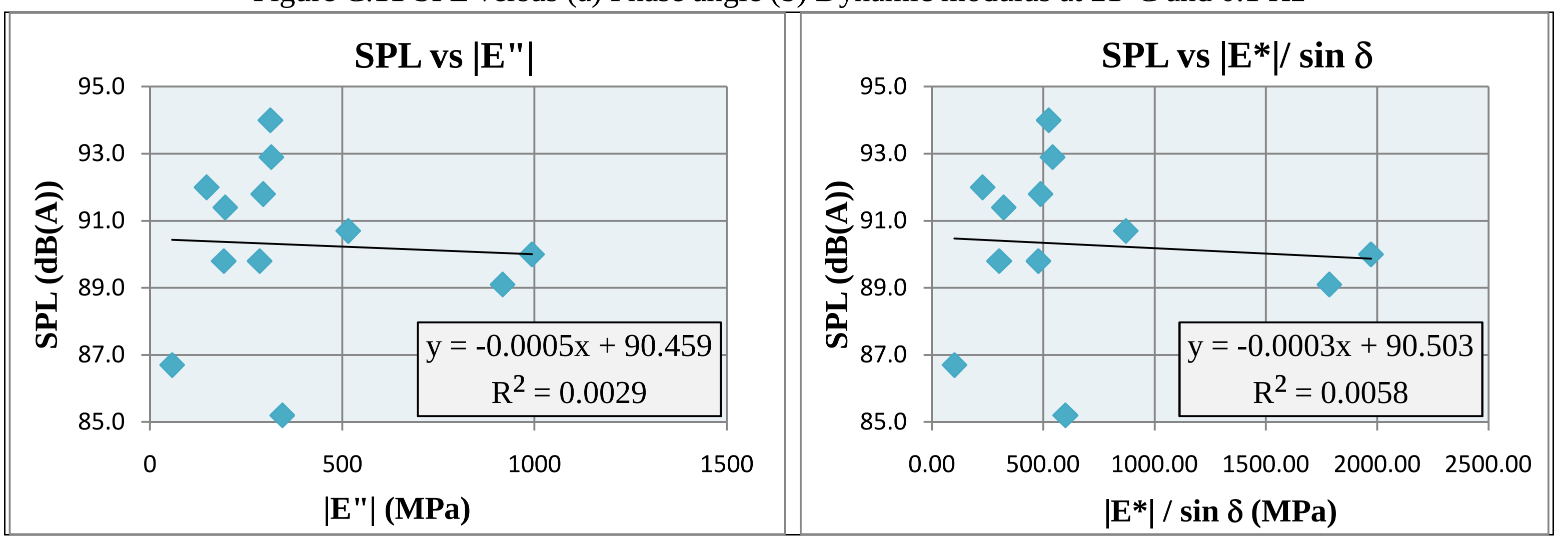

(a) (b)

Figure C.12 SPL versus (a) |E”| (b) |E*|/sin δ at 21^{o}C and 0.1 Hz

REFERENCES

REFERENCES

AASHTO (1993). "American Association of State Highway and Transportation Officials, Guide for Design of Pavement Structures." Washington, D.C.

AASHTO (2009). “Designing Stone Matrix Asphalt (SMA)”. American Association of State Highway and Transportation Officials Standards, Specifications No: R-46, Volume 1B. Washington, D.C.

AASHTO (2009). “Stone Matrix Asphalt (SMA)”. American Association of State Highway and Transportation Officials Standards, Specifications No: M-325, Volume 1B. Washington, D.C.

AASHTO (2009). “Standard Practice for Superpave Volumetric Desing for Hot-Mix Asphalt (HMA)”. American Association of State Highway and Transportation Officials Standards, Specifications No: R-35, Volume 1B. Washington, D.C.

AASHTO (2009). “Superpave Volumetric Mix Design”. American Association of State Highway and Transportation Officials Standards, Specifications No: M-323, Volume 1B. Washington, D.C.

AASHTO (2009). “Preparing and Determining the Density of Hot Mix Asphalt (HMA) Specimens by Means of the Superpave Gyratory Compactor”. American Association of State Highway and Transportation Officials Standards, Test No: T-312, Volume 2B. Washington, D.C.

AASHTO (2009). “Preparation of Cylindrical Performance test Specimens Using the Superpave Gyratory Compactor (SGC)”. American Association of State Highway and Transportation Officials Standards, Test No: PP-60, Provisional Standards. Washington, D.C.

AASHTO (2009). “Developing Dynamic Modulus Master Curves for Hot Mix Asphalt (HMA) Using the Asphalt Mixture Performance Tester (AMPT).” American Association of State Highway and Transportation Officials Standards, Test No: PP-61, Provisional Standards. Washington, D.C.

AASHTO (2009). “Developing Dynamic Modulus Master Curves for Hot Mix Asphalt (HMA).” American Association of State Highway and Transportation Officials Standards, Test No: PP-62, Provisional Standards. Washington, D.C.

AASHTO (2009). “Determining Dynamic Modulus of Hot Mix Asphalt (HMA).” American Association of State Highway and Transportation Officials Standards, Test No: TP-62, Provisional Standards. Washington, D.C.

Ahammed, M.J., Tighe, S.L., (2010). “Sound Absorption characteristics of Typical Pavements: An Ontario Stduy.” Transportation Research Board, 2010. 89th Annual Meeting CD-ROOM.

Ambroziak, M.A., (1999). “Effect of Pavement Type on Traffic Noise Levels.” Ohio Universty, Master of Science Thesis.1999.

Brown, E.R., Cooley, L.A. Jr., (1999). “Designing Stone Matrix Asphalt Mixtures for Rut-Resistant Pavements.” National Cooperative Highway Research Program (NCHRP). Report 42, TRB, National Academy Press, Washington, D.C.

Bucka, M. P., (2002). “Asphalt Rubber Overlay Noise Study Update.” Acoustical Analysis Associates Inc, County of Sacramento Public Works Agency Department of Transportation, Report1272, Project 22110.

Campbell, K., (2000). “Propagation of Sound and Related Shadow Zones: the Reality of Field Measurements versus Modeled Studies, The Wall Journal, Issue No 41.

Carlson D.D., Zhu, H., Xiao, C., (2005). “Analysis of Traffic Noise Before and After Paving with Asphalt Rubber.” Third Joint UNCTAD/IRSG Workshop on Rubber and Environment, International Rubber Forum, Veracruz, Mexico.

Cooley, L.A. Jr., Hurley, G.C. (2004). “Potential of Using Stone Matrix Asphalt (SMA) in Mississippi.” National Center for Asphalt Technology. Auburn University.

Federal Highway Administration (FHWA) Legislation and Regulations, (1997). “Procedures for Abatement of Highway Traffic Noise and Construction Noise.” Federal Aid Policy Guide 23-CFR-772.

Hamet, J.F., Deffayet, C., Palla, M.A., (1990). "Air Pumping Phenomena in Road Cavities.” STU Info NO 794, Proceddings of International Tire/Road Noise Conference, Stockholm, Sweden.

Hanson, D.I., James, R.S., NeSmith, C. (2004) “Tire/Pavement Noise Study.” National Center for Asphalt Technology, Report 04-02.

International Organization for Standardization, (1997). “Measurement of the Influence of Road Surfaces on Traffic Noise: Statistical Pass-By Method.” Part 1, ISO 11819-1.

Kaloush, K.E., Sotil, A., Biligiri, P.K., Golden, J.S. (2006) “The Dynamic Complex Modulus (E*) Test as a Potential Indicator for an Asphalt Mixture’s Tire-Road Noise Characteristics.” Transportation Research Board, Annual Meeting. Washington, DC. 2006.

Kropp, W., Kihlman, T., Forssen, J., and Ivarsson, L., (2007) “Reduction Potential of Road Traffic Noise.” A Pilot Study of Applied Acoustics Chalmers University of Technology, Alpha Print, Stockholm, ISBN 91 7082 770-2.

Kumar P., Chandra, S., Bose, S. (2005). "Comparative Study on Stone Matrix Asphalt Mixes with Different Stabilizers." Transportation Research Board, Annual Meeting. Washington, DC. 2005.

Kutay, M.E., Kocak, S. (2010). "A New Numerical Modeling Approach for Sound Propagation and Generation: the Lattice Boltzmann Method." Transportation Research Board 89th Annual Meeting. Washington, DC.

Lapcik, L., (1998). "Recycled Polymer Based Noise Absorbing Composite Materials." Proceedings of 5th International Conference on Composites Engineering, pp. 515, Las Vegas, USA, ISBN 0-7333-0504-0.

Leasure, W.A. Jr, Bender, E.K., (1975). "Tyre-Road Interaction Noise." Journal of the Acoustical Society of America, 58, pp. 39-50.2.

Malcolm, J.C., Hanson, D., Li, Z., Karjatkar, R., Vissamraju, K.S., (2003). "Measurement of the Acoustical and Mechanical Properties of Porous Road Surfaces and Tire/Pavement Noise." Transportation Research Record: Journal of the Transportation Research Board, Volume 1981/2004, pp 16-22.

Meiarashi S., (1999). " Researches on Low Noise Pavement in Japan." Journal Acoustic Society of Japan, Vol. 20, pp 19-27.

National Asphalt Pavement Association, (1999). "Designing and Constructing SMA Mixtures- State- of- the- Practice, Quality Improvement Series 122. NAPA. Landham, MD.

Narayanan, N., Jason, R.S., Jan, O., (2004). "Research on Enhanced Porosity Concrete." Cementing Future, Volume 15-1.

Nelson, T.J., Kohler E., Ongel, A., Rymer, B., (2008). "Acoustical Absorption of Porous Pavement." Transportation Research Board: Journal of the Transportation Research Board, Volume 2058/2008, pp 125-132.

Rasmussen, R.O., (2006). "Surface Characteristics, Relating Pavement Texture to Tire-Pavement Noise using RoboTex." Presentation at the FHWA Technical Work Group Meeting, ISU-FHWA-ACPA, 2006.

Rasmussen, R.O., Bernard, R.J., Sanberg, U, (2007). "The Little Book of Quieter Pavements." Technical Report No: FHWA-IF-08-004.

Sacramento County Department of Environmental Review and Assessment (SCDERA). (1999). "Report on the Status of Rubberized Asphalt Traffic Noise Reduction in Sacramento County."

Sandberg, U., (1992). "Low Noise Road Surface. A State-of-the-Art Review." Swedish Road and Traffic Research institute, Linkoping. S-581/01.

Sandberg, U., (1999). “Low Noise Road Surfaces: A State-of-the-Art Review.” Journal Acoustic Society of Japan.

Sandberg, U., (2001). “Tyre/road Noise – Myths and Realities.” International Congress and Exhibition on Noise Control Engineering, Inter Noise 2001, The Hague, The Netherlands.

Sandberg, U., Ejsmont, J.A., (2002). “Tyre/Road Noise Reference Book.” Informex, Sweden.

Sandberg, U., (2003). “The Multi-Coincidence Peak around 100 Hz in Tyre/Road Noise Spectra.” Euronoise, Paper ID: 498, Naples.

Shatanawi K.M., Bradley, P.J., Thodesen, C., Amirkhanian, S.N., (2008). “The Effects of Crumb Rubber Particles on Asphalt Pavement Traffic Noise Absorption.” TRIS, Transportation Research Board 88th Annual Meeting, Report No 09-3197.

Von Meier, A., (1988). “Acoustically Porous Road Surfaces: Recent Experiences and New Developments.” Proceedings of Inter-Noise 88, Avignon, France.

Von Meier, A., Van Blockland, G.J., Heerkens J.C.P., (1990). "Noise of Optimized Road Surfaces and Further Improvements by Tire Choice.” Proceedings of INTEROC, Gothenburg, Sweden.

Wayson, R. L. “Relationship Between Pavement Surface Texture and Highway Traffic Noise.” NCHRP19 Synthesis of Highway Practice 268, Transportation Research Board of the National Academies,20 Washington D.C., 1998.

Yamaguchi, M., Nakagawa, H., Mizuno, T., (1999).“Sound Absorption Mechanism of porous Asphalt Pavement.” Journal Acoustic Society of Japan, Vol. 20, pp 29-43.

Zhu, H., Liu, C., Tom, K., Norasit, T., (2008). “Crumb Rubber Blends in Noise Absorption Study.” Materials and Structures, Vol. 41, No. 2,383-390.

Zhu, H., Carlson, D.D., (1999). “A Spray Based Crumb Rubber Technology in Highway Noise Reduction Application.” Rubber Pavement Association.